AD_____

Award Number: DAMD17-96-1-6096

TITLE: Nitric Oxide in Mammary Tumor Progression

PRINCIPAL INVESTIGATOR: Peeyush Lala, M.D., Ph.D.

CONTRACTING ORGANIZATION: The University of Western Ontario
London, Ontario, Canada N6A-5C1

REPORT DATE: July 2000

TYPE OF REPORT: Annual

PREPARED FOR: U.S. Army Medical Research and Materiel Command
Fort Detrick, Maryland 21702-5012

DISTRIBUTION STATEMENT: Approved for Public Release;
Distribution Unlimited

The views, opinions and/or findings contained in this report are
those of the author(s) and should not be construed as an official
Department of the Army position, policy or decision unless so
designated by other documentation.

20001121 069

REPORT DOCUMENTATION PAGE

1. AGENCY USE ONLY (Leave blank)	2. REPORT DATE July 2000	3. REPORT TYPE AND DATES COVERED Annual (1 Jul 99 – 30 Jun 00)

4. TITLE AND SUBTITLE
Nitric Oxide in Mammary Tumor Progression

5. FUNDING NUMBERS
DAMD17-96-1-6096

6. AUTHOR(S)
Peeyush Lala, M.D., Ph.D.

7. PERFORMING ORGANIZATION NAME(S) AND ADDRESS(ES)

The University of Western Ontario
London, Ontario, Canada N6A-5C1

E-MAIL:
pklala@julian.uwo.ca

8. PERFORMING ORGANIZATION REPORT NUMBER

9. SPONSORING / MONITORING AGENCY NAME(S) AND ADDRESS(ES)

U.S. Army Medical Research and Materiel Command
Fort Detrick, Maryland 21702-5012

10. SPONSORING / MONITORING AGENCY REPORT NUMBER

11. SUPPLEMENTARY NOTES
Report contains color photos

12a. DISTRIBUTION / AVAILABILITY STATEMENT
Approved for public release; distribution unlimited

12b. DISTRIBUTION CODE

13. ABSTRACT *(Maximum 200 Words)*

Nitric Oxide (NO) is a potent bioactive molecule produced in the presence of endothelial (e), neuronal (n) and inducible (i) types of NO synthase (NOS) enzymes. We discovered that IL-2 therapy-induced capillary leakage was due to iNOS induction followed by overproduction of NO and then peroxyhnitrite. We also found that tumor-derived NO promoted mammary tumor progression in C3H/HeJ mice. eNOS expression by tumor cells was positively correlated with metastasis in spontaneous C3H/HeJ mammary tumors and transplants of two clonal derivatives of a spontaneous tumor differing in metastatic phenotype: highly metastatic C3L5 and weakly metastatic C10 cell lines. These cell lines also exhibited a parallel difference in invasiveness *in vitro* and growth rates as well as angiogenic abilities *in vivo*. A causal relationship between NO production by the tumor cells and invasive, migratory and angiogenic abilities was demonstrated. Invasion stimulation by NO resulted from an upregulation of MMP-2 and a downregulation of MMP inhibitors TIMP-2 and TIMP-3. Migration stimulation by NO resulted from activation of MAP-kinase pathway Thus NOS inhibitors should have a valuable therapeutic role for blocking multiple steps in mammary tumor growth and metastasis such as tumor cell migration, invasion and angiogenesis.

14. SUBJECT TERMS
Breast Cancer   Nitric Oxide   invasion   metastasis
C3H/HeJ mammary tumor   angiogenesis   IL-2 therapy

15. NUMBER OF PAGES
62

16. PRICE CODE

17. SECURITY CLASSIFICATION OF REPORT Unclassified	18. SECURITY CLASSIFICATION OF THIS PAGE Unclassified	19. SECURITY CLASSIFICATION OF ABSTRACT Unclassified	20. LIMITATION OF ABSTRACT Unlimited

FOREWORD

Opinions, interpretations, conclusions and recommendations are those of the author and are not necessarily endorsed by the U.S. Army.

___ Where copyrighted material is quoted, permission has been obtained to use such material.

___ Where material from documents designated for limited distribution is quoted, permission has been obtained to use the material.

___ Citations of commercial organizations and trade names in this report do not constitute an official Department of Army endorsement or approval of the products or services of these organizations.
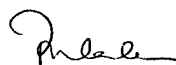
X In conducting research using animals, the investigator(s) adhered to the "Guide for the Care and Use of Laboratory Animals," prepared by the Committee on Care and use of Laboratory Animals of the Institute of Laboratory Resources, national Research Council (NIH Publication No. 86-23, Revised 1985).

N/A For the protection of human subjects, the investigator(s) adhered to policies of applicable Federal Law 45 CFR 46.

N/A In conducting research utilizing recombinant DNA technology, the investigator(s) adhered to current guidelines promulgated by the National Institutes of Health.

N/A In the conduct of research utilizing recombinant DNA, the investigator(s) adhered to the NIH Guidelines for Research Involving Recombinant DNA Molecules.

N/A In the conduct of research involving hazardous organisms, the investigator(s) adhered to the CDC-NIH Guide for Biosafety in Microbiological and Biomedical Laboratories.

_____   27 July 2000
PI - Signature   Date

TABLE OF CONTENTS

page

5.   INTRODUCTION

Overall objectives of the present project are to identify the precise role of nitric oxide (NO) in mammary tumor progression, using a C3H/HeJ mouse mammary tumor model developed in our laboratory. This model employs spontaneous tumors as well as their clones which vary in their ability for spontaneous metastasis.

Biology of NO

Following the discovery (1) that NO accounts for the full biological activity of a factor initially named "endothelium-derived relaxing factor" (2), produced by endothelial cells and causing vasodilation, research on the biology of NO has grown exponentially for many years. This molecule has since been shown to be produced by many other cells in the body, providing additional physiological functions such as inhibition of platelet aggregation, modulation of neurotransmission and mediation of cytotoxic function of macrophages against microbes, parasites and tumor cells (3-8). Sustained high levels of NO produced at the sites of inflammation can also mediate pathological injuries (9).

NO is produced by the conversion of the amino acid L-arginine to L-citrulline by a family of enzymes known as NO synthases (NOS). Three isoforms of NOS have been identified so far: endothelial type or eNOS is a constitutive form present in endothelial cells, myocardial cells and other cells inclusive of certain tumor cells; neuronal type or nNOS is also a constitutive form present in the central nervous system neurons, cells of the myenteric plexus, skeletal muscle cells, renal, bronchial and pancreatic islet cells as well as in tumors of the central nervous system; inducible type or iNOS is usually induced by certain inflammatory cytokines (e.g. IFN-γ, TNF-α) or bacterial products (e.g. LPS) in macrophages, hepatocytes, chondrocytes, endothelial cells and certain tumor cells (10-14). The constitutive forms are Ca^{++} and calmodulin-dependent whereas the inducible form is Ca^{++} and calmodulin-independent. Genes for all the isoforms have been cloned in numerous species (15,16) and disrupted in mice to show that none of the disruptions were embryo-lethal but had pathological effects consistent with known biological functions of NO. For example, eNOS knockout mice are hypertensive (17) because of the loss of vaso-relaxant function of NO; iNOS knockout mice are susceptible to infection and show poor macrophage cytotoxicity against parasites and tumor cells (18), consistent with NO-mediated macrophage defense; nNOS knockout mice (19) show hypertrophic pyloric stenosis, consistent with NO-mediated relaxation of pyloric sphincter muscle. nNOS -deficient males, in addition, show abnormal sexual behavior (20) because of aberrant neurotransmission.

NO is a free radical capable of crossing the cell membrane and reacting with other molecules. Most physiological functions of NO are mediated by increases in intracellular cGMP (21,22), whereas antibacterial, antiparasitic and antitumor functions of macrophage-derived NO

have been ascribed to the inhibition of mitochondrial respiration and DNA synthesis in target cells (23).

Constitutive production of NO occurs in cells at low to moderate levels, and the resulting bioactivity is short lived (T½ = few seconds) and short-range in nature. On the other hand, induced production of NO can be sustained at high local levels for a longer duration if the inducer molecules, e.g. inflammation-associated cytokines are produced in a protracted manner. This often leads to pathological consequences, resulting from NO reaction products. NO reacts with molecular oxygen, transition metals and superoxide to form intermediates which can cause cellular injury. For example, NO reacts with superoxide to make peroxynitrite, which can cause DNA damage (24).

Role of NO in tumor progression

It has been recognized for some time that chronic NO production is genotoxic and thus potentially carcinogenic (24). Recent studies, including our own (25) have revealed that tumor or host-derived NO can profoundly influence tumor progression in a positive or negative manner depending on the circumstances, and that in a large panel of well-established tumors, which have been examined so far, NO usually promotes tumor progression. Elevated serum NO levels have been observed in many cancer patients (26) indicating that tumor cells or host cells serve as the additional source of NO in these patients. A high expression of active NOS enzymes in tumor cells (27,28,31-34), endothelial cells in tumor vasculature (28) or tumor-infiltrating macrophages (29,30,32,34) has been positively correlated with the degree of malignancy in human cancers involving a large number of tissues: cancers of the reproductive tract (uterus, ovary) (27), central nervous system tumors (28), breast cancer (29,34), gastric cancer (30), cancer (squamous cell carcinomas) of the head and neck (31), prostate cancer (32) and lung cancer (33). However, the underlying mechanisms remain unexplored. Unexpectedly an inversion of this relationship was reported for human colonic tumors (35). This anomaly has been explained in a recent study (36) showing that the highest expression of active iNOS was noted in human colonic adenomas prior to their progression into carcinomas, consistent with the hypothesis that this promoted the transition of adenomas into carcinomas by a stimiulation of angiogenesis. Indeed, this group has shown a positive association between certain p53 mutations and iNOS expression in human colonic tumors indicating the promoting role of NO in colonic carcinogenesis (37). A positive correlation between NOS expression or NO production and tumor progression has also been detected in experimental tumor models in the mouse (38) and the rat (39).

A direct evidence for a stimulatory role of NO in tumor progression came from our own findings in a murine mammary adenocarcinoma model that treatments with either of two NOS inhibitors N^G-methyl-L Arginine (NMMA)(40) and N^G-nitro-L-arginine methyl ester (L-NAME) (41) reduced the growth of the primary tumors and their spontaneous lung metastases in mice

6

transplanted with the C3L5 mammary tumor line (reviewed in 25). Similar findings were reported with L-NAME therapy in a rat colonic adenocarcinoma model (39). In support of these results, engineered expression of iNOS in a human colonic adenocarcinoma line resulted in an increased growth rate and vascularity of tumors following transplantation in nude mice (42). In contrast with these results, engineered overexpression of iNOS in an iNOS deficient murine melanoma line (43,44) or a human renal carcinoma line (45) suppressed tumorigenic and metastatic ability of tumor cells *in vivo* because of NO-mediated cytostasis and apoptosis (43,44). Two explanations may be offered for these apparently conflicting results: First, very high NO levels (such as those produced by the iNOS-transduced murine melanoma line) (43,44) can be detrimental to tumor cell survival; for example the iNOS-overexpressing melanoma line had poor survival in the absence of NOS inhibitors *in vitro* and *in vivo* (44). Second, tumor cells may vary in their susceptibility to NO-mediated cytostasis and apoptosis because of their genetic makeup. For example, it has been suggested that the functional status of the tumor suppressor gene p53 dictates susceptibility (if functional) or resistance (if non-functional) to NO-mediated cytostasis or apoptosis (46,47). This suggestion was based on the following findings: iNOS transfected tumor cell lines fell into two distinct categories. Those expressing functional wild type p53 were vulnerable to NO-mediated cytostasis because of an accumulation p53 protein induced by endogenous NO (46,47). On the other hand, tumor cells in which p53 gene was lost or mutated not only withstood the deleterious effects of endogenous NO, but also exhibited faster growth and vascularity when transplanted *in vivo* (47). Since p53 mutation occurs in nearly half of human cancers (48), it was hypothesized that NO would facilitate tumor progression in a large proportion of well-established human tumors (47). We hypothesize that during the clonal evolution of tumors *in vivo*, high NO producing clones susceptible to NO-mediated injury are deleted and selected against those which are genetically resistant to NO-mediated injury and capable of utilizing NO to their advantage for expression of an aggressive phenotype (25). Loss of functional p53 gene may represent one of many genetic changes which can possibly result in the above phenotype. Further studies are needed to identify other genotypic markers in tumors for susceptibility or resistance to NO-mediated injury, so that the information can be utilized in therapeutic designs.

C3H/HeJ mammary tumor model employed in the present project.

Details of this model are provided in Appendix 1. In brief, this model is a combination of spontaneous C3H/HeJ mammary tumors and some of their clonal derivatives produced in our laboratory. Approximately 90% of retired breeder females of this mouse strain spontaneously develop invasive mammary adenocarcinomas with a pseudoglandular architecture, all of which metastasize to the lungs. Tumor development is due to insertional mutagenesis of certain cell growth-regulating loci resulting from the integration of the proviral form of the mouse mammary tumor virus (MMTV) in the developing mammary tissue of mice receiving the virus via mother's milk. Approximately 39% of human breast cancer specimens express a 660 bp sequence of the

MMTV envelop gene (49), the epidemiological significance of which remain to be identified. This finding and the similarity in histological features and metastatic behaviour, as reported by us earlier (50), suggest that C3H/HeJ spontaneous mammary tumors may represent the closest model for the human breast cancer, in particular, the familial form. We have derived two clonal lines, C3L5 and C10, grown from a spontaneous mammary tumor-derived line T58. The metastatic phenotype for C3L5 is high, for C10 is low, and for T58 is intermediate, based on the number of spontaneous lung metastases from subcutaneously transplanted tumors.

Preliminary data provided in the original grant application and substantiated further in the last three annual reports revealed that spontaneous C3H/HeJ primary tumors expressed eNOS protein (based on immunocyto-chemistry) in a heterogenous manner in tumor cells, whereas their metastases in the lungs were uniformly and strongly positive for eNOS (25). This finding suggested that eNOS bearing cells in the primary tumor were more prone to metastasis. This suggestion was strengthened by the findings that C3L5 cells (highly metastatic) were strongly positive for eNOS *in vitro*, as well as *in vivo* both at primary and metastatic sites (25). In addition, iNOS was inducible in C3L5 cells when cultured with IFN-γ and LPS (25). In contrast, C10 cells (poorly metastatic) were weakly positive for eNOS, and the expression was heterogenous. These findings, combined with our observations (25,40,41) that two NOS inhibitors NMMA and L-NAME reduced the growth of C3L5 primary tumors as well as their spontaneous lung metastases, led us to hypothesize that tumor-derived NO promoted tumor progression in this mammary tumor model. A large component of the current project is to validate this hypothesis and to identify the mechanisms underlying NO-mediated promotion of tumor progression in this model.

Role of NO in "capillary leak syndrome"

We discovered that capillary leak syndrome (characterized by fluid leakage from the capillaries into tissue spaces, various organs and body cavities), a life-threatening side effect of interleukin-2 (IL-2) based cancer immunotherapy, is due to the increased production of nitric oxide (40,41,51,52). This was shown by (a) a positive correlation of NO levels in the serum and the body fluids with the severity of IL-2 therapy-induced capillary leakage in healthy and tumor-bearing mice, and (b) an amelioration of this capillary leakage by chronic oral administration of NOS inhibitors NMMA and L-NAME (see ref. 53 for a comprehensive review).

Unexpectedly, we also observed that additional therapy with NOS inhibitors improved antitumor/antimetastatic effects of IL-2 therapy (40,41). This finding led to the suggestion that NO induction by IL-2 therapy interfered with antitumor effects of IL-2 therapy. We tested this hypothesis by investigating the effects of addition of L-NAME on IL-2 induced generation of lymphokine activated killer (LAK) cells *in vivo* and *in vitro* in healthy and tumor bearing mice (54). Results revealed that inhibition of NO production *in vivo* or *in vitro* by addition of

8

L-NAME to IL-2 therapy or IL-2 induced lymphocyte activation *in vitro* caused a substantial enhancement of LAK cell activation. In other words, IL-2 induced NO production interfered with optional LAK cell activation which can be abrogated with NOS inhibitors (54).

A minor component of the current project was to (a) identify the cellular source of NO induced by IL-2 therapy, (b) identify the nature of structural damage to the lungs of mice suffering from IL-2 induced pulmonary edema and pleural effusion, and (c) examine the effects of L-NAME therapy on the above parameters. Results of these studies have been published (52). In brief, IL-2 therapy led to high levels of iNOS protein expression and activity in the tissues of the anterior thoracic wall in accompaniment with pleural effusion. There was structural damage to the lungs (alveolar epithelium and interstitial tissue) and its capillaries by IL-2 therapy, which were mitigated by L-NAME therapy. L-NAME therapy abrogated IL-2 induced rise in iNOS activity but not the expression iNOS protein in the tissues.

6.   BODY OF THE PROGRESS REPORT

Overall Hypothesis: Tumor derived NO promotes C3H/HeJ   mammary tumor progression and metastasis.

Overall Objectives:

(1) To validate the hypothesis of the stimulatory role of NO in mammary tumor progression by further correlation of eNOS expression in clonally derived cell lines with tumor growth, metastasis, and angioigenesis *in vivo*, and migratory and invasive functions *in vitro*, and investigating the effects of blocking NOS activity or down-regulating eNOS gene on tumor cell behaviour *in vitro*, e.g. migration and invasiveness, and *in vivo*, e.g. tumor growth, angiogenesis and metastases.

(2)   To identify mechanisms of NO-mediated stimulation of tumor progression by investigating the role of NO in tumor cell proliferation, migration, invasiveness and tumor-induced angiogenesis.

Our assessment of overall progress in relation to the statement of objectives

Task 1   Relationship between NOS expression and tumor progression/ metastasis:
Progress has matched with our expectations in components 1a and 1b. The molecular biology components have continued to be frustrating. This was initially because of our failure to knockout the eNOS gene in C3L5 cells, evidently because of increased number (3.6) of gene copies in these cells. Subsequently, we adopted the antisense RNA approach to downregulate eNOS. We succeeded in obtaining low or nonexpressing clones more than once, however, all of them proved to be unstable and reverted to the expressor phenotype. During the last year we applied antisense oligonucleotides to achieve downregulation of a shorter duration. While this was achieved with a few antisense oligos, the results were too transient for proceeding with the functional studies 1d and 1e.

Task 2   Identification of mechanisms of tumor progression by NO.   Although this task was initially assigned to Year II onwards, significant progress was achieved in year I and all the goals have been completed in Years II - IV. Based on our findings, we conducted some new experiments and will proceed with additional experimients in the forthcoming year (see later).

Task 3   Mechanisms underlying IL-2 induced capillary leakage and interference with antitumor effects of IL-2 therapy by IL-2-induced NO.   Although this task was initially assigned to Year III onwards, we have completed our goals in this area ahead of the target date, leading to some new experiments and results.   We are in the process of wrapping up these experiments (see later).

10

Record of Research findings during the current year.

Task 1   Relationship between NOS expression and tumor progression and metastasis.

(a) **Relationship between the expression of NOS protein and tumor growth and metastasis.**

(i) **Spontaneous C3H/HeJ mammary tumors.**

We have continued the long process of accrual of a large number of spontaneous tumors developing during the life time of female retired breeder C3H/HeJ mice. During the last year we harvested an additional 12 spontaneous tumors and their metastatic foci for eNOS and iNOS immunostaining. The data confirm the findings presented in Appendix 1, which were based on 20 tumors (excluding 6 which were highly necrotic and thus not usable for immunostaining).

In summary, spontaneous tumors at the primary sites showed heterogenous eNOS expression in tumor cells. Irrespective of tumor growth rates (whether fast, intermediate or slow) a mixture of strongly eNOS positive (40-70%) or completely eNOS negative cells (30-60%) (Appendix 1, Figure 2A) were observed, however, the proportion of positive cells were higher in poorly differentiated areas than in differentiated areas of tumors showing pseudoacinar arrangement of tumor cells (Appendix 1, Figures 2A, 2B). In contrast, virtually all tumor cells at the sites of lung metastasis were strongly and homogenously eNOS positive (Appendix 1, Figure 2C). iNOS expression was restricted to a subset of macrophages within the primary tumors or the tumor stroma (Appendix 1, Figure 2D) as well as the metastatic sites. These results provide a strong validation of our preliminary data (25) suggesting a positive association between eNOS expression and tumor growth and metastasis, leading to the hypothesis that eNOS expression provides tumor cells with a selective advantage for growth and metastasis.

(ii) **C3L5 (highly metastatic) and C10 (weakly metastatic) cell lines and their transplants.**

(a)   The data are detailed in Appendix 1.

In summary, subcutaneous transplants of C3L5 cells grew faster at the primary sites and produced a larger number of spontaneous lung metastasis than those of C10 cells during the same time span (Figure 1, Appendix 1). Weakly metastatic C10 cells expressed low levels of eNOS *in vitro* in a minor proportion of cells, as compared to the highly metastatic C3L5 cells which expressed high eNOS levels in

11

nearly every cell. Similar differences in eNOS protein expressin were observed *in vivo* only at the primary tumor site (Figures 2E and G, Appendix 1), however their lung metastasis were equally and strongly positive for eNOS (Figures 2F and 2H, Appendix 1). iNOS expression was undetectable in either cell line, but noted in a subset of both cell lines *in vitro* only when cultured in the presence of IFN-γ + LPS. C3L5 and C10 tumor cells grown *in vivo* were iNOS negative both at primary and metastatic sites; only a subset of macrophages at either site expressed iNOS. These results were objectively validated by quantitative image analysis (Figures 3A and 3B, Appendix 1), and supported the hypothesis of a causal relationship of eNOS expression to tumor growth and metastasis.

(b) **Attempts to investigate biological alterations of murine mammary adeno-carcinoma cell line (C3L5) by downregulation of eNOS gene expression.**

As reported last year, we failed to knock out eNOS gene in the high eNOS-expressing C3L5 cells because of the presence of a high copy number of eNOS genes (average 3.6). Subsequently, our attempts to knock down this gene by stable transfection with antisense RNA were also met with frustrations, because of the instability of all the eNOS down-regulated clones reverting to eNOS expressing phenotype, possibly because of a variety of reasons suggested or reported by others (55-57). Subsequently, we tried two more antisense constricts based on two different fragments of the eNOS gene (one derived from the tail region) to transform C3L5 cells at different concentrations using the lipofectamine method. These attempts were also unsuccessful and thus will not be detailed here.

Last year, we devoted a good deal of time and energy to apply antisense oligonucleotide knock down stragety to downregulate eNOS in C3L5 cells. In essence, the results were not encouraging for our purpose, because the down-regulation was (a) not always consistent, and (b) not stable enough for the durations required for our functional assays. Below, we provide a summary of our attempts. It is clear from the literature that not all antisense oligonucleotide sequences can downregulate expression of target proteins. Many researchers believe that phosphothioate (PS) oligodeoxy-nucleotides inhibit protein expression by blocking the ribosome as it moves along mRNA. That is why the dogma is that the design of oligonucleotides in the vicinity of AUG (start codon) site on the mRNA are most active. But because almost all PS oligos function as antisense molecules by forming duplex with target mRNA and then serves as substrate for RNase H, Dr. Nic Dean of ISIS Pharmaceutical recommends to design several oligo sequences throughout the mRNA (58). In fact, his group has shown in many instances (58-60) that PS-oligos designed in the vicinity of AUG (start codon) site

have very little or no potential to inhibit target protein expressions, whereas the maximal ability to inhibit target protein expression was shown by PS-oligos designed from some other regions of the mRNA. Furthermore, the phosphothioate modifications of the oligodeoxy-nucleotides, although effective, have some limitations. Their main limitation is that they are metabolised in cells over time, leading to almost total loss of activity over 48-72 h period. Dr. Nic Dean's group has shown that the 2'-O-(2-methoxy) ethyl (2'-MOE) modification of oligodeoxynucleotide result in dramatic enhancement in the ability of the sequence to hybridize to a target mRNA and nuclease resistance when compared with PS-oligos (61). Therefore, we requested him to synthesize 2'-MOE modified antisense murine eNOS oligodeoxynucleotides for us. He kindly synthesized 22 different oligos designed from different regions of the eNOS mRNA for us, the sequences of which remain blinded to us. We utilized these oligos in C3L5 cell cultures in order to screen an active sequence. Lipofectin was tested as oligo uptake enhancer. 100-400 nM concentrations of each oligo were mixed with appropriate concentrations of lipofectin (5 µl lipofectin/ml/100 nm oligo). These mixtures were added to the cells when they are 70-80% confluent. The cells were then allowed to incubate for 4 hrs with occasional swirl. The lipofectin solution was then removed and replaced with media. The cells were then allowed to incubate overnight, and NO (nitrite and nitrate) concentrations in the medium were determined as the end result of eNOS mRNA down regulation.

The results of some six screening attempts were highly variable. In two attempts (attempt # 2 presented in **Fig. 1**), three oligos (#5, 16 and 20) significantly downregulated ($\geq$ 50%) NO production by C3L5 cells as compared with that noted with mock-treated controls (# 23, 24). However, the effects were either too transient (i.e. undetectable after 72 hours) or not adequately reproducible in subsequent screeing (data not presented). We have been advised that our problems, may again, lie in the genetic constitution of our target cell line expressing a high copy number of the eNOS gene.

We have decided that further attempts to downregulate eNOS gene in C3L5 cells are not worth pursuing for the following reasons: (a) we have achieved all the expected resuslts by blocking NOS activity in these cells, and (b) we have, in essence, achieved similar objectives by conducting functional assays with our naturally occurring low eNOS-expressing C10 cell line clonally derived from the same parental tumor, from which the high eNOS-expressing C3L5 cell line was derived.

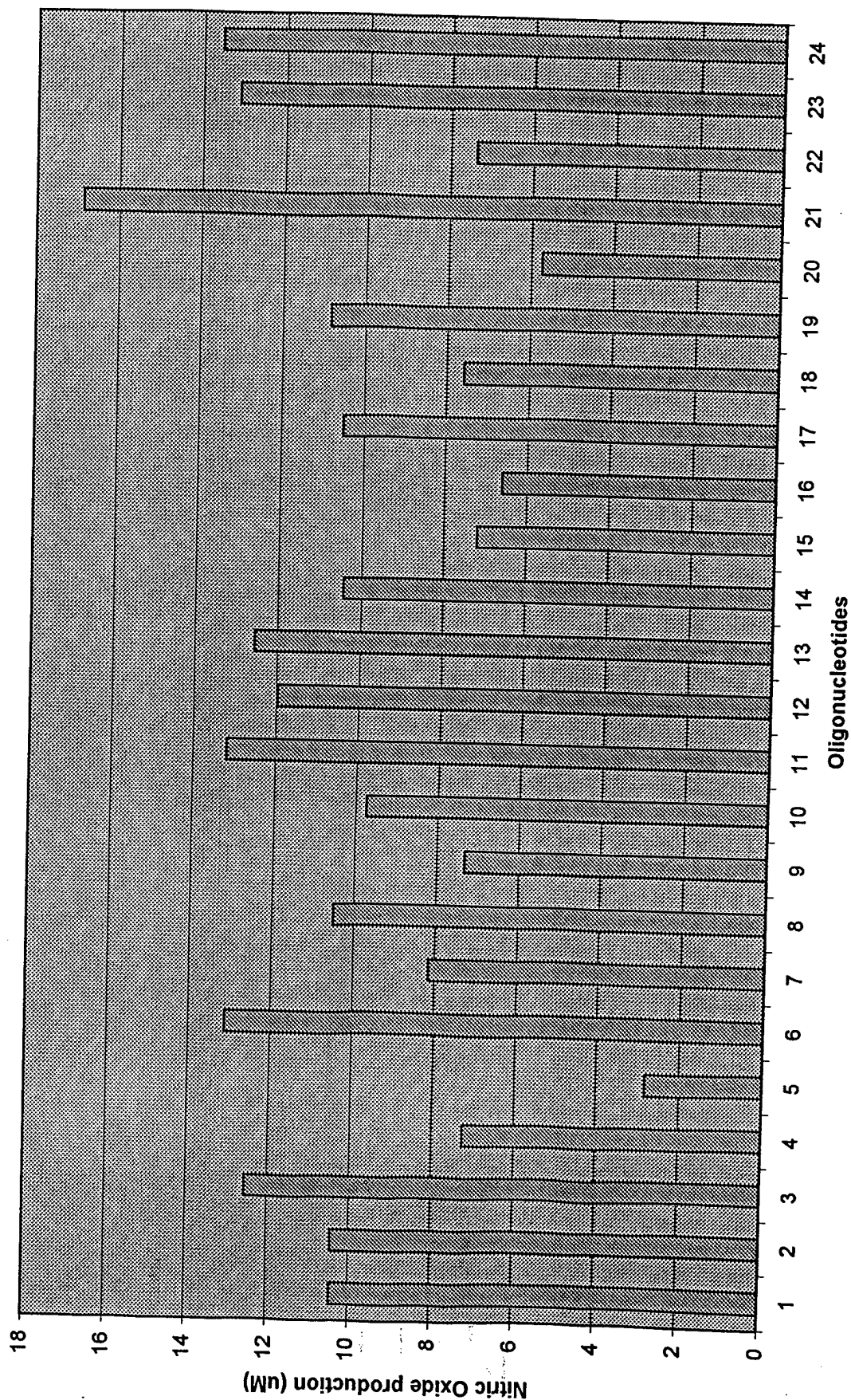# Nitric Oxide Production Measured by the Sum of Nitrate and Nitrite Production

Fig. 1 Numerous oligos reduced NO production to below 50% levels as compared to mock treated cells (# 23,24). Three of them (# 5, 16, 20) reproduced results in another screening (not shown).

Task 2   **Identification of mechanisms underlying NO-mediated promotion of tumor progression.**   We hypothesized that tumor-derived NO facilitates tumor progression and metastasis by **(a)** promoting tumor cell migratory ability, **(b)** promoting tumor cell invasive ability and **(c)**   promoting tumor-induced angiogenesis which is critical for the growth of solid tumors. We had already shown that tumor-derived NO exerted no influence on tumor cell proliferation *in vitro*. Others have shown that tumor-derived NO promotes tumor blood flow and microcirculation which can indirectly promote tumor growth (62-64).

(a)   **Effects of tumor-derived NO on *in vitro* migratory ability of C10 and C3L5 tumor cells. (detailed in Appendices 1, 2 and 3; ref. 71)**

Since migratory ability is an essential component of cellular invasiveness and metastasis, we examined the role of NO on the migration of the two mammary tumor cell lines differing in eNOS expression and metastatic phenotype. First, we compared the migration kinetics of the two cell lines using a transwell migration assay detailed in Appendix 1. Second, we examined the migratory ability of each cell line after treatment with the NOS inhibitor L-NAME in the presence or absence of excess L-arginine (the natural substrate for NOS, which should compete with L-NAME) under conditions detailed in Appendix 1, in order to identify the contributory role of NO which was measured in the medium under identical conditions.

Results (detailed in Appendix 1) revealed that the two cell lines did not differ significantly in their migratory abilities (Figure 4A, appendix 1), however, migration of both cell lines were inhibited in the presence of L-NAME in a dose-dependent manner and restored in the additional presence of excess L-arginine (Figure 5A, Appendix 1). These treatments produced correspondingly similar effects on the NO production by these cells (Figure 6, Appendix 1). These results demonstrate that migration of both cell lines are stimulated by endogenous NO, in spite of differences in the level of NO production by these cells. Thus an absence of any significant difference in the basal migration rates of the two cell lines is possibly explained by differential production of other migration-regulating molecule(s) by these cells. The above is the first demonstration of migration stimulation of tumor cells by tumor-derived NO. The underlying mechanisms of signal transduction are currently being investigated with additional experimentss, not proposed earlier.

We wish to identify intracellular pathways of signal transduction responsible for NO-mediated stimulation of tumor cell migration, utilizing the high eNOS-expressing C3L5 mammary tumor cell line. It has been shown that most

15

physiological functions of NO (e.g. vasorelaxation by endothelium derived NO) are mediated by stimulation of cyclic GMP (cGMP) (10-12). In addition, vascular endothelial growth factor (VEGF)-mediated angiogenesis, involving endothelial cell proliferation, migration and tube formation has been shown to be dependent on stimulation of endothelial NOS (i.e. NO production) followed by activation of mitogen activated protein (MAP) kinase pathway (65,66). We postulate that endogenous NO causes an increase in the level of cGMP leading to the activation of cGMP dependent protein kinase (G kinase), MAP kinase kinase (MAPKK) and MAP kinase (extra cellular regulated kinases or ERK 1 and 2), followed by the activation of the cellular motility apparatus. Following experiments are proposed in C3L5 cells to test this hyposthesis:

(i)   We shall measure cGMP levels with a radioimmunoassay in cell extracts (65) following treatment of cells with L-NAME (to block NO production) ± excess L-arginine (which will restore NO production). Similar experiment will be done following treatment with LPS + IFN-γ to stimulate NO production by induction of iNOS or by addition of sodium nitroprusside (SNP) as an NO donor. Levels of NO (measured with Griess reaction) will be correlated with cGMP levels. Migration index of intact cells will be measured under identical treatment conditions.

(ii)   Cause-effect relationship of cGMP or G-kinase stimulation to cellular migration will be tested by treatment of cells with soluble guanylate cyclase inhibitors LY83583 (65) (0.1-10μM) or 1H (1,2,4) oxadiazolo (4, 3-a) quinoxalin-1-one (ODQ) (0.1-10μM) (66), G-kinase antagonist R p-8-pCPT- cGMPS (1-10nm) (67) and G-kinase inhibitor KT583 (1-10nm) (68) at proven nontoxic doses (i.e. having no effect on cell viability).

(iii) Whether eNOS or iNOS-derived NO causes activation (phosphorylation) of MAPK (ERK1 and 2) will be tested with Western immuno blots of phospho ERK 1 and 2 (66) in lysates of cells pretreated with L-NAME ± excess L-arginine, or LPS + IFN-γ, or SNP, as described in (i).

(iv)   Cause-effect relationship of MAPK activation to cell migration will be tested by treatment of cells with a MAPKK (MEK) inhibitor PD98059 (0-100μM) at proven nontoxic doses. Simultaneously, the effects of the inhibitor on ERK 1,2 phosphorylation will be tested.

(v)   Effects of treating cells with L-NAME (NOS inhibitor) or G-kinase antagonist/inhibitor (see ii above) on ERK 1 and 2 phosphorylation would

16

indicate whether NOS and G-kinase are proximal to MAPK in the signal transduction pathway.

Last year our efforts have been focussed on the role of MAPK pathway in NO-mediated stimulation of mammary tumor cell migration. We have conducted a large number of experiments in C3L5 cells to investigate (a) the time course of changes in MAPK phosphorylation following exposure of C3L5 cells to the NOS inhibitor L-NAME at 200 µM - 1 mM concentrations, which are found to inhibit cell lmigration; (b) the effects of additional treatment with excess L-Arginine (to restore NO production) for various durations on ERK phosphorylation; (c) the effects of additional exposure of cells to the NO donor SNP on ERK phosphorylation; (d) the effects of pretreating cells with the MEK inhibitor PD98059 on C3L5 cell migration and ERK phosphorylation under various conditions. Selected results are presented in Figs. 2 and 3.

In summary, we found that (a) ERK phosphorylation is inhibited with L-NAME at 200 µm - 1mM concentrations; (b) the effects were maximal at 30 mins., followed by a slow recovery even in the presence of L-NAME indicating that endogenous molecules other than NO have important stimulatory role, which can compensate for NO. (c) ERK phosphorylation was restored very rapidly (at 5 - 10 mins.) in the additional presence of excess L-Arginine which restores NO production. This is a key experiment supporting the hypothesis that endogenous NO stimulated ERK phosphorylation in C3L5 cells. (d) Exogenous NO donated by SNP, also rapidly stimulated ERK phosphorylation in NOS-inhibited cells. (e) PD98059 blocked basal as well as NO-stimulated ERK phosphosrylation noted in (c) and (d). (f) PD98059 blocked basal C3L5 cell migration as well as migration-restoring effects of excess L-Arginine following inhibition with L-NAME. These data reveal that migration-stimulating role of endogenous NO in C3L5 cells is mediated via MAPK pathway. Stimulation of MAPK activation by NO is very rapid (matter of minutes) in preparation for the migratory response which is visible in the migration assay at 24-72 hrs.

(b)   Effects of tumor-derived NO on invasiveness of mammary tumor cells.

(i)   A comparison of *in vitro* invasiveness of highly metastatic (and high eNOS expressor) C3L5 with weakly metastatic (and low eNOS expressor) C10 cell lines: role of NO.
Materials, methods and results are detailed in Appendix 1. In brief, C3L5 cells invaded matrigel at a faster rate than C10 cells (Figure 4B, Appendix 1). Furthermore, L-NAME caused a dose-dependent inhibition of invasion in both cells, which was relieved in the presence of excess L-arginine

17

(Figure 5B, Appendix 1) with concomittant restoration of NO production (Figure 6, Appendix 1), indicating that endogenous NO stimulated invasiveness of both cell lines.

(ii)   Mechanism of NO-mediated stimulation of invasiveness, investigated with C3L5 cells.

As presented in the 1997-1998 Progress Report, C3L5 cell invasiveness was shown to be dependent on endogenous NO.

Endogenous (eNOS-derived) NO was shown to downregulate TIMP-2 and TIMP-3 mRNA expression. In addition, when iNOS was induced in C3L5 cells by LPS+IFN-γ *in vitro*, these cells became more invasive, and there was an additional upregulation of MMP-2. Thus NO-mediated promotion of invasiveness was due to an altered balance between MMP-2 and its inhibitors TIMPs 2 and 3 (for details, see published ref. 70).

(iii)   Role of uPA-uPAR system in NO-mediated stiimulation of tumor cell migration or invasiveness.
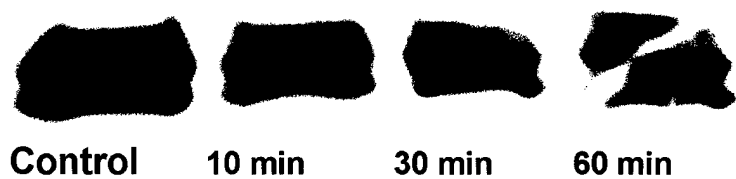
Urokinase type plasminogen activator (uPA) is a major protease made by cancer cells including the present mammary tumor model. uPA has the dual ability of stimulating migration as well as invasiveness of certain cancer cells. In the former case, the effect is independent of the uPA catalytic domain, resulting from binding of the aminoterminal domain of uPA to uPA-receptor (uPAR) which can mediate a migration-stimulatory signal. In the latter case uPAR bound uPA, via the catalytic domain exerts proteolytic action to activate MMP's which, in turn, can degrade the extracellular matrix.

To test whether uPA-uPAR system is involved in regulating C3L5 cell migration or invasiveness, we conducted migration and invasion assays in the presence of anti-uPA as well as anti-uPAR antibodies. As shown in Fig. 4, both antibodies significantly reduced C3L5 cell migration as well as invasiveness. We shall test whether NO stimulates the uPA-uPAR systems as follows: (1) We shall measure the uPA protease activity with casein zymography in the presence of NOS inhibitor L-NAME and NO donor SNP. (2) We shall investigate whether these treatments alter the expression of uPA and uPAR mRNA with Northern blot analysis and uPAR expression with flow cytometry.
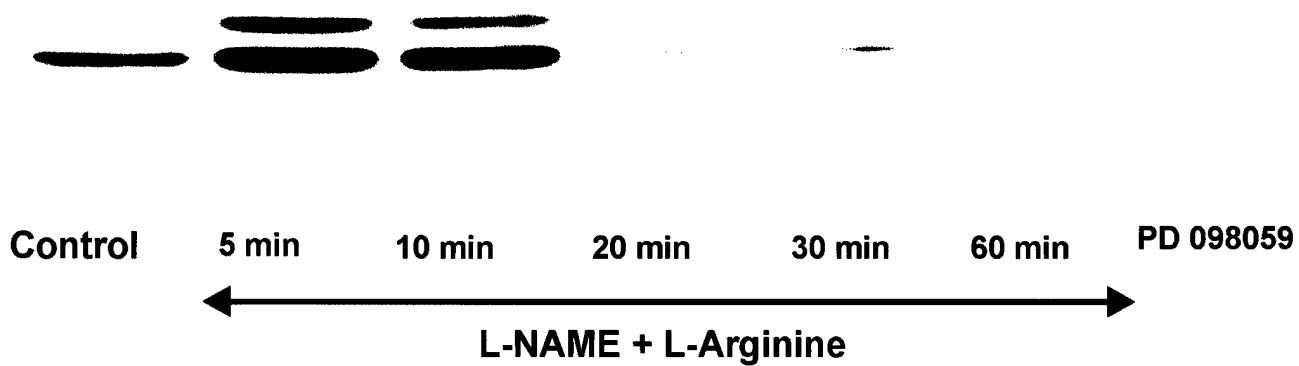
18

Fig. 2 Western blots of MAPK (ERK I and ERK II) phosphorylation in C3L5 cells in three different experiments.

A.   Effects of treatment at O (control) 10, 30 and 60 min with 200 μM L-NAME. The phosphorylation level declined to a maximum at 30 minutes and partially recovered at 60 min.

B.   Effects of treatment with L-NAME for 18 hours, followed by treatment with excess (10 fold) L-Arginine for 5 mins to 60 mins, and treatment with PD98059 for 1 hr. Note that addition of L-Arginine to L-NAME treated cells rapidly stimulated ERK phosphorylation at 5-10 min. followed by a gradual decline. MEK inhibitor PD98059 totally blocked phosphorylation.

C.   Effect of treatment with L-NAME for 18 hours followed by treatment with SNP (NO donor) for 5-60 min; and treatment with PD98059 for 1 hr. Note that addition of SNP rapidly stimulated ERK phosphorylation, reaching a maximum at 5 min followed by a gradual decline. PD980059 totally blocked the phosphorylation event.

A

Control   10 min   30 min   60 min

B

Control   5 min   10 min   20 min   30 min   60 min   PD 098059

L-NAME + L-Arginine

C

Control   5 min   10 min   20 min   30 min   60 min   PD 098059
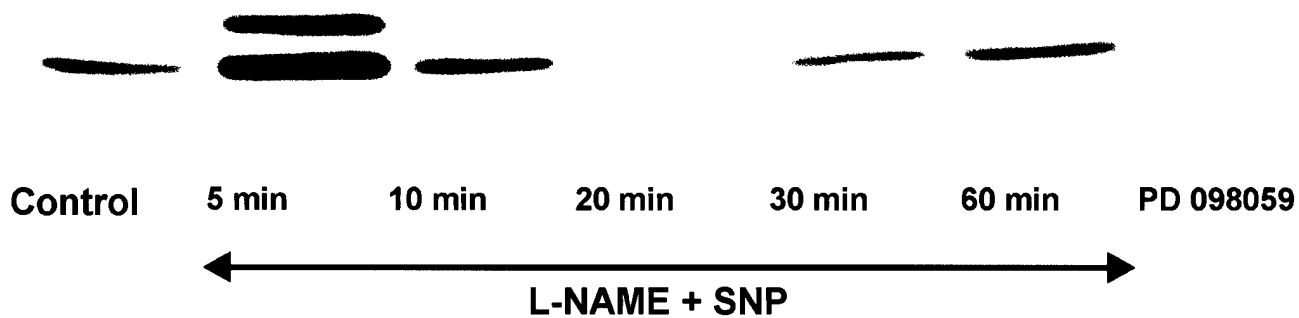
L-NAME + SNP

Fig. 2 Western blots of MAPK (ERK I and ERK II) phosphorylation in C3L5 cells in three different experiments.

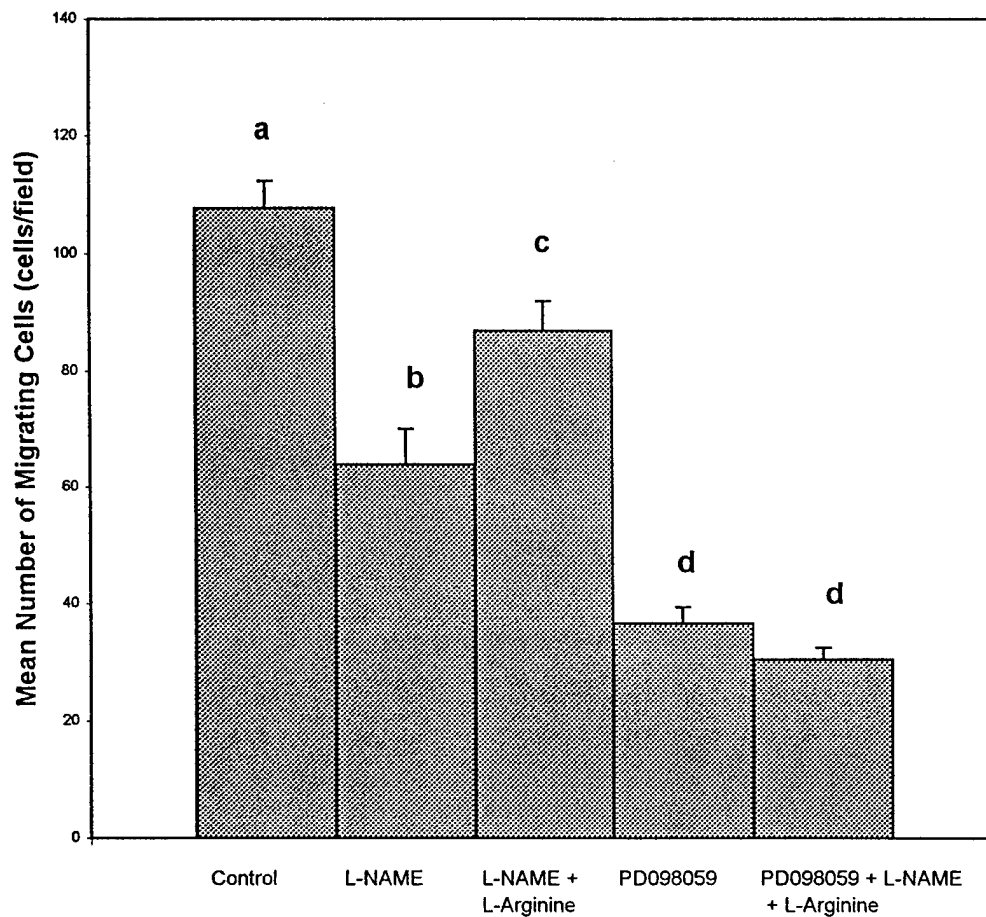**Figure 3.** Twenty-four hour migration of C3L5 cells under different treatment conditions. L-NAME treatment reduced the migration; additional treatment with excess L-Arginine partially restored migration. Treatment with PD098059 blocked basal migration, as well as migration-restoring effects of L-Arginine in L-NAME. Statistical significant differences exist between groups with different superscripts (P < 0.05).
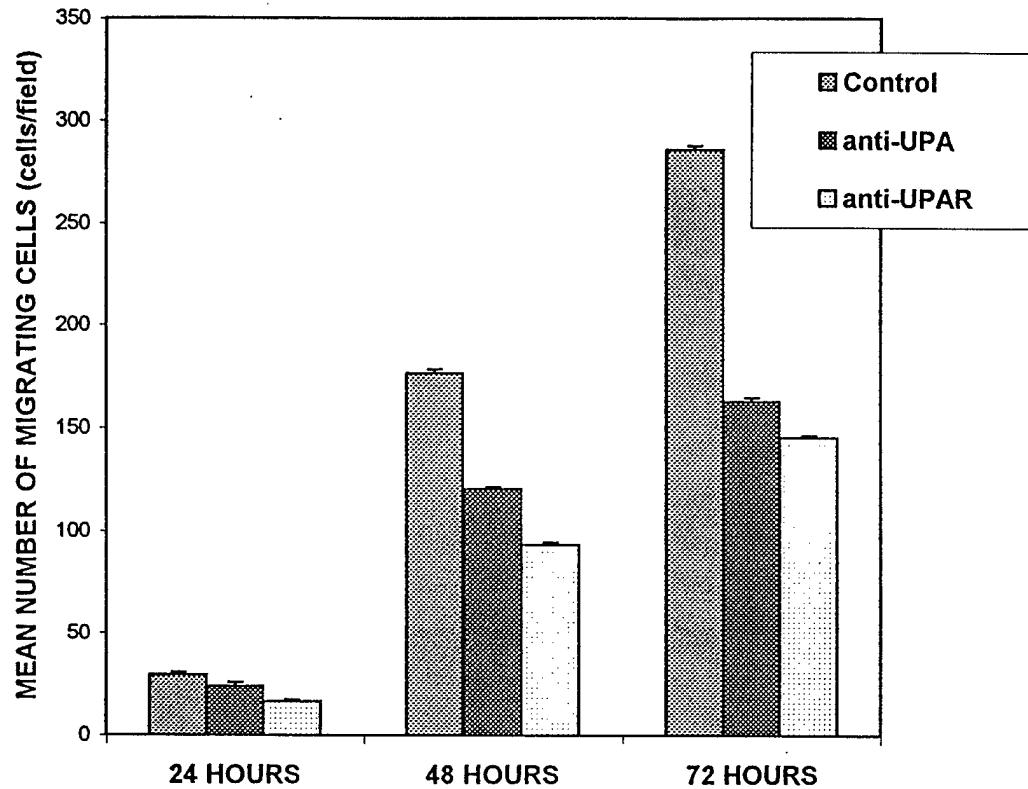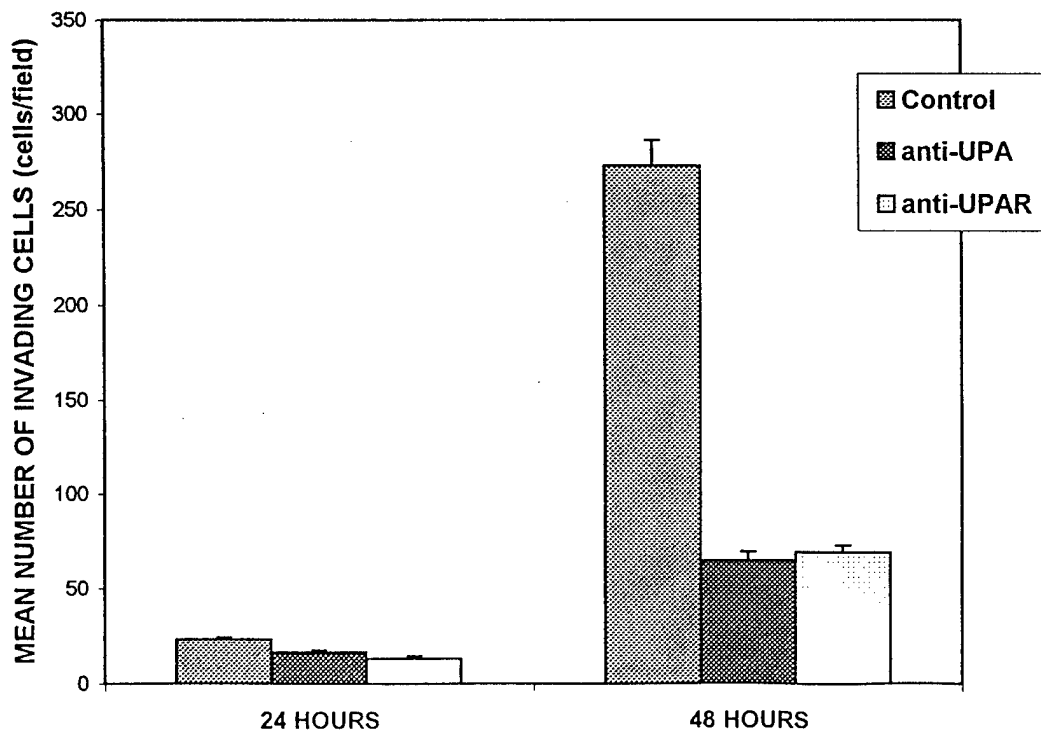
21

Figure 4. Migratory (A) and invasive (B) capacities of C3L5 cells at different time points, and under different experimental conditions. Both anti-uPA and anti-uPAR antibodies significantly inhibited migration of cells at 24, 48 and 72 hours, and invasion of cells at 24 and 48 hours.

22

(c)   Effects of tumor-derived NO on tumor-induced angiogenesis.

(i)   C3L5 tumor model
We have devised a novel tumor angiogenesis assay employing implants of **growth factor-reduced** matrigel, inclusive of tumor cells in the matrigel suspension (part of the data abstracted in Appendix 2; detailed in Appendix 4, ref. 72). Matrigel implants alone had no angiogenic effect, whereas inclusion of tumor cells caused significant angiogenesis. The time course, geography and levels of angiogenesis were objectively measurable after Masson's trichrome staining and CD31 (endothelial cell marker) immunostaining of sections. Animals received L-NAME (NOS inhibitor) or D-NAME (inactive enantiomer of L-NAME used as controls). D-NAME was found to have no effect on basal angiogenesis. Both drugs were given continuously via osmotic mini-pumps, to evaluate the effects of NOS inhibition on tumor-induced angiogenesis measured at 14 days after implantation of matrigel suspended tumor cells. Histological evaluation of implants revealed that neovascularization initially started in the periphery of the implants with concurrent development of stroma. Developing tumors were then fed by secondary vessels growing from the stromal region. At later time points (e.g. 14 days), necrosis was evident in the deeper areas of tumors. It was found that L-NAME treatment caused a dramatic inhibition of angio-genesis both in the stroma as well as tumor tissue as compared to D-NAME, and also a relative reduction in viable tissue mass (stroma and tumor) and an increase in necrosis. Detailed results are presented in Appendix 4. These data show that NO is a key mediator of C3L5 tumor-induced angiogenesis, and that growth inhibitory effects of L-NAME on the primary tumor are partly mediated by reduced tumor-angiogenesis.

(ii)   A comparison of C3L5 (high eNOS expressor) and C10 (low eNOS expressor) tumor models
Materials, methods and results are detailed in Appendix 1 (ref. 71). In brief, in the matrigel implant assay, C3L5 cells were more angiogenic than C10 cells, as expected from their differences in eNOS expression (Figure 7, Appendix 1). Unexpectedly, however, L-NAME treatment did not significantly affect C10 tumor induced angiogenesis indicating that either a certain threshold of NO level was required for angiogenesis stimulation, or that a differential upregulation of other angiogenic factor(s) may have compensated for the L-NAME inhibition of angiogenesis in C10 cells.

We have discovered that C3L5 cells express VEGF, a potent angiogenic factor. VEGF-induced angiogenesis (endothelial cell proliferation, migration and tube formation) has recently been shown to be dependent on NO production in endothelial cells following eNOS activation (evidently due to increase in intracellular calcium), leading to stimulation cGMP and then activation of MAPK pathway (65,66). Thus, it is likely that VEGF expression by C3L5 cells is an additional tool for NO-mediated angiogenesis because of eNOS activation in tumor cells as well as endothelial cells. We shall test whether a neutralization of VEGF activity (with a VEGF neutralizing antibody) in C3L5 cells *in vitro* causes a reduction in Ca++ dependent NO production by C3L5 cells in culture medium. These will be expected if VEGF activates eNOS in C3L5 cells. We shall also test whether this treatment causes a reduction in intracellular Ca++ level in C3L5 cells.

Task 3   **Role of NO in IL-2 induced capillary leakage and mechanisms by which this NO- production compromises antitumor effects of IL-2 therapy.**

This task, as initially proposed, was completed earlier and published (52-54). We showed that IL-2 therapy induced active iNOS in tissues contiguous with pleural effusion and the resulting NO overproduction caused structural damage to the lungs and its capillaries. These injuries were ameliorated with the NOS inhibitor L-NAME.

These results raised the following questions. Was the damage to the lungs and its capillaries due to a direct injury (structural damage and apoptosis) by NO, or injury by certain reaction product of NO? Recently, it has been reported that oxygen-free-radicals play a role in IL-2 therapy-induced capillary damage because it could be ameliorated with dimethylthiourea, a scavanger of oxygen-free-radicals (69). We hypothesise that formation of peroxynitrite, a potent endotheliotoxic molecule, due to a combination of NO with superoxide may be the strongest mediator of IL-2 induced capillary leakage.

Since cytotoxicity due to peroxynitrite is reported to be due to a nitration of important intracellular tyrosine kinases to form nitrotyrosine, nitrotyrosine is considered to provide a good marker for peroxynitrite-mediated cellular injury. We started testing these hypothesis by immunostaining tissues of IL-2-treated mice for nitrotyrosine with the expectation that this marker would appear strongly in tissues of IL-2-treated mice showing capillary leakage, and diminish in mice treated with IL-2 in combination with the NOS inhibitor L-NAME. In last year's report, we presented some preliminary data indicating that normal lungs staind for nitrotyrosine irrespective of IL-2 therapy, possibly because of high levels of basal NOS activity in the normal lungs. However, kidneys (in particular, medullary regions) provided some discrimination for nitrotyrosine as a marker for IL-2-induced capillary leakage.

Last year, we received a fresh batch of human recombinant IL-2 from Chiron Corporation and applied the following protocol to 8-10 week old C3H/HeJ mice (5-6 mice/group): (a) IL-2

injection alone, 50 x 10³ Cetus units i.p. every 8 hours x 10 injections; (b) IL-2 therapy as in (a) combined with continuous therapy with L-NAME given subcutaneously with minipummps for the whole duration (0.5 ml/hr.; 25 mg/200 µl 0.9% NaCl); (c) IL-2 therapy in combination with D-NAME (inactive enantiomer of L-NAME) as above; (d) Therapy with vehicles alone (control). Animals were sacrificed shortly after the injection protocol to measure (a) pleural effusion, (b) water content (wet/dry ratio) of the lungs, (c) water content (wet/dry ratio) of the kidneys as markers for capillary leakage. Frozen sections of kidneys were immunostained for nitrotyrosine (protocol presented in last years report). Sections immunostained with nitrotyrosine antibody preabsorbed with nitrotyrosine provided specificity controls. Capillary leakage data were analysed with one way analysis of variance.

Results revealed that (1) IL-2 alone or IL-2 + D-NAME caused significant pleural effusion and capillary leakage in the lungs as well as the kidneys. There was no difference between these two groups. (2) Addition of L-NAME therapy significantly reduced the IL-2 induced pleural effusion and capillary leakage in the lungs and the kidneys, however, they were not completely ameliorated.

Immunostaining protocol utilizing 1:500 dilution of the primary antibody (or antibody pre-absorbed with nitrotyrosine) and 1:600 dilution of the secondary antibody followed by DAB chromogen treatment provided clean results which were consistent with our hypothesis. The results are summarized as follows and presented in Fig. 5. (a) Strong immunostaining for nitrotyrosine was detected in IL-2 or IL-2 + D-NAME treated mice in their kidneys. The staining was more prominent in the medulla than in the cortex. The stainings were abolished by pre-absorption of the primary antibody with nitrotyrosine, indicative of staining specificity. No difference was found between IL-2 and IL-2+D-NAME treated groups. (b) L-NAME therapy, nearly completely abrogated this immunostaining indicating that abrogation of capillary leakage went hand-in-hand with nitrotyrosine staining. While these correlative data do not establish a cause and effect relationship between the production of peroxynitrite (as indicated by nitrotyrosine staining) and IL-2 induced capillary leakage, they are highly suggestive. In future experiments, we wish to test whether therapy with peroxynitrite scavangers, e.g. Lazaroids (73), can block or reduce IL-2 induced capillary leakage as well as nitrotryosine immunostaining in the tissues.

Fig. 5 Immunostaining for nitrotyrosine (brown color) in the kidneys (cortical regions on the left and medullary region on the right) of mice receiving different treatments.

A, B: IL-2 alone.   C,D: Specificity controls of the same kidneys in A,B. Sections were treated with primary antibody preabsorbed with nitrotyrosine. E,F: IL-2 + D- NAME treated.   G,H: IL-2 + L-NAME treated.

Note that specific staining is noted in the cortex and the medulla but more strongly in the medulla of IL-2 treated or IL-2 + D-NAME treated mice. Preabsorption of the primary ab with the antigen completely abrogated the staining (C,D). L-NAME therapy nearly completely eliminated the presence of immunreactive nitrotyrosine which is a marker for peroxynitrite (G,H).
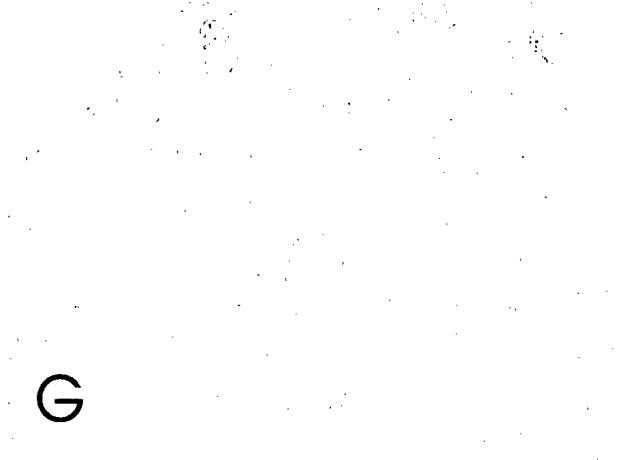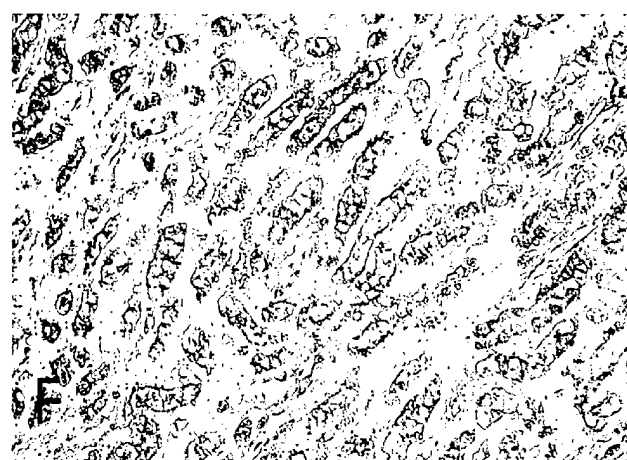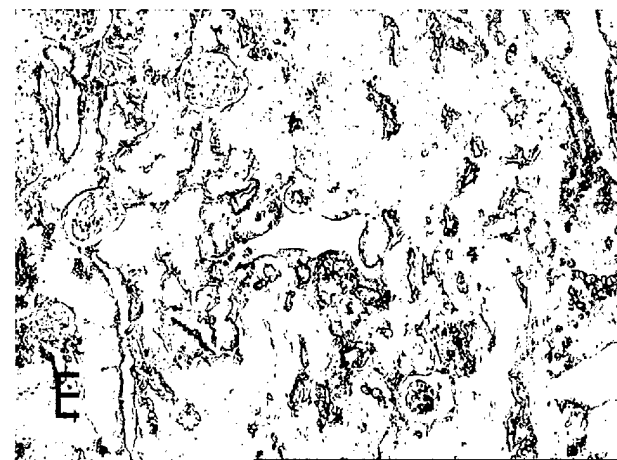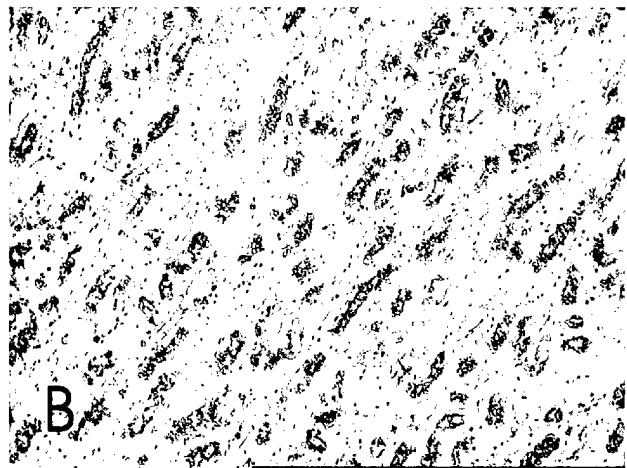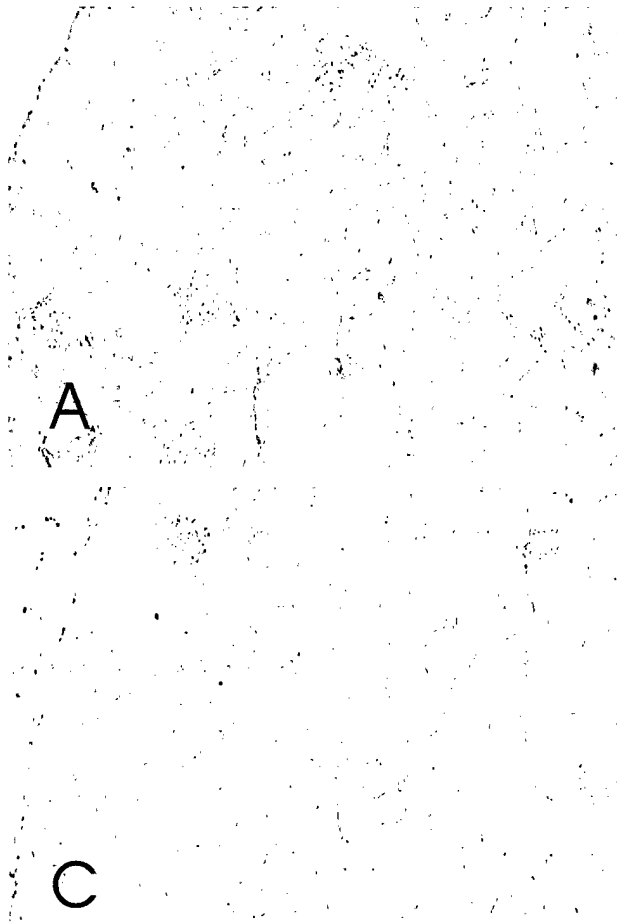
A   B

C   D

E   F

G   H

Fig. 5

7. KEY RESEARCH ACCOMPLISHMENTS

Following were the achievements during the project period.

I.   We have expanded and validated our earlier data showing that:

(a) Spontaneous primary C3H/HeJ tumors show a heterogeneity in eNOS-bearing tumor cells; this expression was unrelated to tumor growth rate. However, the incidence of eNOS bearing cells was higher in undifferentiated than in differentiated zones of primary tumors, and metastatic foci resulting from each primary tumor was mostly eNOS positive.

(b) All C3L5 tumor cells (a highly metastatic clone of a spontaneous tumor) expressed eNOS *in vitro*; a minority expressed iNOS under inductive conditions (IFN-γ + LPS). When transplanted *in vivo*, most tumor cells at the primary site and a high proportion at the metastatic site expressed eNOS. C10 tumor cells originally shown to be a poorly metastatic clone of the same spontaneous tumor were shown to have a lower *in vivo* growth rate of primary tumors and a lower rate of spontaneous lung metastasis than C3L5 cells. These differences were positively correlated with their differences in eNOS protein expression *in vitro* as well as *in vivo* in primary tumors but not in metastatic foci which were equally positive for eNOS.

These findings substantiated further our hypothesis that eNOS expression provided an advantage for metastasis.

II.   We abandoned our futile attempts to knockout eNOS gene in C3L5 cells because we found that they have increased (3.6) number of gene copies. Subsequently we adopted the alternative approach of downregulating eNOS by antisense RNA transfection and isolated eNOS downregulated clones. However, all the clones proved to be unstable and thus could not be applied to functional assays *in vitro* or *in vito*. Applicatyion of ethoxy-methoxy derivatives of antisense oligos for short-term biological assays, also proved to be non-productive and thus abandoned. However, the same objectives were achieved with inhibitors of NOS activity and use of a naturally occurring low eNOS-expressing clone.

III.   We have shown that endogenous NO promoted migratory function of C3L5 and C10 tumor cells.

This is the first definitive evidence of NO-mediated stimulation of tumor cell migration, which is an essential component of invasion and metastasis.

28

We have partly identified the pathway for signal transduction for NO-mediated stimulation of tumor cell migration. We have shown that it involves stimulation of the MAP kinase pathway. Further experiments are intended for a further characterization of the pathway.

IV. **(a)** We have shown that endogenous NO promoted invasiveness of C3L5 and C10 tumor cells. The invasive function of the highly metastatic C3L5 cell line was investigated in detail. Their invasiveness was further stimulated by additional NO production when treated with IFN-γ and LPS because of the induction of iNOS in tumor cells.

This is the first definitive evidence of NO-mediated promotion of tumor cell invasiveness.

(b) We have identified some of the mechanisms responsible for NO-mediated stimulation of invasiveness. Endogenous and IFN-γ + LPS-induced NO down-regulated the expression of TIMP-2 and TIMP-3 genes. Induced NO further up-regulated the expression of MMP-2 gene. Thus, NO-mediated promotion of invasiveness resulted from an alteration in the balance between MMP-2 and TIMP's.

This is the first demonstration of mechanisms for NO-mediated promotion of tumor cell invasiveness. We are currently testing the role of NO on the uPA-uPAR system.

V. By devising a novel tumor-induced angiogenesis assay *in vivo*, we have obtained substantial data showing that endogenous NO promotes C3L5 tumor-induced angiogenesis, which was higher than the level of angiogenesis induced by C10 cells expressing a lower level of eNOS.

This novel and objective angiogenesis assay is highly suitable for testing anti-angiogenic agents against human tumor cells grown in nude mice.

We are currently testing the role of endogenous VEGF in eNOS activation in C3L5 cells.

VI We had shown that active, inducible NOS expression, leading to high NO production *in vivo* is responsible for IL-2 therapy-induced capillary leakage in healthy mice. We identified the iNOS-expressing cells in the vicinity of the leakage (pulmonary edema, pleural effusion) and have shown that NOS inhibitors can restrain the IL-2 therapy-induced structural damage to the lungs. We have provided further evidence in support of our hypothesis that NO-mediated capillary damage following IL-2 therapy is

owing to the formation of peroxynitrite, as revealed by immunostaining for nitrotyrosine in the kidney which was abrogated with L-NAME therapy.

In summary, our progress matched with our expectations in most areas. In one area we had no progress because of unexpected difficulties arising from the genetic constitution of our tumor cells. In other areas we had an accelerated progress, leading to some newer findings and proposals for experimentation within the overall objectives of the project.

8.   REPORTABLE OUTCOMES

A.   Journal Publications (published, in press or submitted)

A1.   Orucevic A, Hearn S, Lala PK: The role of active inducible nitric oxide synthase expression in the pathogenesis of capillary leak syndrome resulting from interleukin-2 therapy in mice. Lab Investigation. 76, 53-75, 1997.

A2.   Lala PK, Orucevic A: Role of nitric oxide in tumor progression: Lessons from experimental tumors. Cancer and Metastasis Reviews. 17: 91-106, 1998.

A3.   Orucevic A, Lala PK: Role of nitric oxide in interleukin-2 therapy induced capillary leak syndrome. Cancer and Metastasis Reviews. 17: 127-142, 1998.

A4.   Orucevic A, Bechberger J, Green AM, Shapairo RA, Billiar TR and Lala PK: Nitric oxide production by murine mammary adenocarcinoma cells promotes tumor cell invasiveness. Int J Cancer 81: 889-896, 1999.

A5.   Jadeski LC, Lala PK: NOS inhibition by N^G-Nitro-L-Arginine Methyl Ester (L-NAME) inhibits tumor-induced angiogenesis in mammary tumors. Amer J Path 155: 1381-1390, 1999.

A6.   Jadeski LC, Hum KO, Chakraborty C, Lala PK: Nitric oxide promotes murine mammary tumor growth and metastasis by stimulating tumor cell migration, invasiveness and angiogenesis. Int J Cancer 86: 30-39, 2000.

B. **Conference presentations (Abstracts/extended abstracts)**

B1. Lala PK, Hum K, Jadeski I, Orucevic A: Nitric Oxide (NO) mediated mammary tumor progression: Role of NO in tumor cell invasiveness. Proceedings of the Department of Defense Breast Cancer Program Meeting, Era of Hope, Vol. 2, 709-710, 1997.

B2. Hum K, Lala PK: Nitric oxide synthase expression promotes murine mammary tumor progression and metastasis. Proc Amer Assoc Cancer Res 39: # 1450, 212, 1998.

B3. Jadeski L, Lala PK: Role of nitric oxide in mammary tumor angiogenesis. Proc Amer Cancer Res 39, # 2574, 378, 1998.

B4. Hum K, Jadeski L, Lala PK: Nitric oxide synthases and murine mammary tumor progression. Proc Amer Assoc Cancer Res 40: # 3715, 563, 1999.

B5. Lala PK, Hum K, Jadeski L: Nitric oxide (NO) synthase expression promotes growth and metastasis of murine breast cancer cells due to invasion and migration stimulation by NO. Abstract: Reasons for Hope Conference in Breast Cancer Research, sponsored by the Canadian Breast Cancer Research Initiative. p 185, 1999.

B6. Jadeski L, Lala PK: The role of nitric oxide in murine mammary tumor induced angiogenesis. Abstract: Reasons for Hope Conference in Breast Cancer Research, sponsored by the Canadian Breast Cancer Research Initiative. p 182, 1999.

B7. Lala PK, Jadeski L, Hum K, Rozic J and Chakraborty C: Cyclooxygenase and nitric oxide synthase inhibitors inhibit murine mammary tumor growth and metastasis by blocking tumor cell migration, invasion and angiogenesis. Proc. AACR-NCI-EORTC International Conf. Abstract # 406, p 83, 1999.

B8. Jadeski L, Hum KO, Gleeson LM, Chakraborty C and Lala PK: Nitric oxide mediated promotion of murine mammary tumor cell progression: Role in tumor cell migration. Proc. Amer Assoc Cancer Res 41, Abstract # 1024, p 160, 2000.

9. CONCLUSIONS

Results of this project so far reveals that:

(a) Tumor-derived nitric oxide promotes murine mammary tumor progression by multiple mechanisms including stimulation of tumor cell migration, invasiveness and tumor-induced angiogenesis.

Since NOS activity correlates with the progression of human breast cancer, the above information is highly relevant for designing breast cancer therapy in the human. NOS inhibitors should have a valuable role by blocking multiple steps in breast cancer progression and metastasis.

(b) Induction of iNOS leading to increased NO production and peroxynitrite formation in various tissue is responsible for IL-2 induced "capillary leak syndrome" which can be mitigated with NOS inhibitors. NOS inhibitors also improved the anti-cancer effects of IL-2 therapy.

High-dose IL-2 therapy, in spite of proven benefit in certain human cancers, has lately been abandoned because of this side effect. This therapy can now be reviewed in combination with selective iNOS inhibitors.

REFERENCES

1. Palmer RMJ, Ferrige AS, Moncada S: Nitric oxide release accounts for the biological activity of endothelium-derived relaxing factor. Nature 327: 524-526, 1987.

2. Furchgott RF, Zawadzki JV: The obligatory role of endothelial cells in the relaxation of arterial smooth muscle by acetylcholine. Nature 288: 377-386, 1980.

3. Furchgot RF: Studies on endothelium-dependent vasodilation and the endothelium-derived relaxing factor. Acta Physiol Scand 139: 257-270, 1990.

4. Moncada S, Palmer RMJ, Higgs EA: Byosynthesis of nitric oxide from L-arginine: a pathway for the regulation of cell function and communication. Biochem Pharmacol 38: 1709-1715, 1989.

5. Marletta MA: Nitric oxide: Biosynthesis and biological significance. Trends Biochem Sci. 14: 488-492, 1989.

6. Snyder SH, Bredt DS: Biological roles of nitric oxide. Sci Am 266: 68-71, 1992.

7. Nathan CF, Hibbs JB, Jr.: Role of nitric oxide synthesis in macrophage antimicrobial activity. Curr Opin Immunol 3: 65-70, 1991.

8. Stuehr DJ, Nathan CF: Nitric oxide: A macrophage product responsible for cytostasis and respiratory inhibition in tumor target cells. J Exp Med 469: 1543-1555, 1989.

9. Tamair S, Tannenbaum SR: The role of nitric oxide (NO) in the carcinogenetic process. BBA 1288: f31-f36, 1996.

10. Moncada S, Higgs A: The L-arginine-nitric oxide pathway. N Eng J Med 329: 2002-2012, 1993.

11. Knowles RGL, Moncada S: Nitric oxide synthases in mammals. Biochem J 298: 249-258, 1994.

12. Kobil L, Schmidt HHHW: Immunohistochemistry of nitric oxide synthase and nitric oxide related products. In: Feelisch M, Stamler J (eds) Methods in Nitric Oxide. John Wiley & Sons, New York, pp. 229-236, 1996.

13. Morris SM, Billiar TR: New insights into the regulation of inducible nitric oxide synthesis. Am J Physiol 266: E829-E839, 1994.

14. Billiar TR: Nitric oxide: Novel biology with clinical relevance. Ann Surg 221: 339-349, 1995.

15. Michel T, Xie QW, Nathan C: Molecular biological analysis of nitric oxide synthases. In: Feelisch M, Stamler J (eds) Methods in Nitric Oxide Research. John Wiley & Sons, New York, pp. 161-175, 1996.

16. Gnanapandithen K, Chen Z, Kau CL, Gorenzynski RM, Marsden PA: Cloning and characterization of murine endothelial constitutive nitric oxide synthase. Biochimica et Biophysica Acta 1308: 103-106, 1996.

17. Huang PL, Huang Z, Mashimo H, Bloch KD, Moskowitz MA, Bevan JA, Fishman MC: Hypertension in mice lacking the gene for endothelial nitric oxide synthase. Nature 377: 239-242, 1995.

18. MacMicking JD, Nathan C, Horn G, Chartrain N, Fletcher DS, Trumbauer M, Stevens K, Xie Q-W, Sokol K, Hutchinson N, Chen H, Mudgett JS: Altered responses to bacterial infection and endotoxic shock in mice lacking inducible nitric oxide synthase. Cell 81: 641-650, 1995.

19. Huang PK, Dawson TM, Bredt DS, Synder SH, Fishman MC: Targeted disruption of the neuronal nitric oxide synthase gene. Cell 175: 1273-1286, 1993.

20. Nelson RJ, Demas GE, Huang PL, Fishman MC, Dawson VL, Dawson TM, Snyder SH: Behavioral abnormalities in male mice lacking neuronal nitric oxide synthase. Nature 378: 383-386, 1995.

21. Moncada S, Palmer RMJ, Higgs EA: Nitric Oxide: Physiology, pathophysiology and pharmacology. Pharmacol Rev 43: 109-142, 1991.

22. Bredt DS, Snyder SH: Nitric oxide mediates glutamate-linked enhancement of cGMP levels in the cerebellum. Proc Natl Acad Sci USA 86: 9030-9033, 1989.

23. Stuehr DJ, Nathan CF: Nitric oxide: A macrophage product responsible for cytostasis and respiratory inhibition in tumor target cells. J Exp Med 169: 1543-1555, 1989.

24. Beckman JS, Koppenol WH: Nitric oxide, superoxide and peroxynitrite: The good, the bad and the ugly. Am J. Physiol 271: C1424-C1437, 1996.

25. Lala PK, Orucevic A: Role of nitric oxide in tumor progression: Lessons from experimental tumors. Cancer & Metastasis Reviews. 17: 91-106, 1998.

26. Miles D, Thomsen L, Balkwill F, Thavasu P, Moncada S; Association between biosynthesis of nitric oxide and changes in immunological and vascular parameters in patients treated with interleukin-2. Eur J Clin Invest 24: 287-290, 1994.

27. Thomsen LL, Lawton FG, Knowles RG, Beesley JE, Riveros-Moreno V, Moncada S: Nitric oxide synthase activity in human gynecological cancer. Cancer Res 54: 1352-1354, 1994.

28. Cobbs CS, Brenman JE, Aldape KD, Bredt DS, Israel lMA: Expression of nitric oxide synthase in human central nervous system tumors. Cancer Res 55: 727-730, 1995.

29. Thomsen LL, Miles DW, Happerfield L, Bobrow LG, Knowles RG, Moncada S: Nitric oxide synthase activity in human breast cancer. Br J Cancer 72: 41-44, 1995.

30. Thomsen LL, Miles DW: Role of nitric oxide in tumor progression: Lessons from human tumors. Cancer and Metastasis Reviews 17: 107-118, 1998.

31. Gallo O, Masini E, Morbidelli L, Franchi A, Fini-Storchi I, Vergari WA, Ziche M: Role of nitric oxide in angiogenesis and tumor progression in head and neck cancer. J Nat Cancer Inst 90: 586-596, 1998.

32. Klotz T, Bloch W, Volberg C, Engelmann W, Addicks K: Selective expression of inducible nitric oxide synthase in human prostate carcinoma. Cancer. 82: 1897-1903, 1998.

33. Fujimoto H, Ando Y, Yamashita T, Terazaki H, Tanaka Y, Sasaki J, Matsumoto M, Suga M, Ando M: Nitric oxide synthase activity in human lung cancer. Japanese J of Cancer Res 88: 1190-1198, 1997.

34. Vakkala M, Kahlos K, Lakari E, Paakko P, Kinnula V, Soini Y: Inducible nitric oxide synthase expression, apoptosis and angiogenesis in *in situ* and invasive breast carcinomas. Clinical Cancer Research 6: 2408-2415, 2000.

35. Moochhala S, Chhatwal VJS, Chan STF, Ngoi SS, Chia YW, Rauff A: Nitric oxide synthase activity and expression in human colorectal cancer. Carcinogenesis 17: 1171-1174, 1996.

36. Ambs S, Merriam WG, Bennett WP, Felly-Bosco E, Ogunfusika MO, Oser SM, Klein S, Shields PG, Billiar TR, Harris, CC. Frequent nitric oxide synthase-2 expression in human colon adenomas: Implications for tumor angiogenesis and colon cancer progression. Cancer Res 58: 334-341, 1998.

35

37. Ambs S, Bennett WP, Merrium WG, Ogunfusika MO, Oser SM, Harrington AM, Shields PG, Felley-Bosco E, Houssain P, Harris CC: Relationship between p53 mutations and inducible nitric oxide synthase expression in human colorectal cancer. J Nat Cancer Inst 91: 86-88, 1999.

38. Buttery LDK, Springall DR, Andrade SP, Riveros-Moreno V, Hart I, Piper PJ, Polak JM: Induction of nitric oxide synthase in the neo-vasculature of experimental tumours in mice. J Path 171: 311-319, 1993.

39. Kennovin GD, Hirst DG, Stratford MRL, Flitney FW: Inducible nitric oxide synthase is expressed in tumour-associated vasculature: Inhibition retards tumor growth *in vivo*. In: Moncada S, Feelisch M, Busse R, Higgs EA (eds) Biology of Nitric Oxide. Part 4: Enzymology, Biochemistry and Immunology. Partland Press, London, pp. 473-479, 1994.

40. Orucevic A, Lala PK: Effects of N^G-Methyl-L-arginine, an inhibitor of nitric oxide synthesis on IL-2 induced capillary leakage and anti-tumor responses in healthy and tumor-bearing mice. Cancer Immunol Immunother 42: 38-46, 1996.

41. Orucevic A, Lala PK: N^G-Nitro-L-arginine methyl ester, an inhibitor of nitric oxide synthesis, ameliorates interleukin-2 induced capillary leakage and reduces tumor growth in adenocarcinoma bearing mice. Br J Cancer 72: 189-197, 1996.

42. Jenkins DC, Charles IG, Thomsen LL, Moss DW, Holmes LS, Baylis SA, Rhodes P, Westmore K, Emson PC, Moncada S: Roles of nitric oxide in tumor growth. Proc Natl Acad Sci USA 82: 4392-4396, 1995.

43. Dong Z, Staroselski AH, Qi X, Hie K, Fidler IJ: Inverse correlation between expression of inducible nitric oxide synthase activity and production of metastasis in K-1735 murine melanoma cells. Cancer Res 54: 789-793, 1994.

44. Xie K, Huang S, Dong Z, Juang S-H, Gutman M, Zie Q-W, Nathan C, Fidler IJ: Transfection with the inducible nitric oxide synthase gene suppresses tumorigenicity and abrogated metastasis by K-1753 murine melanoma cells. J Exp Med 181: 1333-1343, 1995.

45. Juang S, Xie K, Xu L, Shi Q, Wang Y, Yoneda G, Fidler I: Suppression of tumorigenicity and metastasis of human renal carcinoma cells by infection with retroviral vectors harboring the murine nitric oxide synthase gene. Human Gene Therapy 9: 845-854, 1998.

46. Forrester K, Ambs S, Lupoid SE, Kapust RB, Spillare EA, Weinberg WC, Felly- Bosco E, Wang XW, Geller DA, Tzeng E, Billiar TR, Harris C: Nitric oxide induced p53 accumulation of regulation of inducible nitric oxide synthase expression by wild type p53. Proc Natl Acad Sci USA 93: 2442-2447, 1996.

47. Ambs S, Hussain SP, Harris CC: Interactive effects of nitric oxide and the p53 tumor suppressor gene in carcinogenesis and tumor progression. FASEB J 11: 443-448, 1997.

48. Hollstein M, Sidranski D, Vogelstein B, Harris CC: P53 mutations in human cancer. Science 253: 49-53, 1991.

49. Wang Y, Holland JF, Bleiweiss IJ, Melena S, Liu X, Pellisson I, Cantarella A, Stellract K, Mari S, Pogo BGT: Detection of mammary tumor virus ENV gene-like sequences in human breast cancer. Cancer Res 55: 5173-5179, 1995.

50. Lala PK, Al-Mutter N, Orucevic A: Effects of chronic indomethacin therapy on the development and progression of spontaneous mammary tumors in C3H/HeJ mice. Int J Cancer 73: 371-380, 1997.

51. Orucevic A, Lala PK: N^G-Nitro-L-arginine methyl ester, an inhibitor of nitric oxide synthesis, ameliorates interluekin-2 induced capillary leak syndrome in healthy mice. J. Immunother. 18: 210-220, 1996.

52. Orucevic A, Hearn S, Lala PK: The role of active inducible nitric oxide synthase expression in the pathologenesis of capillary leak syndrome resulting from interleukin-2 therapy in mice. Lab Investigation 76: 53-65, 1997.

53. Orucevic A, Lala PK: Role of nitric oxide in interleukin-2 therapy induced capillary leak syndrome. Cancer & Metastatic Reviews 17: 127-142, 1998.

54. Orucevic A, Lala PK: Effects of N^G-Nitro-L-arginine methyl ester, an inhibitor of nitric oxide synthesis on IL-2 induced LAK cell generation *in vivo* and *in vitro* in healthy and tumor-bearing mice. Cell Immunol 169: 125-132, 1996.

55. Scherczinger CA, Yates AA, Knecht DA: Varibles affecting antisense RNA inhibition of gene expression. Ann NY Acad Sci 660: 45-56, 1992.

56. Kerr SM, Stark GR, Kerr IM: Excess antisense RNA from infectious recombinant SV40 fails to inhibit expression of a transfected, interferon-inducible gene. Eur J Biochem 175: 65-73, 1988.

57. Salmons B, Groner B, Friis R, Muellener D, Jaggi R.: Expression of anti-sense mRNA in H-ras transfected NIH/3T3 cells does not suppress the transformed phenotype. Gene 45: 215-220, 1986.

58. Dean NM, McKay R, Miraglia L, Geiger T, Muller M, Fabbro D, Bennett CF: Antisense oligonucleotides as inhibitors of signal transduction: development from research tools to therapeutic agents. Biochem Soc Trans 24: 623-629, 1996.

59. Dean NM, McKay RA, Holmlund J: Antisense oligonucleotides as inhibitors of genes that regulate AP-1: Pharmacology and clinical development. Antisense & Nucleic acid Drug Der. 8: 147-151, 1998.

60. Zuo Z, Dean NM, Honkanen RE: Serine/threonine protein phosphatase type 5 acts upstream of p53 to regulate the induction of p212$^{WAF1/Cip1}$ and mediate growth arrest. J Biol Chem 20: 12250-12258, 1998.

61. McKay RA, Miraglia LJ, Cummins LL, Owens SR, Sasmor H, Dean NM: Characterization of a potent and specific class of antisense oligonucleotide inhibitor of human protein kinase C-α expression. J Biol Chem 274: 1715-1722, 1999.

62. Andrade SP, Hart IR, Piper PJ: Inhibition of nitric oxide synthase selectively reduces flow in tumour-associated neovasculature. Br J Pharmacol 107: 1092-1095, 1992.

63. Meyer RE, Shan S, DeAngelo J, Dodge RK, Bonavenuta J, Ong ET, Dewhirst MW: Nitric oxide synthase inhibition irreversibly decreases perfusion in the R3230AC rat mammary adenocarcinoma. Br J Cancer 71: 1169-1174, 1995.

64. Fukumura D, Yuan F, Endo M, Jain RK: Role of nitric oxide in tumor microcirculation; Blood flow, vascular permeability and leukocyte-endothelial interactions. Am J Pathol 150: 713-725, 1997.

65. Ziche M, Morbidelli L, Choudhuri R, Zhang HT, Donnini S, Granger HJ: Nitric oxide synthase lies downstream from vascular endothelial growth factor-induced but not basic fibroblast growth factor-induced angiogenesis. J Clin Invest 99: 2625-2634, 1997.

66. Parenti A, Morbidelli L, Cui ZL, Douglast JG, Hood JD, Granger HJ, Ledda F, Ziche M: Nitric oxide is an upstream signal of vascular endothelial growth factor-induced extracellular signal-regulated kinase 1/2 activation in post capillary endothelium. J Biol Chem 273: 4220-4226, 1998.

67. VanUfflelen BE, deKoster BM, VanSteveniinck J, Elferink JGR: Carbon monoxide enhances human neutrophil migration in a cyclic GMP-dependent way. Biochem Biophys Res Com 226: 21-26, 1996.

68. Elferink JG, deKoster BM: The involvement of protein kinase G in stimulation of neutrophil migration by endothelins. Europ J Pharmacol 350: 285-291, 1998.

69. Gutman M, Laufer R, Eisenthal A, Goldman G, Ravid A, Inbar M, Klausner JM: Increased microvascular permeability induced by prolonged interleukin-2 administration is attenuated by the oxygen-free-radical scavenger dimethylthiourea. Cancer Immunol Immunother 43: 240-244, 1996.

70. Orucevic A, Bechberger J, Green AM, Shapiro RA, Billiar TR, Lala PK: Nitric oxide production by mammary carcinoma cells promotes tumor cell invasiveness. Int J Cancer 81: 889-896, 1999.

71. Jadeski LC, Hum KD, Chakraborty C, Lala PK: Nitric oxide promotes murine mammary tumor growth and metastasis by stimulating tumor cell migration, invasiveness and angiogenesis. Int J Cancer 86: 30-39, 2000.

72. Jadeski LC, Lala PK: Nitric oxide synthase inhibition by N^G-Nitro-L-Arginine methyl ester inhibits tumor-induced angiogenesis in mammary tumors. Amer J Pathol 155: 1381-1390, 1999.

73. Althaus JS, Fici GJ, vonVoightlander PF: The pharmacology of peroxynitrite-dependent nitric oxide blockade. In: Rubanyi GM (ed) Pathophysiology and Clinical Application of Nitric Oxide. Harwood Academic Publishers. pp. 523-528, 1999.

APPENDICES

1. Jadeski LC, Hum KO, Chakraborty C and Lala PK: Nitric oxide promotes murine mammary tumor growth and metastasis by stimulating tumor cell migration, invasiveness and angiogenesis. Int J Cancer 86: 30-339, 2000.

2. Lala PK, Jadeski L, Hum K, Rozic J and Chakraborty C: Cyclooxygenase and nitric oxide synthase inhibitors inhibit murine mammary tumor growth and metastasis by blocking tumor cell migration, invasion and angiogenesis. Proc AACR-NCI-EORTC International Conf. Abstract ## 406, p 83, 1999.

3. Jadeski L, Hum KO, Gleeson LM, Chakraborty C and Lala PK: Nitric oxide mediated promotion of murine mammary tumor cell progression: Role in tumor cell migration. Proc. Amer Assoc Cancer Res. 41: Abstract # 1024, p 160, 2000.

4. Jadeski LC and Lala PK: NOS inhibition by N^G-Nitro-L-Arginine Methyl Ester (L-NAME) inhibits tumor-induced angiogenesis in mammary tumors. Amer J Path. 155: 1381-1390, 1999.

NITRIC OXIDE PROMOTES MURINE MAMMARY TUMOUR GROWTH AND METASTASIS BY STIMULATING TUMOUR CELL MIGRATION, INVASIVENESS AND ANGIOGENESIS

Lorraine C. Jadeski, Kathleen O. Hum, Chandan Chakraborty and Peeyush K. Lala*

Department of Anatomy and Cell Biology, The University of Western Ontario, London, Ontario, Canada

The contributory role of nitric oxide (NO) on tumour growth and metastasis was evaluated in a murine mammary tumour model. NO synthase (NOS) protein expression levels were examined in spontaneously arising C3H/HeJ mammary adenocarcinomas and respective lung metastases. In addition, 2 clonal derivatives of a single spontaneous tumour differing in metastatic phenotype (C3L5 and C10; highly and weakly metastatic, respectively) were utilised to investigate *(i)* the relationship between NOS expression levels and the biological behaviour of tumour cells (e.g., *in vitro* migratory and invasive capacities, *in vivo* tumour growth rate and metastatic and angiogenic capacities) and *(ii)* whether tumour-derived NO stimulated the invasive, migratory and angiogenic capacities of tumour cells. A heterogeneous pattern of endothelial NOS (eNOS) expression was observed in tumour cells in spontaneous primary tumours, and eNOS expression was higher in undifferentiated relative to differentiated tumour zones. However, tumour cells in lung metastatic sites were always strongly eNOS-positive, suggesting that eNOS expression facilitated metastasis. Findings using clonal derivatives supported this notion; s.c. primary tumour growth rate, efficiency of spontaneous metastasis and eNOS expression were higher for C3L5 relative to C10 cell lines. Nevertheless, lung metastases derived from both tumour cell lines were always strongly and homogeneously eNOS-positive. C3L5 cells were more invasive than C10 cells *in vitro*, but the migratory capacities of the cell lines did not differ. However, migration and invasiveness of both cell lines were inhibited with L-NAME and restored with excess L-arginine. Tumour-associated angiogenesis, measured in Matrigel implants inclusive of tumour cells, was higher for C3L5 relative to C10 cells, and C3L5-induced angiogenesis was reduced with chronic L-NAME treatment of host animals. These findings suggest that tumour-derived eNOS promoted tumour growth and metastasis by multiple mechanisms: stimulation of tumour cell migration, invasiveness and angiogenesis. *Int. J. Cancer 86:30–39, 2000.*
© 2000 Wiley-Liss, Inc.

Nitric oxide (NO), an inorganic free radical gas, is synthesised from the amino acid L-arginine by a group of enzymes, the nitric oxide synthases (NOS). Three isoforms of the enzyme have been identified: endothelial (e) and neuronal (n) isoforms are Ca^{2+}/calmodulin-dependent and constitutively expressed. The inducible isoform (iNOS) is Ca^{2+}/calmodulin-independent and induced in the presence of inflammatory cytokines or bacterial products. When constitutively expressed, NO produced at low levels is an important mediator of physiological functions such as vasodilation, inhibition of platelet aggregation and neurotransmission. Under inductive conditions, high levels of NO can mediate antibacterial and anti-tumour functions; however, sustained, chronically produced NO contributes to many pathological conditions, including inflammation and cancer (reviewed by Moncada and Higgs, 1993; Knowles and Moncada, 1994).

The role of NO in tumour biology has been extensively studied; overall, an overwhelming amount of evidence suggests a positive association between NO and tumour progression (Lala and Orucevic, 1998; Thomsen and Miles, 1998). Over-expression of NOS enzymes and/or NOS activity has been positively correlated with the degree of malignancy in the human reproductive tract (*i.e.,* ovarian, uterine) cancers (Thomsen *et al.,* 1994), CNS tumours (Cobbs *et al.,* 1995) and mammary tumours (Thomsen *et al.,* 1995; Dueñas-Gonzalez *et al.,* 1997). iNOS has been detected in stromal elements and eNOS in tumour vasculature in a majority of gastric carcinomas (Thomsen and Miles, 1998); relative to benign prostatic hyperplasia, iNOS expression was higher in prostatic carcinomas (Klotz *et al.,* 1998). Total NOS activity is increased in carcinomas of the larynx, oropharynx, oral cavity (Gallo *et al.,* 1998) and adenocarcinomas of the lung (Fujimoto *et al.,* 1997) relative to normal healthy control tissue.

Experimental tumour models have provided direct evidence for a promoting role of NO in tumour progression. Treatment with the NOS inhibitor N^G-nitro-L-arginine methyl ester (L-NAME) reduced NO production and tumour growth in a rat adenocarcinoma model (Kennovin *et al.,* 1994). Induction of iNOS with lipopolysaccharide (LPS) and interferon (IFN)-γ in EMT-6 murine mammary tumour cells stimulates tumour growth and metastasis *in vivo* (Edwards *et al.,* 1996). Furthermore, iNOS transduction in a human colon adenocarcinoma line results in enhanced tumour growth and vascularity when transplanted in nude mice (Jenkins *et al.,* 1995). We have studied the role of NO in tumour progression/metastasis using a murine mammary tumour model which includes spontaneously arising mammary adenocarcinomas and 2 clonal derivatives of a spontaneous tumour which differ in metastatic capacity. Preliminary studies of spontaneously arising mammary tumours in C3H/HeJ retired breeder female mice revealed that cells in primary tumours were distinctly heterogeneous in eNOS protein expression. However, a strong and homogeneous expression pattern was observed at metastatic lung sites, suggesting that eNOS expression provides a selective advantage to metastasis (Lala and Orucevic, 1998). Further evidence supported this notion. A highly metastatic cell line, C3L5, clonally derived from a spontaneously arising mammary tumour, strongly expressed eNOS protein *in vitro* and *in vivo* and iNOS protein upon stimulation with LPS and IFN-γ (Orucevic *et al.,* 1999). Treatment of C3L5 mammary tumour-transplanted animals with the NOS inhibitors N^G-methyl-L-arginine (L-NMMA) or L-NAME reduced both primary tumour growth and spontaneous lung metastases (Orucevic and Lala, 1996a,b; Lala and Orucevic, 1998). The present study used this murine mammary tumour model to further examine the contributory role of NO in tumour progression and metastasis and the underlying mechanisms. A large number of spontaneous mammary tumours and respective lung metastases were utilised to examine the relationship between levels of NOS protein expression at primary tumour sites and the degree of morphological differentiation of tumour cells and tumour growth rates and to compare the levels of NOS expression between primary and metastatic lesions. Clonally derived C3L5 (highly metastatic) and C10 (weakly metastatic) tumour cell lines were utilized to examine *(i)* levels of NOS protein expression *in vitro* and *in vivo* (at primary and metastatic tumour sites), *(ii)* whether the levels of NOS protein

expression and NO production by tumour cells were correlated with invasive or migratory abilities *in vitro* or to their biological behaviour *in vivo* (*i.e.,* tumour growth rate, capacities for metastases formation and angiogenesis) and *(iii)* whether NO production by tumour cells was causally related to invasion, migration and angiogenesis.

MATERIAL AND METHODS

Mice

Female C3H/HeJ mice were obtained from the Jackson Laboratory (Bar Harbor, ME); retired breeder mice (approx. 6 months old) were utilised in spontaneous mammary tumour experiments, and 6- to 8-week-old mice were used in experiments related to tumour transplantation and angiogenesis with C3L5 and C10 cells. Upon arrival, animals were randomised into treatment groups; experimental procedures began after a 1-week acclimatization period. Throughout the investigation, animals had free access to food (standard mouse chow) and water and were maintained on a 12 hr light/dark cycle. Animals were treated in accordance with guidelines set by the Canadian Council on Animal Care.

Spontaneous mammary tumour development

Fifty C3H/HeJ female retired breeder mice were monitored 2 times per week for spontaneous mammary tumour development (20 tumours studied) as previously reported (Lala *et al.,* 1997). After initial localisation of a primary tumour, tumour growth rate was monitored daily; minimum and maximum diameters were measured using digital calipers, and tumour volume was calculated using the equation tumour volume $= 0.52a^2b$, where a and b are the minimum and maximum tumour diameters, respectively (Baguley *et al.,* 1989). When tumours had grown for 8 to 12 weeks, mice were killed using an overdose of pentobarbital and primary tumours and lungs inclusive of metastatic foci were removed, processed for paraffin embedding and immunostained for eNOS and iNOS antigens.

Tumour cell lines

Two murine mammary adenocarcinoma cell lines were utilised: C3L5, a highly metastatic line, and C10, a weakly metastatic line. Both were originally derived from a spontaneous tumour that developed in a C3H/HeJ female retired breeder mouse. Cells from the primary tumour (T58) demonstrated moderate metastatic capacity in early *in vitro* passages (Brodt *et al.,* 1985). Two clones were then derived from T58 cells: the weakly metastatic C10 line currently used and C3, a highly metastatic line. Since the metastatic capacity of the C3 line declined after several years of repeated *in vitro* passages (Lala *et al.,* 1986), a highly metastatic C3L5 line was derived by 5 cycles of repeated *in vivo* selections for spontaneous lung micrometastases following s.c. transplantation of C3 cells into C3H/HeJ mice and retransplantation of dispersed lung micrometastases s.c. in syngeneic mice. This led to production of the highly metastatic cell line C3L5 (Lala and Parhar, 1993), which has since maintained its strong metastatic phenotype. C3L5 and C10 cells were grown from frozen stock and maintained in RPMI-1640 medium (GIBCO, Burlington, Canada) supplemented with 5% FCS (GIBCO) and 1% penicillin–streptomycin (Mediatech, Washington, DC) in a humidified incubator with 5% CO_2.

Tumour transplantation studies

C3L5 and C10 cells, grown in monolayer, were harvested by brief exposure to 0.05% trypsin–PBS–EDTA solution. C3L5 or C10 cells (5×10^5), suspended in 0.5 ml of RPMI, were injected s.c. in the mammary line in the left axillary region of 6- to 8-week-old C3H/HeJ female mice (n = 15 mice/group). Trypan blue exclusion staining ensured adequate tumour cell viability (*i.e.,* >95%). Tumour growth was monitored using digital calipers; 2 times per week, the minimum and maximum diameters were recorded and tumor volume was calculated as described for spontaneous tumours. Twenty-one days after tumour transplantation,

mice were killed using an overdose of pentobarbital and primary tumours removed, fixed in 4% paraformaldehyde and processed for paraffin embedding. Lungs were inflated *in situ* with Bouin's fixative, removed and assessed for lung surface colonies using a dissecting microscope (experimenter blind to experimental condition). Immunostaining of both primary tumours and the corresponding lung metastases for eNOS and iNOS protein was conducted as described below.

Immuno-cytochemical detection of NOS enzymes in cells propagated in vitro

C3L5 and C10 cells were grown in complete RPMI-1640 medium alone or in complete medium containing IFN-γ (1,000 U/ml; GIBCO BRL, Grand Island, NY) and LPS (100 ng/ml; Sigma, St. Louis, MO) for 24 hr on chamber slides (Nunc, Naperville, IL) in a humidified incubator (37°C, 5% CO_2). Cells were fixed in ice-cold methanol (–20°C, 5 min). Endogenous peroxidase activity was blocked with methanol containing 3% H_2O_2 (room temperature, 5 min), and cell membranes were permeabilized using 0.25% Triton X-100 in 0.2% BSA in PBS prior to application of blocking antibody: normal horse serum diluted in 0.2% BSA (1:10; 1 hr at room temperature in a humidified chamber). Cells were then incubated with primary antibody: mouse monoclonal antibody (MAb) anti-eNOS or mouse anti-macrophage iNOS MAb (1:80 diluted in 0.2% BSA overnight at 4°C or 1:50 diluted in 0.2% BSA overnight at 4°C; Transduction Laboratories, Lexington, KY) for eNOS and iNOS localisation, respectively. Secondary antibody, biotinylated horse anti-mouse (1:200 diluted in 0.2% BSA, 1 hr at room temperature), was then applied, followed by avidin–biotin complex (Vector, Burlingame, CA) (1 hr at room temperature) and DAB chromogen (Sigma). Negative controls were incubated with the equivalent concentration of mouse IgG (Dako, Horsholm, Denmark) in place of primary antibody. Immuno-cyto-chemical staining of human umbilical vein endothelial cells (HUVECs) for eNOS served as positive controls.

Immuno-histochemical detection of NOS enzymes in spontaneous and transplanted tumours

Paraformaldehyde-fixed, paraffin-embedded primary tumours and lungs inclusive of metastatic foci were sectioned at 7 μm thickness. Following deparaffinization and rehydration of sections, endogenous peroxidase activity was blocked using methanol containing 3% H_2O_2 prior to application of blocking serum and primary and secondary antibodies, as described above. Sections were lightly counterstained with Mayer's haemalum, and those sections used to quantify immunostaining intensities were incubated with metal-enhanced DAB (Pierce, Rockford, IL) and not counterstained.

Quantitative analysis of immuno-histochemical staining in tissue sections

The intensity of immuno-histochemical staining was quantified using a method similar to that of Lehr *et al.* (1997). Digitized images of non-counterstained primary tumour sections and lung metastases were obtained and imported into the image analysis software program Mocha (Jandel, San Rafael, CA); pixels of the black and white images were inverted and remapped (*i.e.,* black pixels converted to white and white converted to black); therefore, absolute white was measured as 0 and absolute black as 255 grey level units. The average intensity of immuno-histochemical staining in healthy (non-necrotic) tumour tissue was quantified and compared between experimental groups (*i.e.,* C3L5 and C10) and corresponding negative control sections.

In vitro *invasion and migration assays*

Both invasion and migration assays were conducted in transwells fitted with millipore membranes (6.5 mm filters, 8 μm pore size; Costar, Toronto, Canada). In the invasion assay, cells degraded and passed through a Matrigel barrier prior to migrating through membrane pores. Thus, in the invasion assay,

membranes were coated with 120 µl growth factor–reduced Matrigel (1:20 dilution in RPMI-1640 medium; Collaborative Research, Bedford, MA). For both assays, 2.5 × 10⁴ C3L5 or C10 cells/100 µl complete RPMI were plated in upper wells of transwell chambers containing either 200 µl complete RPMI, complete RPMI and L-NAME (0.01, 0.1 or 1 mM; Sigma) or complete RPMI, L-NAME and excess L-arginine (5 mM, Sigma) (total volume in upper chamber 200 µl). Bottom wells contained 800 µl complete RPMI. Chambers were gently shaken for 1 hr at room temperature, followed by 24, 48 or 72 hr incubation (37°C, 5% CO₂). After incubation, cells from the upper surface of millipore membranes were completely removed with gentle swabbing and remaining migrant cells were fixed and stained using the Diff-Quik Stain Set (Dada, Düdingen, Switzerland). Membranes were then rinsed with distilled H₂O, gently cut from transwells and mounted onto glass slides. Cellular invasion and migration indices were determined by counting the number of stained cells on membranes in 5 randomly selected, non-overlapping fields at 400× magnification under a light microscope (researcher blind to experimental condition).

Assay for in vitro NO production

C3L5 and C10 cell culture media were collected at the same time points and, in conditions identical with those used in invasion and migration assays, stored at –20°C until assayed. Levels of NO were measured by determining levels of inorganic NO₂-, a stable product of oxidized NO (Moncada and Higgs, 1993), in the Greiss reaction (Green *et al.*, 1982), using a procedure previously established in this laboratory (Orucevic and Lala, 1996a). Briefly, samples of culture medium were diluted in de-ionized H₂O (1:1) and proteins precipitated using 50 µl 30% ZnSO₄ and 1 ml of dilute sample, followed by centrifugation (8,000 g, 5 min); 1 ml of supernatant was incubated (room temperature, 30 min) with 300 µl 0.5 M ammonium chloride, 100 µl 0.06 M sodium borate and 50 mg acid-washed cadmium filings (Davison and Woof, 1978). The mixture was centrifuged (400 g, 7 min), and 1 ml of supernatant was added to Greiss reagent and incubated (room temperature, 10 min). Greiss reagent was prepared by mixing equal parts 1% sulphanilic acid (Sigma) and 0.1% naphthylethylenediamine (Sigma) in 2% phosphoric acid. Absorbance of samples at 543 nm was measured using a spectrophotometer; concentration of NO₂– in media samples was determined from the sodium nitrite standard curve, which was linear for 0 to 100 µM of nitrite.

In vivo tumour-induced angiogenesis assay

Levels of tumour-induced angiogenesis *in vivo* were quantified using a novel assay devised in our laboratory and based on our observation that angiogenesis was induced in s.c. implants of growth factor–reduced Matrigel only when tumour cells were suspended in the Matrigel (Jadeski and Lala, 1999). We compared angiogenesis induced by C3L5 and C10 cells and examined the effects NOS inhibition by chronically administering L-NAME or its inactive enantiomer, D-NAME, to implant-bearing mice using osmotic minipumps.

In the inguinal region, mice received s.c. implants of 5 × 10⁴ C3L5 or C10 cells suspended in growth factor–reduced Matrigel (3.5 mg Matrigel in 0.5 ml RPMI) and, on the contralateral side as controls, the equivalent amount of Matrigel alone. Immediately thereafter, osmotic minipumps (ALZA, Palo Alto, CA) were implanted s.c., providing a constant systemic supply (0.5 µl/hr, 25 mg/200 µl 0.9% NaCl) of L-NAME (n = 15/group) or D-NAME (n = 15/group) (both drugs purchased from Sigma) for the duration of the experiment (14 days).

Mice were killed using an overdose of pentobarbital and Matrigel implants removed, fixed in 4% paraformaldehyde, processed for paraffin embedding, sectioned and stained with Masson trichrome. Sections were scanned at low power for areas containing new blood vessels (researcher blind to experimental condition); these areas were systematically imaged at 160× magnifica-

tion using Northern Exposure (Empix Imaging, Mississauga, ON) and individual vessel counts for each field documented using Mocha Image Analysis Software (Jandel) to identify fields of maximum blood vessel density (*i.e.*, hot spots). Subsequently, hot spots were statistically analysed for between-group differences by determining the average (n = 15 animals/group) of 3 fields of maximal blood vessel density (taken in descending order) per animal.

Statistical analysis

Data were analysed using the SAS (Cary, NC) system for Windows, release 6.12. Data comparing 2 means were tested using Student's *t*-test; those comparing multiple (*i.e.*, more than 2)
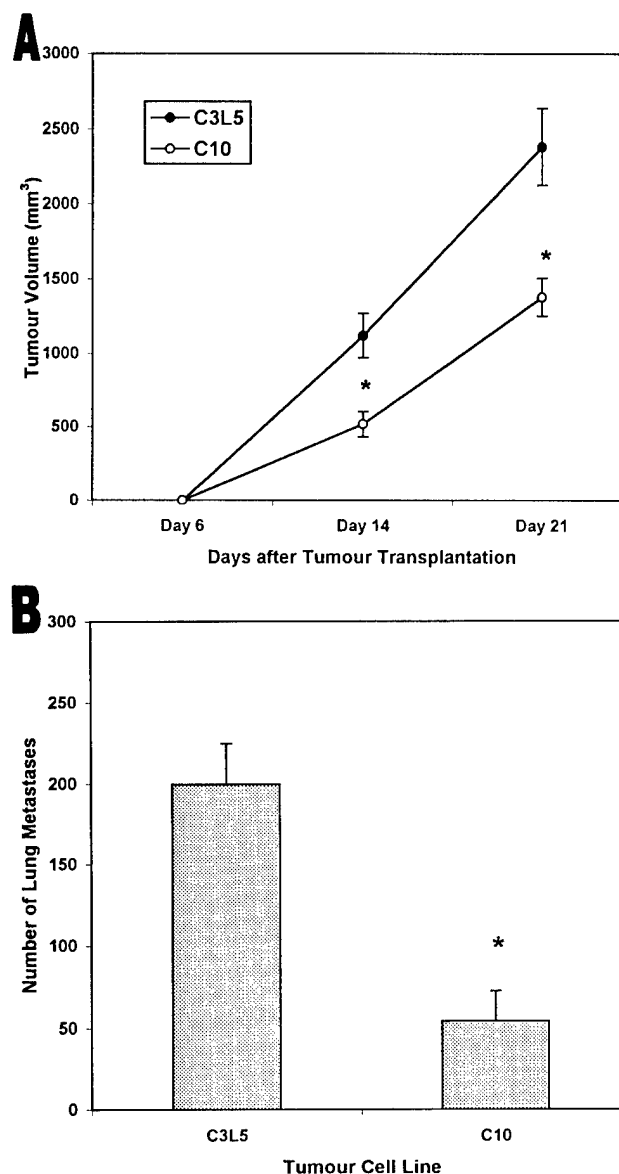
FIGURE 1 – Primary tumour growth rate and metastatic lung colony formation in C3H/HeJ mice after s.c. injection of 5 × 10⁵ C3L5 or C10 tumour cells. *(a)* At 14 and 21 days after tumour transplantation, primary tumour volumes were significantly lower (*p < 0.0001) for C10 than for C3L5 transplants. Data represent means ± SE (n = 15/group). *(b)* Mean number of metastatic lung nodules 3 weeks after tumour transplantation. Fewer lung colonies formed in mice bearing C10 than C3L5 tumour transplants (*p < 0.001). Data represent means ± SE (n = 15/group).
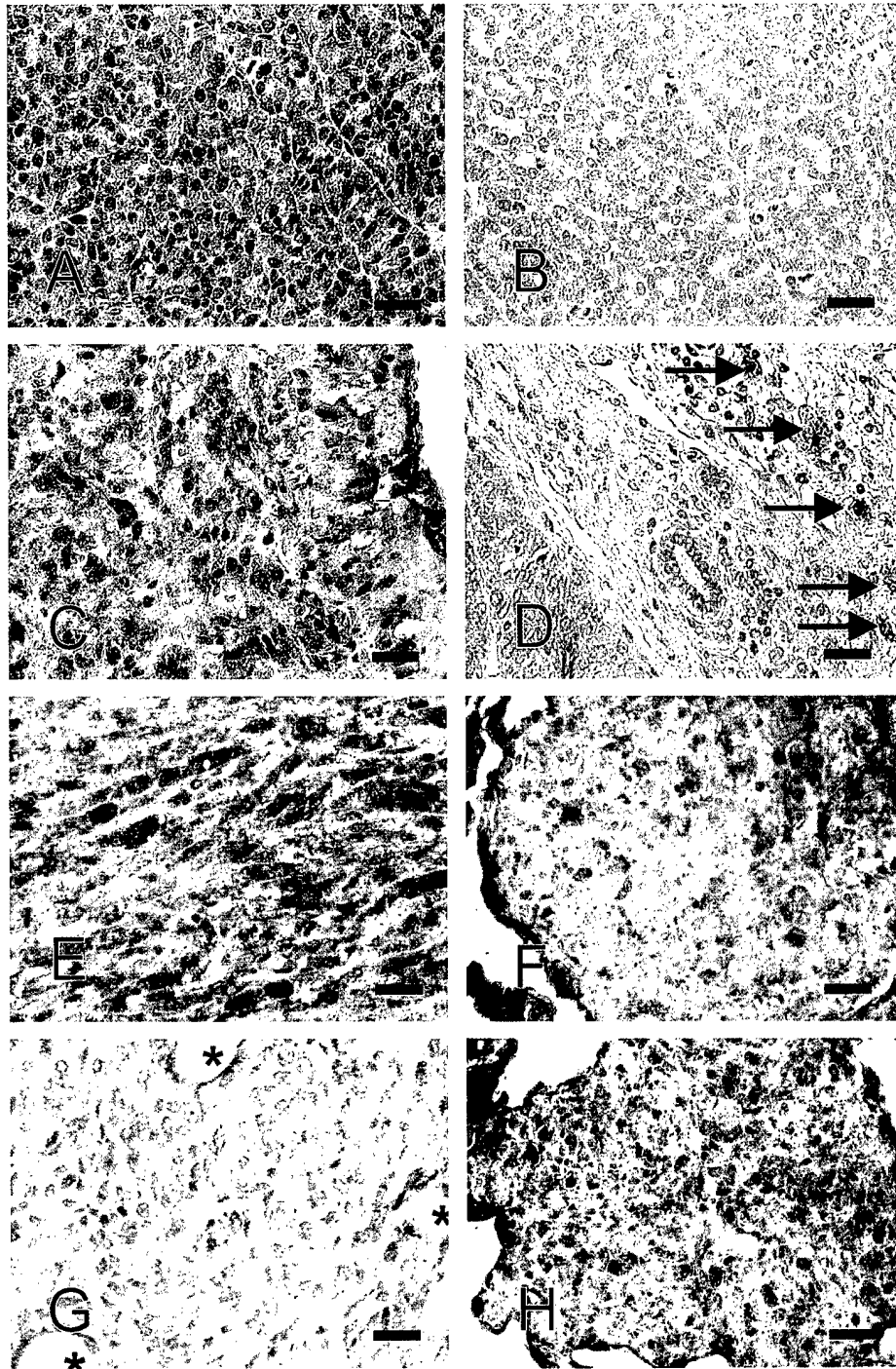
FIGURE 2 – Immuno-histochemical localisation of eNOS and iNOS proteins in spontaneous *(a–d)* and transplanted *(e–g)* mammary tumours (C3L5 or C10) at primary and metastatic sites. *(a)* Spontaneous primary tumour showing both eNOS-positive and -negative tumour cells arranged in pseudo-acinar formation. *(b)* Representative negative control. *(c)* Lung metastasis of tumour depicted in *(a)*; metastases were always strongly and homogeneously eNOS-positive. *(d)* Spontaneous primary tumour immunostained for iNOS; macrophages, present in tumour stroma, stained positively for iNOS, whereas tumour cells did not express iNOS. *(e)* C3L5 primary tumours transplanted s.c. exhibited strong and homogeneous eNOS positivity, whereas C10-derived tumours *(g)* showed weak and heterogeneous eNOS staining. Constitutive eNOS protein was expressed in endothelial cells lining blood vessels (* in *g*) in tumour tissue. eNOS expression was similar in metastatic lung colonies arising after C3L5 or C10 transplantation (*f* and *h*, respectively). Scale bars = 30 μm.

means for a single main effect were tested using 1-way ANOVA. Data from the *in vivo* pulmonary metastasis assay were analyzed using the Mann-Whitney rank sum test. Main effects of tumour type (*i.e.,* C3L5 and C10) and treatment (*i.e.,* L-NAME and D-

NAME) were tested for the dependent variable (blood vessel formation) using 2-way ANOVA in the *in vivo* angiogenesis assay. A probability of 0.05 was always used in determining statistical significance.

RESULTS

Primary tumour growth rate and metastatic lung colony formation

Figure 1 shows the volume of primary tumours and the number of lung metastases forming in C3H/HeJ mice receiving s.c. im-

A

Legend:
- ▨ eNOS Intensity
- ☐ eNOS Intensity–Blood Vessel Devoid Regions

Y-axis: Average Intensity (Grey Levels)
X-axis: Primary Tumour Sample — Negative Control, C3L5, C10

B

Legend:
- ▨ eNOS
- ☐ iNOS

Y-axis: Average Intensity (Grey Levels)
X-axis: Lung Metastases — Negative Control, C3L5, C10

plants of C3L5 or C10 tumour cells (n = 15 mice/group). C3L5-derived primary tumours grew faster, resulting in larger tumours, than those derived from C10 cells at day 14 ($p < 0.0001$) and day 21 ($p < 0.0001$) after tumour transplantation (Fig. 1*a*). In addition, the number of spontaneous metastatic lung colonies harvested at 21 days (Fig. 1*b*) was higher in mice receiving s.c. implants of C3L5 cells relative to those receiving C10 cells (C3L5 199.6 ± 25.0, C10 54.1 ± 18.3; $p < 0.001$).
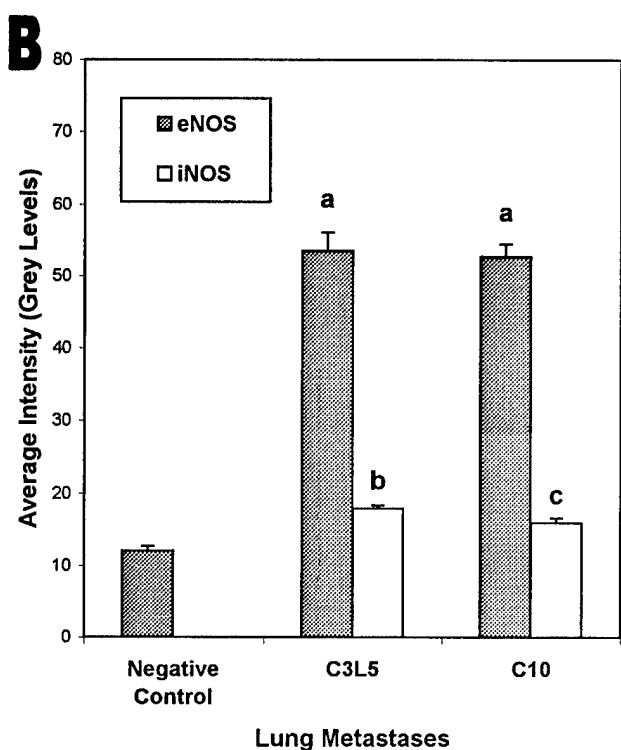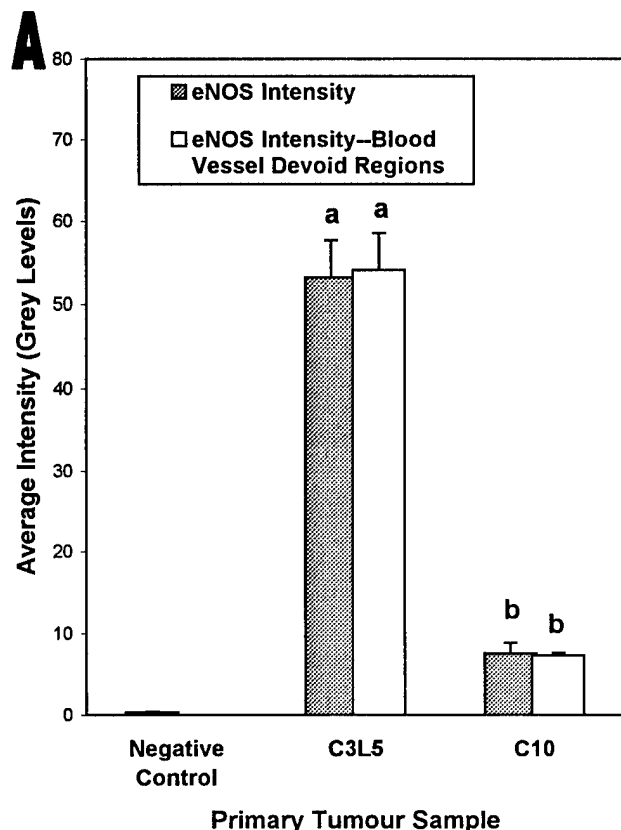
Immuno-cytochemical detection of NOS (eNOS and iNOS) enzymes

Strong and homogeneous eNOS staining was observed *in vitro* in 100% of cultured C3L5 mammary adenocarcinoma cells, as reported by Orucevic *et al.* (1999), suggesting that these cells constitutively express high levels of eNOS. In contrast, *in vitro* eNOS immunostaining in C10 cells was much weaker and more heterogeneous relative to C3L5 cells (data not shown). Under normal culture conditions, C3L5 and C10 cells did not express iNOS; however, iNOS expression was induced in both cell lines using IFN-γ and LPS in approximately 40% to 50% of cells (data not shown), as previously reported for C3L5 cells (Orucevic *et al.*, 1999).

Spontaneous mammary tumours developing in C3H/HeJ female retired breeder mice (tumour diameter at 8 to 12 weeks' = 8 to 20 mm) showed localised variations in levels of morphological differentiation within primary tumours, irrespective of tumour growth rate. Differentiated zones were comprised of tumour cells arranged in pseudo-acini, whereas poorly differentiated sites constituted spindle-shaped tumour cells arranged in sheets, whorls or clusters. A heterogeneous pattern of eNOS expression was seen in both differentiated and poorly differentiated zones of tumour tissue; cells were either strongly eNOS-positive or completely eNOS-negative (differentiated zone, Fig. 2*a*); however, the proportion of eNOS-positive cells was consistently higher in poorly differentiated zones relative to differentiated zones (data not shown). Overall, approximately 40% to 70% of tumour cells in individual primary tumours were eNOS-positive. A clear correlation between eNOS expression patterns and tumour growth rates was not observed (high tumour growth rate = 13 to 20 mm tumour diameter at 8 to 12 weeks, n = 4; moderate growth rate = 8 to 12 mm, n = 11; low growth rate = <8 mm, n = 5). In contrast, all spontaneous lung metastases were strongly and homogeneously eNOS-positive; virtually all (76% to 100%) tumour cells at metastatic sites expressed eNOS (Fig. 2*c*). Tumour cells within primary and metastatic sites did not express iNOS; however, some tumour-associated macrophages, located in the primary tumour tissue and surrounding stroma (Fig. 2*d*) and occasionally at metastatic sites (data not shown), stained positively for iNOS.

Figure 2*e–h* shows eNOS staining in primary and metastatic tumours 3 weeks after transplantation of C3L5 (Fig. 2*e*, primary tumour; Fig. 2*f*, lung metastasis) and C10 (Fig. 2*g*, primary tumour; Fig. 2*h*, lung metastasis) cells. Primary tumours derived

---

FIGURE 3 – Quantification of the average staining intensity of primary tumours from C3H/HeJ mice bearing C3L5 or C10 tumour transplants immunostained for eNOS protein. *(a)* The intensity of immuno-histochemical staining for eNOS was higher in tumour cells within primary C3L5 tumours than in those derived from C10 cells ($p < 0.001$). eNOS immunostaining intensity did not differ in regions containing blood vessels *vs.* those devoid of blood vessels, and this was observed for both C3L5 and C10-derived tumours (C3L5 $p =$ 0.8969, C10 $p =$ 0.9012), indicating that endothelial cells did not alter the relative amount of eNOS staining between C3L5- and C10-derived tumours. *(b)* The intensity of eNOS immunostaining did not differ in lung metastases derived from C3L5 or C10 cells ($p =$ 0.8008). iNOS immunostaining was slightly higher in lung metastases derived from C3L5 cells relative to those derived from C10 cells ($p < 0.0197$). Bars not sharing a common letter (*i.e.*, a, b or c) in each diagram are significantly different.
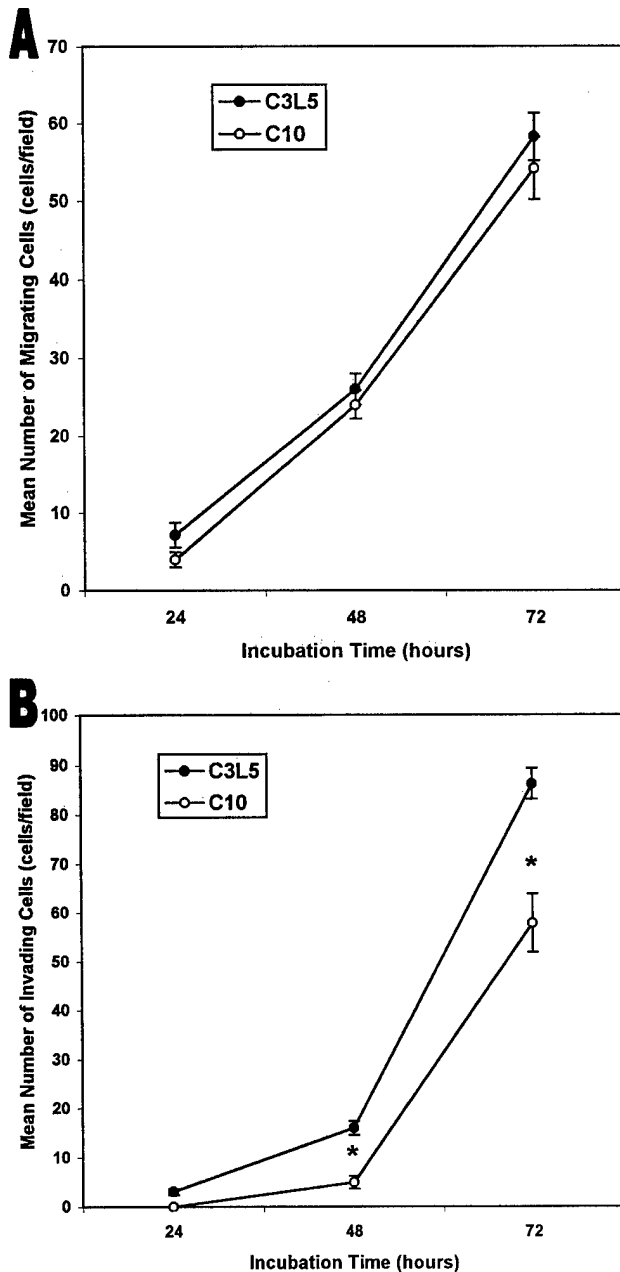
Figure 4 – Temporal kinetics of *in vitro* migration and invasion. *(a)* Kinetics of migration of C3L5 and C10 tumour cells; C3L5 and C10 cells did not differ in migratory capacity (n = 20 fields/group). *(b)* Kinetics of invasion of C3L5 and C10 tumour cells; invasion rate of C10 cells was slower than that of C3L5 cells (*p < 0.0011, n = 20 fields/group).

from the weakly metastatic C10 cell line showed weak and heterogeneous eNOS staining; relatively weak eNOS positivity was noted in approximately 20% to 50% of tumour cells (Fig. 2*g*). Primary tumours derived from the highly metastatic C3L5 cell line (Fig. 2*e*) were strongly and homogeneously eNOS-positive; most (>90%) tumour cells expressed eNOS. However, regardless of the tumour cell line transplanted (*i.e.*, C3L5 or C10), lung metastases were always strongly and homogeneously eNOS-positive; approximately 60% to 80% of tumour cells within metastatic lung colonies showed strong staining for eNOS (Fig. 2*f*, C3L5; Fig. 2*h*, C10). Cells within primary tumours and metastases did not express

iNOS. However, iNOS expression was observed in tumour-associated macrophages at primary and metastatic sites of both tumour types (data not shown).

Quantification of NOS staining intensity of primary tumours and lung metastases

Figure 3 shows quantification of the staining intensity within primary, healthy (non-necrotic) tumour tissue and lung metastases (Fig. 3*a,b*) harvested 3 weeks after transplantation of C3L5 or C10 cells. The average intensity of immuno-histochemical staining for eNOS was higher in cells within primary tumours derived from C3L5 cells relative to those derived from C10 cells (C3L5 53.2 ± 4.9, C10 7.5 ± 1.3; p < 0.001). Since eNOS staining intensity did not differ in regions of tumour sections containing blood vessels compared with those devoid of blood vessels and this relationship was observed for both C3L5- and C10-derived tumours (C3L5 blood vessel–containing regions = 53.2 ± 4.9, blood vessel–devoid regions = 54.0 ± 4.5, p = 0.8969; C10 blood vessel–containing regions = 7.5 ± 1.3, blood vessel–devoid regions = 7.3 ± 1.2, p = 0.9012), it appears that endothelial cells did not alter the relative amount of eNOS staining between C3L5- and C10-derived tumours. The intensity of eNOS immunostaining did not differ in lung metastases derived from C3L5 and C10 cells (C3L5 53.5 ± 2.6, C10 52.6 ± 1.8; p = 0.8008). iNOS immunostaining was higher in metastatic lung colonies derived from C3L5 relative to those derived from C10 cells (C3L5 17.9 ± 0.4, C10 15.9 ± 0.7; p > 0.0197).

Kinetics of in vitro migration and invasion by C3L5 and C10 cells

The temporal kinetics of migration and invasion are shown in Figure 4. Migration rates of the 2 cell types did not differ (p = 0.429 at 72 hr); however, C3L5 cells were more invasive than C10 cells (C3L5 86.2 ± 3.6, C10 57.8 ± 6.9; p < 0.0011 at 72 hr).

Migration and invasiveness under different treatment conditions

The effects of L-NAME treatment at various doses ± 5-fold excess L-arginine (natural substrate for NOS, competes with and blocks NO-specific effects of L-NAME) on the migratory and invasive abilities of both cell lines at 24, 48 and 72 hr were examined. Since the effects were qualitatively similar at all time points, only the 72 hr time point is shown (Fig. 5). L-NAME treatment at varying doses (0.01, 0.1 and 1 mM) reduced the migratory capacity of both C3L5 (p < 0.0001) and C10 (p < 0.0001) cells relative to untreated control cells. Migratory capacities of both cell lines were restored to baseline levels after additional treatment with excess L-arginine, indicating that the inhibitory effects of L-NAME on migration were NO-specific (Fig. 5*a*).

The invasion indices of C3L5 and C10 cells after 72 hr incubation, under different treatment conditions, are shown in Figure 5*b*. As shown earlier, C3L5 cells invaded the Matrigel barrier at a faster rate than C10 cells (p < 0.0011). In addition, L-NAME treatment at the various doses reduced the invasive capacity of both C3L5 (p < 0.0001) and C10 (p < 0.0001) cells relative to untreated control cells. Invasive capacities of both cell lines were restored to near baseline levels after additional treatment with excess L-arginine, indicating that the effects of L-NAME on invasion were NO-specific.

NO production assay

Figure 6 shows the levels of NO produced by C3L5 and C10 cells as measured by the nitrate/nitrite levels present in the culture media collected after 72 hr incubation under the treatment conditions examined in invasion and migration assays. Under normal culture conditions, nitrate/nitrite levels were higher in culture media from C3L5 cells compared with C10 cells (C3L5 78.4 ± 1.2, C10 67.4 ± 0.5; p < 0.0001). For both cell lines, treatment of cells with L-NAME at the various doses reduced levels of nitrate/nitrite produced relative to untreated control cells (C3L5 p <
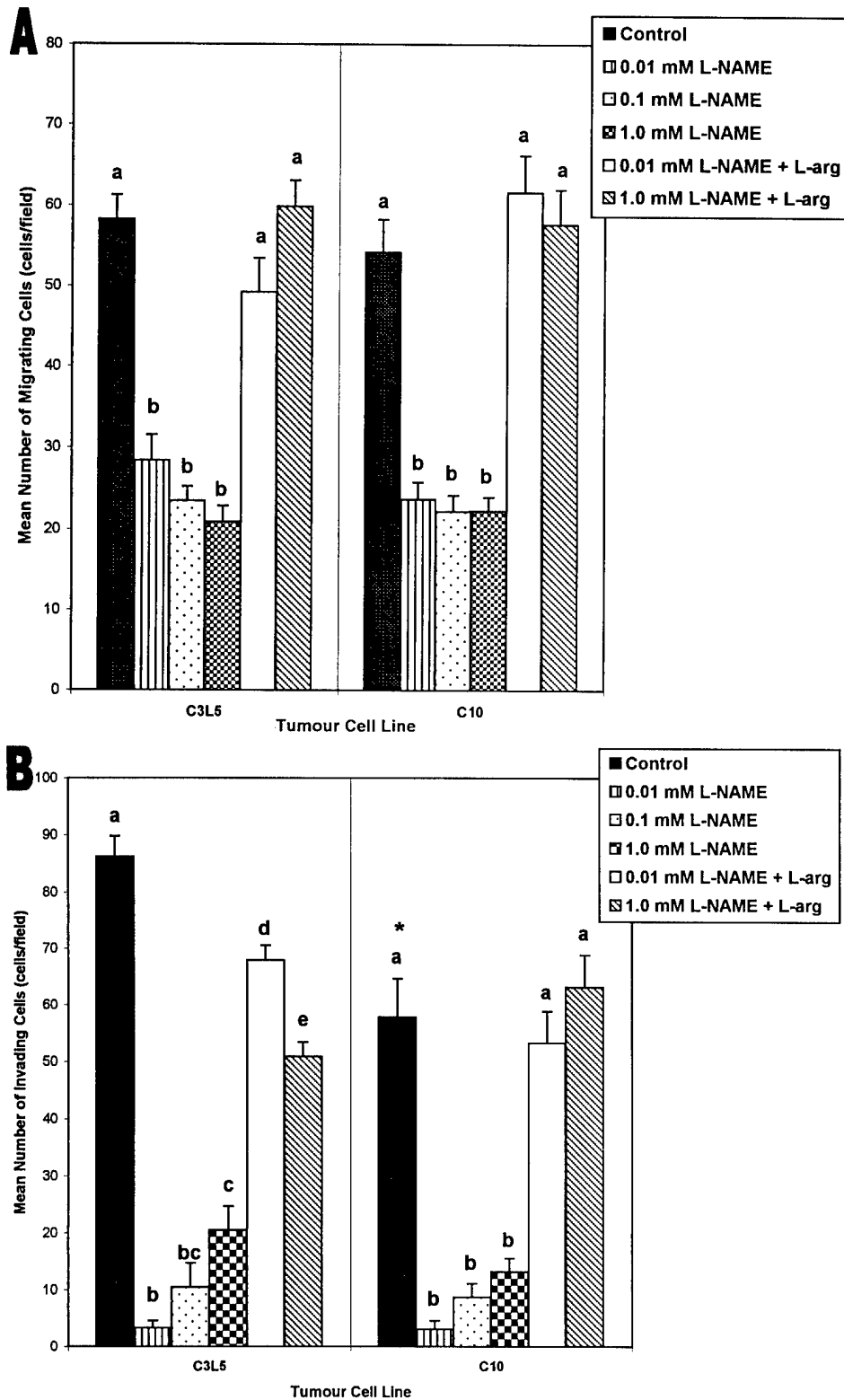
JADESKI ET AL.

FIGURE 5 – Migration and invasion indices of C3L5 and C10 cells under different treatment conditions (72 hr incubation). (a) Migratory ability of both C3L5 and C10 cells was reduced after treatment with L-NAME at various concentrations (0.01, 0.1 and 1 mM) relative to control cells (C3L5 $p < 0.0001$, C10 $p < 0.0001$), and migration of both cell lines was restored to basal levels after additional treatment with L-arginine (0.01, 1.0 mM). (b) Basic invasiveness of C10 cells was lower (*) than that of C3L5 cells. Treatment of C3L5 and C10 cells with L-NAME reduced invasive ability relative to untreated controls (C3L5 $p < 0.0001$, C10 $p < 0.0001$). Additional treatment with L-arginine increased invasion of both cell lines, restoring it to near basal levels. Within each cell line, bars not sharing a common letter (i.e., a–e) are significantly different.
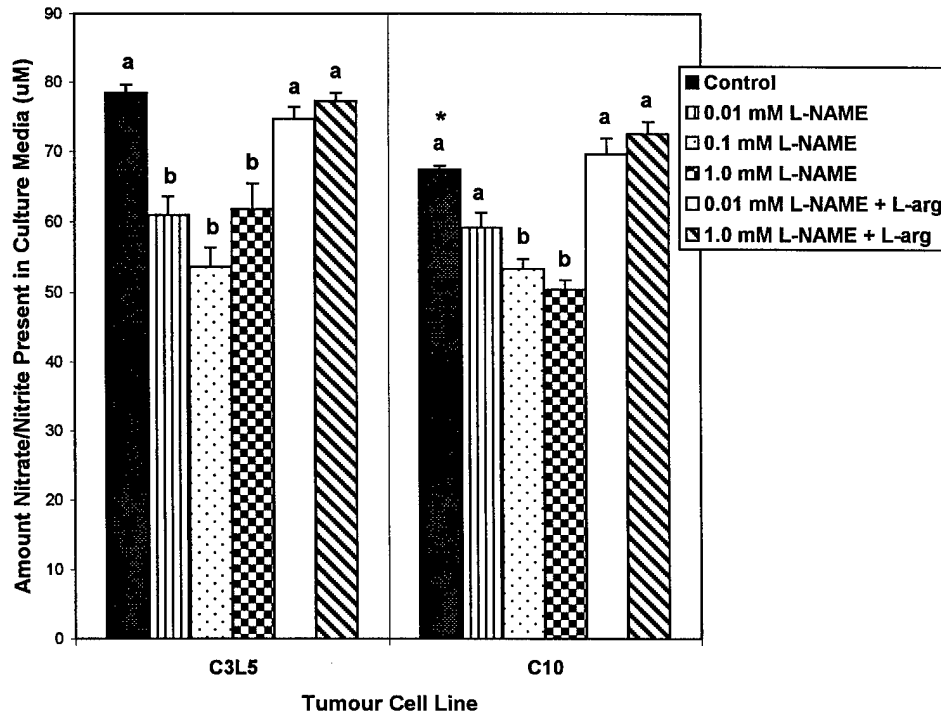
FIGURE 6 – NO production by C3L5 and C10 cells measured by nitrate/nitrite levels in culture media under different treatment conditions (72 hr incubation). Concentrations of nitrate/nitrite were higher for C3L5 than for C10 cells (*$p < 0.0001$). Relative to untreated C3L5 and C10 cells, production of NO by both cell lines decreased significantly after treatment with L-NAME at various concentrations (0.01, 0.1, 1.0 mM; C3L5 $p < 0.0001$, C10 $p < 0.0001$). Levels of nitrate/nitrite increased and were restored to near basal values with additional exposure of C3L5 and C10 cells to L-arginine (0.01, 1.0 mM). Bars not sharing a common letter (*i.e.*, a or b) are significantly different.

0.0001, C10 $p < 0.0001$), and these levels were restored with additional exposure of cells to excess L-arginine.

In vivo *tumour-induced angiogenesis assay*

Figure 7 shows the number of blood vessels per unit area in Matrigel implants containing C3L5 or C10 cells, retrieved from animals treated with L-NAME or D-NAME (control animals). C3L5 cells were more angiogenic than C10 cells; in control animals treated with D-NAME, neovascularisation was lower in C10-containing implants than in those containing C3L5 cells (C3L5 71.9 ± 5.33, C10 39.1 ± 4.9; $p < 0.0001$). L-NAME therapy reduced angiogenesis in C3L5-containing implants relative to control animals but did not affect neovascularisation in C10-containing implants (C3L5 L-NAME 34.2 ± 4.7, D-NAME 71.9 ± 5.3, $p < 0.0001$; C10 L-NAME 38.1 ± 4.7, D-NAME 39.1 ± 4.9, $p = 0.8903$).

DISCUSSION

We have investigated the role of endogenous NO, resulting from eNOS expression by tumour cells, in tumour progression and metastasis using a C3H/HeJ murine mammary adenocarcinoma model that includes spontaneously arising tumours and 2 clonal derivatives that differ in metastatic phenotype. Examination of a large number of spontaneous tumours confirmed our preliminary findings (Lala and Orucevic, 1998) that tumour cells at primary sites were distinctly heterogeneous in eNOS protein expression, whereas those at spontaneous lung metastatic sites had a strong and homogeneous expression pattern, suggestive of a metastasis-promoting role of eNOS. This concept was further validated by our findings of a positive correlation between levels of eNOS expression in primary tumours and primary tumour growth rate and formation of spontaneous pulmonary metastases, using 2 transplanted, clonally derived cell lines: C10, a weakly metastatic cell

line (Lala *et al.*, 1986), and C3L5, a highly metastatic cell line (Lala and Parhar, 1993).

The 2 cell lines differed in eNOS expression *in vitro* and *in vivo* at primary transplant sites. However, as revealed using objective, computer-assisted quantification, eNOS expression in tumour cells did not differ at metastatic sites. Exclusion of eNOS-positive vascular endothelial cells from the analysis did not alter *in vivo* results, suggesting that tumour-derived eNOS contributed to the observed variations in eNOS expression between the 2 cell lines. Furthermore, because iNOS expression (observed in macrophages within primary tumour tissue, in surrounding stroma and at metastatic sites) did not differ between C3L5 and C10-derived tumours, it is likely that the observed differences in tumour growth and metastasis were eNOS-mediated. However, this relationship, on its own, did not establish causality. A causal relationship between NO production and tumour progression was earlier demonstrated in C3L5 tumour-bearing mice; anti-tumour and anti-metastatic effects were observed with NOS inhibition using NMMA and L-NAME (Orucevic and Lala, 1996*a,b*). The present study further explored the underlying mechanisms utilising both tumour cell lines.

Key cellular processes that determine primary tumour growth rate are tumour cell proliferation, survival and capacity for angiogenesis; invasiveness and metastasis depend on migration and matrix degradation by tumour cells. We earlier found that endogenous NO did not alter C3L5 cell proliferation (Orucevic *et al.*, 1999); we have also observed that *in vitro* growth rates of C10 and C3L5 cells did not differ (data not shown). In the present study, we compared migratory, invasive and angiogenic capacities of the 2 cell lines and the role of endogenous NO in these processes.

Despite differences in eNOS expression and NO production by C3L5 and C10 cell lines *in vitro*, the migratory capacities did not differ. However, for both cell lines, migration and NO production
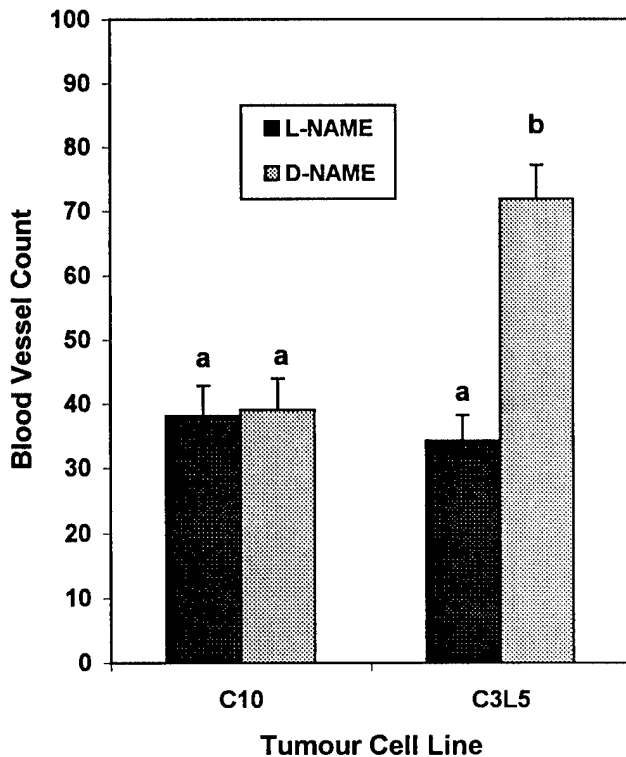
FIGURE 7 – Levels of angiogenesis in C10 and C3L5 implants in L-NAME–treated and control (D-NAME–treated) animals. For control animals treated with D-NAME, the neovascular response was higher in Matrigel implants containing C3L5 cells than in those containing C10 cells ($p < 0.0001$). L-NAME treatment reduced angiogenesis in implants containing C3L5 cells relative to control animals ($p < 0.0001$) but did not alter angiogenesis in implants containing C10 cells relative to control animals ($p = 0.8903$). Bars not sharing a common letter (*i.e.*, a or b) are significantly different.

were inhibited in the presence of L-NAME and inhibitory effects were abrogated with additional exposure of cells to L-arginine, indicating that endogenous NO stimulated migration. Thus, the absence of differences in the basal migration rates may be explained by the presence of additional migration regulatory factor(s) differentially expressed by the 2 cell lines. The present report demonstrates a migration-promoting role of endogenous, tumour-derived NO. The precise pathway of signal transduction responsible for this role remains to be examined.

C3L5 cells were more invasive than C10 cells, consistent with the differences in their metastatic capacities *in vivo*. For both cell lines, invasiveness and NO production were suppressed with L-NAME and restored with additional exposure of cells to L-arginine, suggesting that endogenously-derived NO promoted inva-

sion. Therefore, varied capacities for invasion could be explained, in part, by differences in NO production between the 2 cell lines. Because cellular invasiveness depends on multiple steps, including matrix degradation and migration, and migration did not differ between the 2 cell lines, it is likely that the differences in their invasiveness were due to differences in their matrix-degrading capabilities. Orucevic *et al.* (1999) demonstrated that endogenous NO promoted matrix degradation by C3L5 cells by altering the balance between matrix metalloproteases (MMPs) and their natural inhibitors, tissue inhibitors of metalloproteases (TIMPs): constitutively produced NO by C3L5 cells down-regulated TIMP-2 and TIMP-3 mRNA, whereas induction of additional NO production by LPS and IFN-γ up-regulated MMP-2 mRNA. Additional mechanisms of NO-mediated stimulation of cellular invasiveness may exist. For example, NO was shown to stimulate degradation of articular cartilage by stimulating other MMPs (collagenases and stromelysin) in human, bovine and rabbit chondrocytes (Murrell *et al.*, 1995; Tamura *et al.*, 1996).

Finally, C3L5 and C10 cells differed in their angiogenic capacities *in vivo*, consistent with differences in their NO-producing abilities. This may partly explain the observed differences in primary tumour growth rates following transplantation of equivalent numbers of C3L5 or C10 cells at identical sites in syngeneic mice. For C3L5 cells, endogenous NO promoted vascularisation; angiogenesis was markedly reduced in L-NAME–treated mice relative to those receiving D-NAME, confirming earlier findings using the novel *in vivo* angiogenesis assay devised in our laboratory (Jadeski and Lala, 1999). However, in C10-derived Matrigel implants, L-NAME treatment did not reduce the angiogenic response relative to D-NAME treatment. Two explanations may be offered for this finding: (i) the cell lines differentially express other angiogenesis-regulating factor(s) and (ii) a certain threshold level of NO is required to stimulate angiogenesis in the present tumour model. Angiogenesis promotion by NO has been reported utilizing *in vitro* and *in vivo* assays (Ziche *et al.*, 1994, 1997) and has been demonstrated in numerous tumour models. For example, iNOS over-expression in a human colonic adenocarcinoma cell line led to increased growth rate and enhanced vascularity of transplanted tumours in nude mice (Jenkins *et al.*, 1995). Furthermore, NOS inhibition reduced angiogenesis in the rabbit cornea following xenotransplantation of human squamous-cell carcinoma cells (Gallo *et al.*, 1998). Taken together, these findings suggest that promotion of angiogenesis is a key event responsible for NO-mediated stimulation of tumour growth and metastasis.

In summary, our results in the C3H/HeJ murine mammary tumour model have established that tumour-derived NO plays a stimulatory role in tumour progression and metastasis by multiple mechanisms: promotion of migration, matrix degradation and angiogenesis. Thus, NOS inhibitors may prove to be important components of combination therapy protocols in certain human tumours, including breast cancer, which exhibits a positive association of NOS activity with tumour grade (Thomsen *et al.*, 1995; Dueñas-Gonzalez *et al.*, 1997).

REFERENCES

BAGULEY, B.C., CALVELEY, S.B., CROWE, K.K., FRAY, L.M. and O'ROUKE, S.A., Comparison of the effects of flavone acetic acid, fostriecin, homoharrgtone and tumour necrosis factor α on colon 38 tumours in mice. *Europ. J. Cancer clin. Oncol.*, **25**, 263–269 (1989).

BRODT, R., PARHAR, R., SANKAR, P. and LALA, P.K., Studies on clonal heterogeneity in two spontaneously metastasizing mammary carcinomas of recent origin. *Int. J. Cancer*, **35**, 265–273 (1985).

COBBS, C.S., BRENMAN, J.E., ALDAPE, K.D., BREDT, D.S. and ISRAEL, M.A., Expression of nitric oxide synthase in human central nervous system tumors. *Cancer Res.*, **55**, 727–730 (1995).

DAVISON, W. and WOOF, C., Comparison of different forms of cadmium as reducing agents for the batch determination of nitrate. *Analyst*, **103**, 403–406 (1978).

DUEÑAS-GONZALEZ, A., ISALES, C.M., DEL MAR ABAD-HERNANDEZ, M.,

GONZALEZ-SARMIENTO, R., SANGUEZA, O. and RODRIGUEZ-COMMES, J., Expression of inducible nitric oxide synthase in breast cancer correlates with metastatic disease. *Mod. Pathol.*, **10**, 645–649 (1997).

EDWARDS, P., CENDAN, J.C., TOPPING, D.B., MOLDAWER, L.L., MACKAY, S., COPELAND, E.M. and LIND, D.S., Tumor cell nitric oxide inhibits cell growth *in vitro*, but stimulates tumorigenesis and experimental lung metastasis *in vivo*. *J. Surg. Res.*, **63**, 49–52 (1996).

FUJIMOTO, H., ANDO, Y., YAMASHITA, T., TERAZAKI, H., TANAKA, Y., SASAKI, J., MATSUMOTO, M., SUGA, M. and ANDO, M., Nitric oxide synthase activity in human lung cancer. *Jpn. J. Cancer Res.*, **88**, 1190–1198 (1997).

GALLO, O., MASINI, E., MORBIDELLI, L., FRANCHI, A., FINI-STORCHI, I., VERGARI, W.A. and ZICHE, M., Role of nitric oxide in angiogenesis and

tumor progression in head and neck cancer. *J. nat. Cancer Inst.*, **90**, 587–596 (1998).

GREEN, L.C., WAGNER, D.A., GLOGOWSKI, J., SKIPPER, P.L., WISHNOK, J.S. and TANNENBAUM, S.R., Analysis of nitrate, nitrite, and [^{15}N]nitrate in biological fluids. *Anal. Biochem.*, **126**, 131–138 (1982).

JADESKI, L.C. and LALA, P.K., NOS inhibition by N^G-nitro-L-arginine methyl ester (L-NAME) inhibits tumour-induced angiogenesis in mammary tumours. *Amer. J. Pathol.*, **155**, 1381–1390 (1999).

JENKINS, D.C., CHARLES, I.G., THOMSEN, L.L., MOSS, D.W., HOLMES, L.S., BAYLIS, S.A., RHODES, P., WESTMORE, K., EMSON, P.C. and MONCADA, S., Roles of nitric oxide in tumor growth. *Proc. nat. Acad. Sci. (Wash.)*, **92**, 4392–4396 (1995).

KENNOVIN, G.D., HIRST, D.G., STRATFORD, M.R.L. and FLITNEY, F.W., Inducible nitric oxide synthase is expressed in tumor-associated vasculature: inhibition retards tumor *in vivo*. *In:* S. Moncada, M. Feelisch, R. Busse and E.A. Higgs (eds.), *Biology of nitric oxide. Part 4, Enzymology, biochemistry, and immunology,* pp. 473–479, Portland Press, London (1994).

KLOTZ, T., BLOCH, W., VOLBERG, C., ENGELMANN, U. and ADDICKS, K., Selective expression of inducible nitric oxide synthase in human prostate carcinoma. *Cancer*, **82**, 1897–1903 (1998).

KNOWLES, R.G. and MONCADA, S., Nitric oxide synthases in mammals. *Biochem. J.*, **298**, 249–258 (1994).

LALA, P.K., AL-MUTTER, N. and ORUCEVIC, A., Effects of chronic indomethacin therapy on the development and progression of spontaneous mammary tumors in C3H/HeJ mice. *Int. J. Cancer*, **73**, 371–380 (1997).

LALA, P.K. and ORUCEVIC, A., Role of nitric oxide in tumor progression: lessons from experimental tumors. *Cancer Metastasis Rev.*, **17**, 91–106 (1998).

LALA, P.K. and PARHAR, R.S., Eradication of spontaneous and experimental adenocarcinoma metastases with chronic indomethacin and intermittent IL-2 therapy. *Int. J. Cancer*, **54**, 677–684 (1993).

LALA, P.K., PARHAR, R.S. and SINGH, P., Indomethacin therapy abrogates the prostaglandin-mediated suppression of natural killer activity in tumour-bearing mice and prevents tumour metastasis. *Cell. Immunol.*, **99**, 108–118 (1986).

LEHR, H.-A., MANKOFF, D.A., CORWIN, D., SANTEUSANIO, G. and GOWN, A.M., Application of photoshop-based image analysis to quantification of hormone receptor expression in breast cancer. *J. Histochem. Cytochem.*, **45**, 1559–1565 (1997).

MONCADA, S. and HIGGS, A., The L-arginine–nitric oxide pathway. *N. Engl. J. Med.*, **329**, 2002–2012 (1993).

MURRELL, G.A.A., JANG, D. and WILLIAMS, R.J., Nitric oxide activates metalloprotease enzymes in articular cartilage. *Biochem. Biophys. Res. Comm.*, **206**, 15–21 (1995).

ORUCEVIC, A., BECHBERGER, J., GREEN, A.M., SHAPIRO, R.A., BILLIAR, T.R. and LALA, P.K., Nitric-oxide production by murine mammary adenocarcinoma cells promotes tumor-cell invasiveness. *Int. J. Cancer*, **81**, 889–896 (1999).

ORUCEVIC, A. and LALA, P.K., Effects of N^G-methyl-L-arginine, an inhibitor of nitric oxide synthesis, on IL-2-induced capillary leakage and anti-tumor responses in healthy and tumor-bearing mice. *Cancer Immunol. Immunother.*, **42**, 38–46 (1996a).

ORUCEVIC, A. and LALA, P.K., N^G-Nitro-L-arginine methyl ester, an inhibitor of nitric oxide synthesis, ameliorates interleukin-2-induced capillary leakage and reduces tumor growth in adenocarcinoma-bearing mice. *Brit. J. Cancer*, **73**, 189–196 (1996b).

TAMURA, T., TAKANISHI, T., KIMURA, Y., SASAKI, D., NORIMATSU, H., TAKAHASHI, D. and TAKIGAWA, M., Nitric oxide mediates interleukin-2-induced matrix degradation and basic fibroblast growth factor release in cultured rabbit articular chondrocytes. A possible mechanism of pathological neovascularization in arthritis. *Endocrinology*, **137**, 3729–3737 (1996).

THOMSEN, L.L., LAWTON, F.G., KNOWLES, R.G., BEESLEY, J.E., RIVEROS-MORENO, V. and MONCADA, S., Nitric oxide synthase activity in human gynecological cancer. *Cancer Res.*, **54**, 1352–1354 (1994).

THOMSEN, L.L. and MILES, D.W., Role of nitric oxide in tumor progression: lessons from human tumors. *Cancer Metastasis Rev.*, **17**, 107–118 (1998).

THOMSEN, L.L., MILES, D.W., HAPPERFIELD, L., BOBROW, L.G., KNOWLES, R.G. and MONCADA, S., Nitric oxide synthase activity in human breast cancer. *Brit. J. Cancer*, **72**, 41–44 (1995).

ZICHE, M., MORBIDELLI, L., CHOUDHURI, R., ZHANG, H.T., DONNINI, S., GRANGER, H.J. and BICKNELL, R., Nitric oxide synthase lies downstream from vascular endothelial growth factor-induced but not fibroblast growth factor-induced angiogenesis. *J. clin. Invest.*, **99**, 2625–2634 (1997).

ZICHE, M., MORBIDELLI, L., MASINI, E., AMERINI, S., GRANGER, H.J., MAGGI, C.A., GEPPETTI, P. and LEDDA, F., Nitric oxide mediates angiogenesis *in vivo* and endothelial cell growth and migration *in vitro* promoted by substance P. *J. clin. Invest.*, **94**, 2036–2044 (1994).

Appendix 2

#406 Cyclo-oxygenase and nitric oxide synthase inhibitors inhibit murine mammary tumor growth and metastasis by blocking tumor cell migration, invasion and angiogenesis. Lala Peeyush K., Jadeski Lorraine, Hum Kathleen, Rozic Jerry and Chakraborty Chandan. *Department of Anatomy and Cell Biology, The University of Western Ontario, London, Ontario, Canada N6A 5C1.*

Productions of prostaglandins (PG) ascribed to cyclo-oxygenase-2 (COX-2) and nitric oxide (NO), ascribed to endothelial type (e) NO synthase (NOS) expression by tumor cells were both found to promote tumor growth and metastasis in a murine breast cancer model, which could be mitigated with respective treatments with the COX-inhibitor indomethacin (Indo) or NOS inhibitors NMMA or L-NAME. Present study explored the underlying mechanisms, utilizing two mammary adenocarcinoma cell lines, clonally derived from a single C3H/HeJ spontaneous tumor, which differed in metastatic phenotype (C3L5-highly metastatic, high eNOS and high COX-2 expressing; C10-weakly metastatic, low eNOS and moderate COX-2 expressing). Cellular migratory ability *in vitro*, quantitated with a transwell migration assay, was found to be similar in both cell lines, and was suppressed by treatments with Indo (C3L5 cells) as well as L-NAME (C3L5 and C10 cells) and respectively restored with addition of PGE_2 or L-Arginine indicating that endogenous PGE_2 and NO had migration-stimulating effects. Cellular ability to invade Matrigel *in vitro* was higher in C3L5 than in C10 cells. However, using similar experiments as in the migration assay, endogenous NO was shown to promote invasiveness of both cell lines. Invasion stimulation by NO was found to be due to an upregulation of matrix metalloprotease (MMP)-2 mRNA and downregulation of tissue inhibitor of metalloproteases (TIMP)-2 and -3 mRNA in C3L5 cells. Finally, endogenous NO was shown to promote tumor-induced angiogenesis *in vivo* quantitated in sc implants of tumor cells suspended in growth factor-reduced Matrigel: (a) angiogenesis was lower with low-eNOS-expressing C10 than with high eNOS-expressing C3L5 cells; (b) L-NAME therapy of C3L5 but not C10 implant-bearing mice substantially reduced tumor angiogenesis as compared to control mice receiving D-NAME the inactive enantiomer. Similarly, endogenous PG was shown to be angiogenic in C3L5 implants; Indo therapy dramatically reduced angiogenesis. However, a combination of L-NAME and Indo therapy failed to produce any additive or synergistic effect, indicating that angiogenic stimulus by PG and NO may be mediated by a final common pathway. Thus antitumor and anti-metastatic effects of COX/NOS inhibitors were due to inhibition of migration, invasion and angiogenesis in this tumor model. Since COX-2 and iNOS expression are positively correlated with human breast cancer progression, selective COX-2 and iNOS inhibitors may prove useful in human breast cancer therapy. (Supported by the US Army Grant DAMD 17-96-6069 and the Breast Cancer Society of Canada).

#1024 NITRIC OXIDE-MEDIATED PROMOTION OF MURINE MAMMARY TUMOR PROGRESSION: ROLE IN TUMOR CELL MIGRATION.

Lorraine C Jadeski, Kathy O Hum, Louise M Gleeson, Chandan Chakraborty, and Peeyush K Lala, The Univ of Western Ontario, London, ON, Canada

We had earlier shown that tumor-derived nitric oxide (NO) resulting from expression of endothelial (e) type NO synthase (NOS) by tumor cells promoted tumor growth and metastasis in a murine mammary tumor model inclusive of spontaneous C3H/HeJ mammary tumors and two clonal derivatives: C3L5 (high eNOS expressor, highly metastatic) and C10 (low eNOS expressor, weakly metastatic). This was shown to be due to multiple mechanisms: NO-mediated promotion of tumor cell invasiveness resulting from an upregulaton of MMP-2 and downregulation of TIMP-2 and 3, and stimulation of tumor-induced angiogenesis. Present study utilized highly metastatic C3L5 and weakly metastatic C10 cells to examine whether endogenous NO promoted tumor cell migration, and if intracellular signalling via the MAP kinase (K) pathway was involved. In spite of parallel differences in eNOS expression, invasive, angiogenic and metastatic capacities of the two cell lines, the migratory function of C10 and C3L5 cells were indistinguishable in a transwell migration assay. However, there was a dose-dependent reduction of migration of both cell lines in the presence of the NOS inhibitor L-NAME; this effect was abrogated in the additional presence of excess L-Arginine, the natural substrate for NOS activity, indicating that endogenous NO promoted migration of both cell lines. Migration of both cells was blocked in the presence of a MAPKK (MEK) inhibitor, PD098059, irrespective of L-NAME and L-Arginine treatment. These results reveal that (a) migration stimulation by endogenous NO is an additional mechanism of NO-mediated promotion of metastasis, and (b) the signalling pathway for this stimulation involves MAPK. (Supported by US AMRAA, Grant # 966096)

Animal Model

Nitric Oxide Synthase Inhibition by N^G-Nitro-L-Arginine Methyl Ester Inhibits Tumor-Induced Angiogenesis in Mammary Tumors

Lorraine C. Jadeski and Peeyush K. Lala

From the Department of Anatomy and Cell Biology, The University of Western Ontario, London, Ontario, Canada

Using a murine breast cancer model, we earlier found a positive correlation between the expression of nitric oxide synthase (NOS) and tumor progression; treatment with inhibitors of NOS, N^G-methyl-L-arginine (NMMA) and N^G-nitro-L-arginine methyl ester (L-NAME), had antitumor and antimetastatic effects that were partly attributed to reduced tumor cell invasiveness. In the present study, we used a novel *in vivo* model of tumor angiogenesis using subcutaneous implants of tumor cells suspended in growth factor-reduced Matrigel to examine the angiogenic role of NO in a highly metastatic murine mammary adenocarcinoma cell line. This cell line, C3L5, expresses endothelial (e) NOS *in vitro* and *in vivo*, and inducible (i) NOS *in vitro* on stimulation with lipopolysaccharide and interferon-γ. Female C3H/HeJ mice received subcutaneous implants of growth factor-reduced Matrigel inclusive of C3L5 cells on one side, and on the contralateral side, Matrigel alone; L-NAME and D-NAME (inactive enantiomer) were subsequently administered for 14 days using osmotic minipumps. Immediately after sacrifice, implants were removed and processed for immunolocalization of eNOS and iNOS proteins, and measurement of angiogenesis. Neovascularization was quantified in sections stained with Masson's trichrome or immunostained for the endothelial cell specific CD31 antigen. While most tumor cells and endothelial cells expressed immunoreactive eNOS protein, iNOS was localized in endothelial cells and some macrophages within the tumor-inclusive implants. Measurable angiogenesis occurred only in implants containing tumor cells. Irrespective of the method of quantification used, tumor-induced neovascularization was significantly reduced in L-NAME-treated mice relative to those treated with D-NAME. The quantity of stromal tissue was lower, but the quantity of necrotic tissue higher in L-NAME relative to D-NAME-treated animals. The total mass of viable tissue (ie, stroma and tumor cells) was lower in L-NAME relative to D-NAME-treated animals. These data suggest that NO is a key mediator of C3L5 tumor-induced angiogenesis, and that the antitumor effects of L-NAME are partly mediated by reduced tumor angiogenesis. *(Am J Pathol 1999, 155:1381–1390)*

Nitric oxide, an inorganic free radical gas, is synthesized from the amino acid L-arginine by a group of enzymes, the NO synthases (NOS). At least three isoforms of NOS have been cloned, characterized, and localized: endothelial (e) and neuronal (n) NOS isoforms are Ca^{2+}/calmodulin-dependent and are expressed constitutively in these and other cells. The inducible (i) isoform is Ca^{2+}/calmodulin-independent and usually induced in the presence of inflammatory cytokines and bacterial products in macrophages, hepatocytes, and other cells. Under certain conditions, iNOS can also be expressed constitutively in some cells. When constitutively expressed, NO produced at low levels is an important mediator of physiological functions such as vasodilation, inhibition of platelet aggregation, and neurotransmission. Under inductive conditions, high levels of NO produced by macrophages and other effector cells can mediate antibacterial and antitumor functions. However, chronic induction of NOS may contribute to many pathological processes including inflammation and cancer.[1,2]

Much scientific research has focused on the role of NO in tumor progression; although two apparently conflicting views exist, overall an overwhelming amount of clinical and experimental evidence supports a positive association between NO production and tumor progression. The level of NOS protein and/or activity in the tumor has been positively correlated with the degree of malignancy for

tumors of the human reproductive tract,[3] breast,[4,5] and central nervous system.[6] In a majority of gastric carcinomas, iNOS was detected in stromal elements, and eNOS was detected in the tumor vasculature.[7] iNOS expression was higher in prostatic carcinomas relative to benign prostatic hyperplasia.[8] Similarly, relative to normal healthy control tissue, total NOS activity was higher in carcinomas of the larynx, oropharynx, oral cavity,[9] and adenocarcinomas of the lung.[10]

Experimental tumor models have provided more direct evidence of a contributory role of NO in tumor progression. Using a rat adenocarcinoma model in which cells of the tumor vasculature expressed iNOS, treatment of the host with the NOS inhibitor N^G-nitro-L-arginine methyl ester (L-NAME) reduced NO production and tumor growth.[11] Furthermore, despite *in vitro* cytostatic effects of NO induction with lipopolysaccharide (LPS) and interferon (IFN)-γ in EMT-6 murine mammary cells, this induction stimulated tumor growth and metastasis *in vivo*.[12] Finally, in our own studies using a murine mammary adenocarcinoma model (C3H/HeJ spontaneous mammary tumors and their clonal derivatives), NO-mediated stimulation of tumor progression was observed.[13] The spontaneously developing tumors showed heterogeneous expression of eNOS within primary tumors, whereas their metastatic counterparts were homogeneously eNOS positive, suggesting that eNOS expression promoted metastasis. A highly metastatic cell line, C3L5, clonally derived from a spontaneous mammary tumor showed strong eNOS expression *in vitro* and *in vivo*, and iNOS *in vitro* on stimulation with LPS and IFN-γ.[13] Treatment of C3L5 mammary tumor-bearing mice with inhibitors of NOS, L-NAME and N^G-methyl-L-arginine (NMMA), had antitumor and antimetastatic effects.[14,15] Reduced tumor cell invasiveness was identified as one of the mechanisms mediating these effects.[13,16] We hypothesized that, in this tumor model, additional mechanisms likely played critical roles in mediating the therapeutic effects of NOS inhibition.

In contrast to the above, some studies reported an inverse association between NO and tumor progression. For example, the levels of NOS enzymes and NOS activity declined during the transition of human colonic mucosa to polyps, and then to carcinomas.[17] However, a later study revealed higher NOS activity in adenomatous polyps, which was believed to promote increased angiogenesis before the transition of adenomas into carcinomas.[18] In a murine melanoma cell line, NOS activity was inversely correlated with capacity for metastasis.[19] When genetically transduced to overexpress iNOS, the melanoma cells,[19] as well as renal carcinoma cells,[20] lost their tumorigenic and metastatic abilities as a result of NO-mediated tumor cell apoptosis. These opposing findings suggest a dual role for NO in tumor growth and metastasis; the susceptibility of tumor cells to NO-mediated injury may depend on levels of NO produced and the genetic makeup of the tumor cells. During clonal evolution of tumors, high NO-producing cells may self-delete by apoptosis, and those making lower levels of NO or capable of resisting NO-mediated injury may have an *in vivo* advantage, resulting from NO-mediated stimulation

of tumor cell invasiveness, tumor blood flow or tumor angiogenesis.[13]

A body of recent evidence suggests a stimulatory role of NO in angiogenesis. For example, NO donors were found to increase proliferation and migratory function of endothelial cells *in vitro*.[21,22] Using the *in vivo* rabbit cornea assay, angiogenesis induced by vasoactive molecules such as substance P and prostaglandin E_1 was blocked with NOS inhibition.[22] Similarly, NOS inhibitors reduced neovascularization in acetic acid-induced gastric ulcers in rats,[23] and human squamous cell carcinoma xenografts in the rabbit cornea.[9] An angiogenesis-promoting role for tumor-derived NO was also suggested by the *in vivo* behavior of a human colon adenocarcinoma cell line engineered to continuously express iNOS. When transplanted into nude mice, the iNOS-transduced cells resulted in tumors with enhanced growth rate and vascularity relative to those derived from wild-type control cells.[24]

In the present study, we have evaluated the contributory role of NO in C3L5 mammary tumor-induced angiogenesis. To achieve this, we devised a novel *in vivo* Matrigel implant model of tumor-induced angiogenesis and subjected the host animals to chronic treatment with the NOS inhibitor L-NAME, or as controls, its inactive enantiomer, D-NAME.

Materials and Methods

Animals

Female C3H/HeJ mice (6–8 weeks old) were obtained from Jackson Laboratories (Bar Harbor, ME). On arrival at the vivarium, animals were immediately randomized to treatment groups (ie, L-NAME and D-NAME); experimental procedures began after a one-week acclimatization period. Throughout the investigation, animals had free access to food (standard mouse chow) and water and were maintained on a 12-hour light/dark cycle. Animals were treated in accordance with guidelines set out by the Canadian Council on Animal Care.

Tumor Cell Line

A spontaneously occurring mammary tumor in a female retired breeder C3H/HeJ mouse was the source of a primary transplantable tumor T58 from which a metastatic C3 cell line was derived. Since the metastatic potential of the C3 line declined over a number of years following repeated *in vitro* passages, a highly metastatic C3L5 line was derived by five cycles of repeated *in vivo* selections for spontaneous lung micrometastases following subcutaneous transplantation of C3 cells into C3H/HeJ mice.[25] The C3L5 cells used in the present study were grown from frozen stock and maintained in RPMI 1640 medium (GIBCO; Burlington, ON) supplemented with 5% fetal calf serum (GIBCO) and 1% penicillin-streptomycin (Mediatech; Washington, DC) in a humidified incubator, 5% CO_2.

In Vivo *Assay for Tumor-Induced Angiogenesis*

We devised a novel *in vivo* model of tumor angiogenesis based on the protocol of Kibbey et al.[26] These authors used conventional Matrigel, a reconstituted basement membrane, which is liquid at 4°C and forms a solid gelatinous mass at body temperature. Measurable angiogenesis occurred within these implants, possibly due to angiogenic growth factors present in the conventional Matrigel. In our application of the assay we used growth factor-reduced Matrigel, which, unlike conventional Matrigel, did not stimulate angiogenesis on its own. However, when tumor cells were suspended in growth factor-reduced Matrigel as a component of the subcutaneous implant, a strong angiogenic response was observed, which was easily and objectively quantifiable. Based on several pilot experiments in which the implant volume, tumor cell number, and implant duration were varied, we standardized the assay (the detailed kinetics of tumor-induced angiogenesis in these implants are not presented here). This assay was used to examine the effects of NO on the angiogenic response by administering L-NAME or its inactive enantiomer, D-NAME, to mice using osmotic minipumps (pilot experiments established an equivalent angiogenic response in animals receiving D-NAME and those receiving no treatment). The angiogenic response was evaluated by examining the gross morphology of the Matrigel implants and quantifying neovascularization in sections stained with Masson's trichrome or immunostained for the endothelial-specific CD31 antigen (PECAM). In addition, we documented the mass (weight in mg) of the implants on retrieval and systematically analyzed sections of tumor cell-inclusive implants for area quantification of three histologically distinct regions: peripheral tumor-free stromal tissue feeding blood vessels into the more deeply located tumor tissue; viable tumor tissue; and necrotic regions, to determine the effects of therapy on the various components of the implants.

In the inguinal region, mice received subcutaneous implants of 5×10^4 C3L5 cells suspended in growth factor reduced Matrigel (Collaborative Research, Bedford, MA) (3.5 mg of Matrigel in 0.5 ml of RPMI 1640), and on the contralateral side as controls, the equivalent amount of Matrigel alone. Immediately thereafter, osmotic minipumps (ALZA Corporation, Palo Alto, CA) were implanted subcutaneously, providing a constant systemic supply (0.5 ml/hour; 25 mg/200 μl 0.9% NaCl) of L-NAME to one group ($n = 15$), or D-NAME to the other group ($n = 15$) (both drugs purchased from Sigma Chemical Co., St. Louis, MO) for the experiment duration (14 days). This experiment was performed on two separate occasions; both experiments were conducted using the same protocol and sample size (ie, $n = 15$ animals/group).

Mice were sacrificed using an overdose of pentobarbital and the Matrigel implants were removed and divided in half; therefore paraffin and frozen sections were obtained from the same sample. Samples fixed in 4% paraformaldehyde, processed for paraffin embedding, and sectioned were stained with Masson's trichrome or immunostained for eNOS and iNOS proteins. Alternatively,

samples frozen in OCT were sectioned and analyzed immunohistochemically for CD31. Both types of sections (ie, Masson's trichrome stained or CD31 immunostained) were scanned at low power for areas containing new blood vessels (researcher blind to experimental condition); these areas were systematically imaged at 160× magnification using Northern Exposure (Empix Imaging Inc.), and individual vessel counts for each field were documented using Mocha Image Analysis Software (Jandel Scientific) to identify fields of maximum blood vessel density (ie, "hot spots"). Subsequently, "hot spots" were statistically analyzed for between-group differences using two different approaches: the average ($n = 15$ animals/group) of the maximal number of blood in one field per animal, and the average ($n = 15$ animals/group) of the average of three fields of maximal blood vessel density (taken in descending order) per animal. Masson's trichrome-stained sections were also used to quantify histologically distinct regions within implants (ie, peripheral stromal, healthy tumor, and necrotic regions); entire cross sections of the implants were digitally imaged; areas were then quantified, and data expressed as the number of pixels, using Mocha Image Analysis Software (researcher blind to experimental condition).

Immunohistochemical Localization of CD31 Antigen (PECAM-1)

OCT-fixed samples were stored at −80°C until sectioned; samples were sectioned at 5 μm thickness and stored at −20°C before immunostaining (sections stored for maximum of 2 days at −20°C). Frozen sections were fixed in ice-cold methanol (5 minutes, −20°C). Endogenous peroxidase activity was blocked with methanol containing 3% H_2O_2 (30 minutes, room temperature) before application of blocking serum: normal mouse serum (Cedarlane Laboratories Limited, Hornby, ON) diluted in 1% bovine serum albumin (1:10; 1 hour at room temperature in humidified chamber). Sections were then incubated with primary antibody: purified rat anti-mouse CD31 monoclonal antibody (1:50; overnight at 4°C in humidified chamber; Cedarlane Laboratories) followed by secondary antibody: biotinylated mouse anti-rat IgG-2a monoclonal antibody (1:100; 1 hour at room temperature in humidified chamber; Caltag Laboratories, San Francisco, CA). Avidin-biotin complex (ABC) (Vector Laboratories, Inc., Burlingame, CA) was then applied (1 hour at room temperature), followed by diaminobenzidine chromogen (Sigma); sections were then lightly counterstained with Mayer's hemalum. Negative controls were incubated with the equivalent concentration of rat IgG-2a (Caltag Laboratories) in place of primary antibody.

Immunohistochemical Localization of eNOS and iNOS Antigens

Paraffin-embedded implants were sectioned at 7 μm thickness. Following deparaffinization and rehydration of sections, endogenous peroxidase activity was blocked

using methanol containing 3% H_2O_2 before application of blocking serum (normal horse serum, 1:10; 1 hour at room temperature). Sections were then incubated with primary antibody: mouse monoclonal anti-eNOS or mouse monoclonal anti-macrophage iNOS (1:80; overnight at 4°C, or 1:50; overnight at 4°C; Transduction Laboratories, Lexington, KY) for eNOS and iNOS localization, respectively. Secondary antibody (biotinylated horse anti-mouse, 1:200; 1 hour at room temperature) was then applied, followed by ABC (1 hour at room temperature) and diaminobenzidine chromogen. Sections were lightly counterstained with Mayer's hemalum.

Data Analysis

Data were analyzed using SAS v6.12 on a Unix mainframe computer, and treatment groups (ie, L-NAME and D-NAME) compared using one-way analysis of variance. In quantifying neovascular response for each treatment group (n = 15 mice/group), results were expressed as the mean of the maximum number of microvessels in a single field (160× magnification) and the mean number of microvessels in three fields of maximum blood vessel density (160× magnification). Data from the duplicate experiment (n = 15 mice/group) were analyzed in the same manner. A probability of 0.05 was used in determining statistical significance.

Results

Gross Morphology of Implants

Figure 1 shows the gross morphology of tumor-exclusive implants (Figure 1A) and tumor-inclusive implants obtained from L-NAME and D-NAME-treated (Figure 1, B and C, respectively) animals. Tumor-exclusive implants from L-NAME and D-NAME-treated animals were small, translucent, and avascular. Tumor-inclusive implants were larger, and implants obtained from L-NAME-treated animals were less vascular than those obtained from D-NAME-treated animals.

Histological Evaluation of Vascularity of Implants—Masson's Trichrome Staining

Figure 1 shows Masson's trichrome staining of tumor-exclusive Matrigel implant (Figure 1D) (sections of tumor cell-exclusive implants were identical for L-NAME and D-NAME-treated animals) and tumor-inclusive implants obtained from L-NAME (Figure 1E) and D-NAME-treated animals (Figure 1F). This method stains fibrous tissue and stroma bluish-green. Blood vessels containing red blood cells stand out because of bright red staining of red blood cells. Other cells (including tumor cells) show pink staining of cytoplasm and dark magenta colored nuclei. Tumor-exclusive Matrigel implants obtained from L-NAME and D-NAME-treated animals were avascular and contained a few fibroblasts. Tumor-inclusive implants obtained from both treatment groups consisted of

three histologically distinct regions, shown in Figure 1G (implant obtained from L-NAME-treated animal): a peripheral zone of stroma (S) containing feeder blood vessels; healthy tumor areas (T); and more centrally located necrotic areas (N) infiltrated with leukocytes. Areas of highest microvascular count were best identified in the stroma of tumor-inclusive implants in Masson's trichrome-stained sections. The stroma of tumor-inclusive implants obtained from L-NAME-treated animals appeared thinner and less vascular relative to those obtained from D-NAME-treated animals.

Histological Evaluation of Vascularity of Implants—CD31 Immunostaining

Figure 2 shows immunohistochemical localization of CD31 antigen in implants obtained from D-NAME and L-NAME-treated animals (Figure 2, A and B, respectively). This method stains endothelial cells brown and correctly identifies cells lining the microvasculature within the tumor component of the implants (in contrast to Masson's trichrome-stained sections, which predominantly identifies blood vessels within stromal areas). Nuclei are lightly counterstained with Mayer's hemalum. Neovascularization was reduced in tumor-inclusive implants obtained from L-NAME-treated animals relative to those obtained from D-NAME-treated animals.

Histological Evaluation of Implants—eNOS and iNOS Immunostaining

Immunohistochemical localization of eNOS antigen in tumor-inclusive implant and a negative control are shown in Figure 2, C and D, respectively. eNOS expression was observed in endothelial cells of the tumor vasculature (Figure 2C, inset), and a high proportion of tumor cells within implants obtained from animals treated with either L-NAME or D-NAME. Immunohistochemical localization of iNOS antigen is shown in Figure 2, E and F. Regardless of treatment group, tumor cells within the implants did not stain positively for iNOS. However, positive immunoreactivity for iNOS protein was observed in a significant proportion of macrophages located in peripheral stroma (Figure 2E), in the healthy tumor bordering the necrotic area (Figure 2F), and within the central necrotic area (not shown in Figure 2). Endothelial cells also stained positively for iNOS (Figure 2E, small arrow).

Quantification of Tumor-Induced Neovascularization—Masson's Trichrome Staining and CD31 Immunostaining

Figure 3 shows the number of blood vessels per unit area for Masson's trichrome-stained and CD31 immunostained sections; data are expressed as the maximum number of blood vessels per field and as the average number of blood vessels in three fields of maximal density. Irrespective of staining protocol or method of quan-
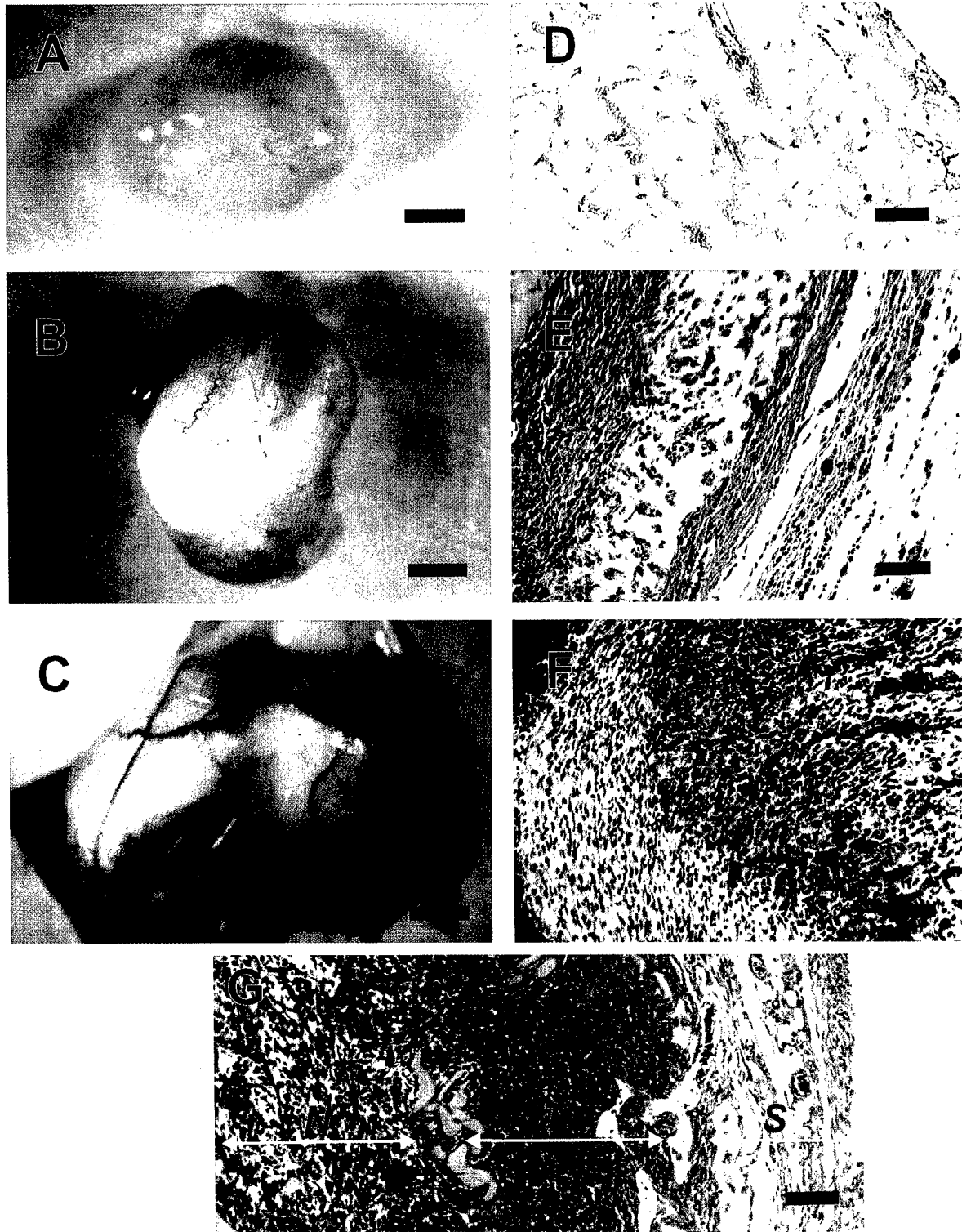
Figure 1. Gross morphology is shown for tumor-exclusive Matrigel implants (A) and tumor-inclusive Matrigel implants obtained from L-NAME- and D-NAME-treated animals (B and C, respectively). Tumor-exclusive implants were translucent, avascular, and unaffected by L-NAME or D-NAME treatment. Tumor-inclusive implants were larger, and those obtained from L-NAME-treated animals were less vascular relative to those obtained from D-NAME-treated animals. Photomicrographs of Masson's trichrome staining are shown for tumor-exclusive (D) and tumor-inclusive Matrigel implants obtained from L-NAME-treated (E) and D-NAME-treated (F) animals. Tumor-exclusive implants obtained from L-NAME- and D-NAME-treated animals were avascular and contained a few fibroblasts. The sections of tumor-inclusive implants in both treatment groups showed three histologically distinct areas, shown in G (from L-NAME-treated animal): peripheral stroma (S), adjacent tumor-dominant area (T), and central zone of necrosis (N). The stromal components in L-NAME-treated animals appeared thinner and less vascular relative to those in D-NAME-treated animals. Scale bars: **A–C**, 1 mm; **D–G**, 30 μm.
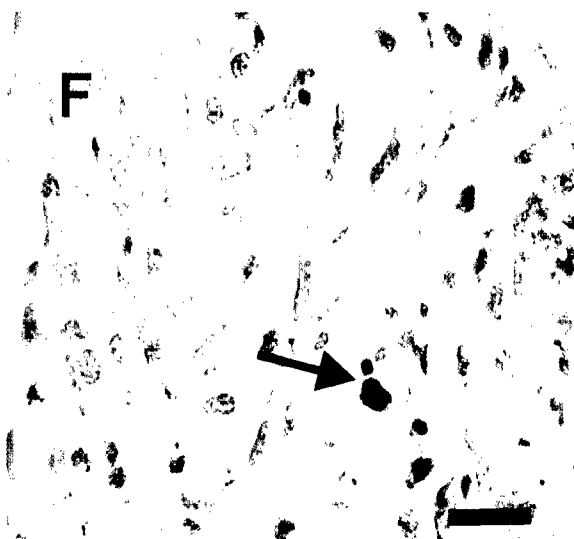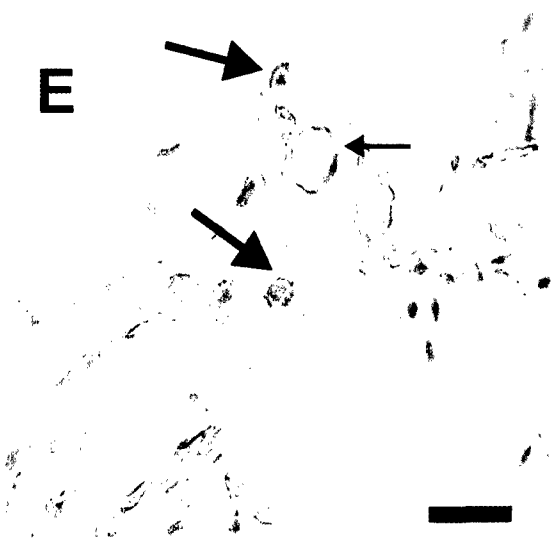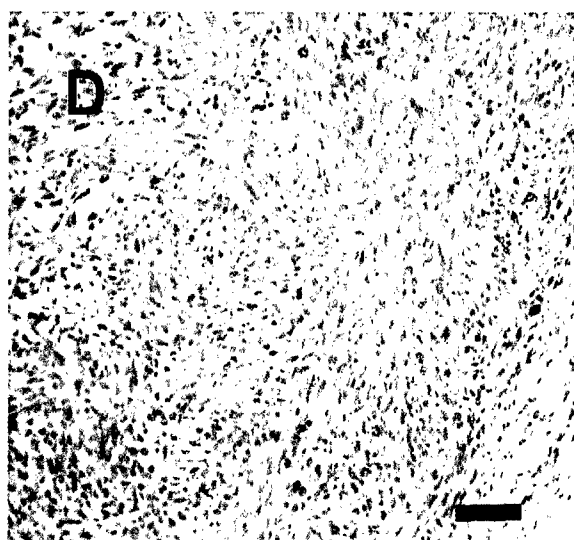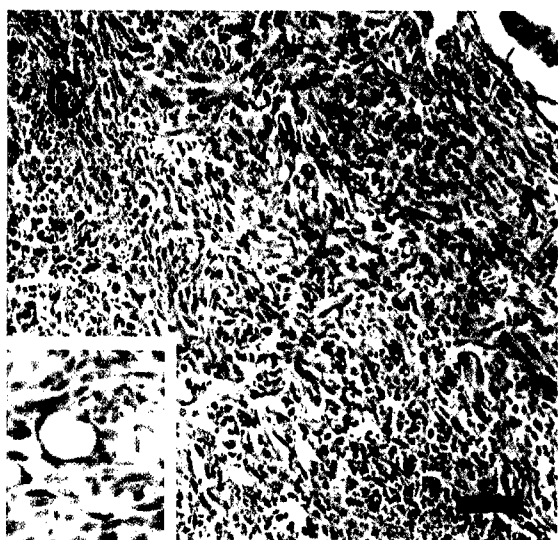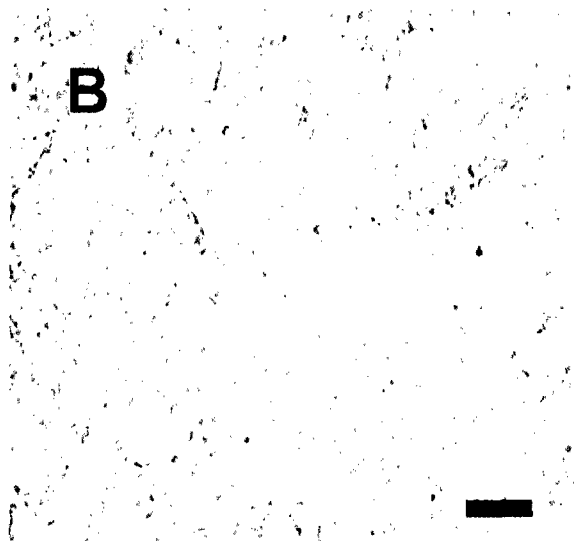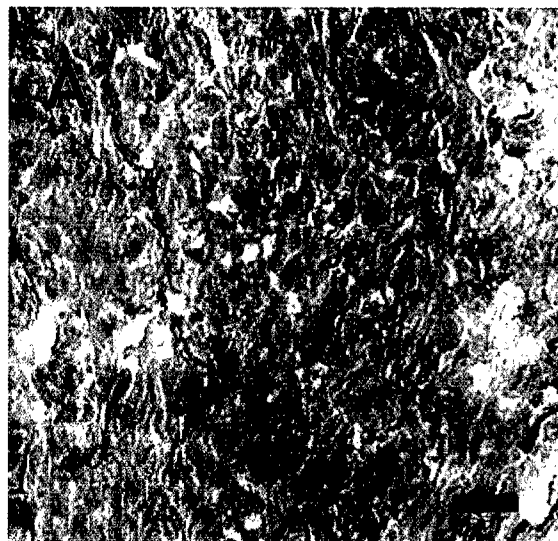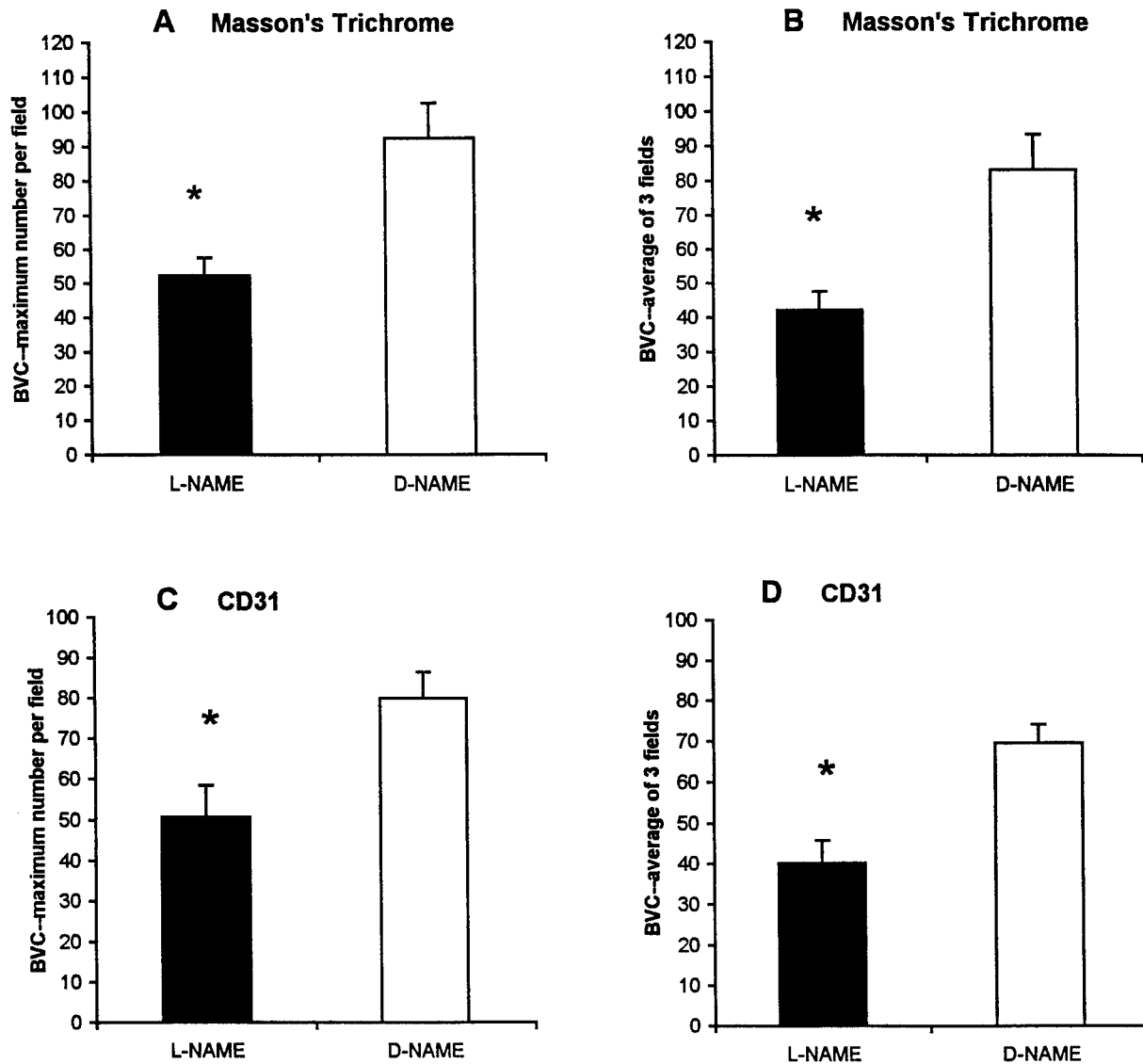
Figure 3. Quantification of tumor-induced neovascularization in sections stained with Masson's trichrome (A and B) and immunostained for CD31 (C and D). The data were expressed as the maximum number of blood vessels per field (mean ± SE; n = 15 animals/group) and as the average number of blood vessels in 3 fields of maximal density (mean ± SE; n = 15 animals/group). Irrespective of staining protocol or method of quantification used, the neovascular response was reduced in L-NAME-treated mice relative to those treated with D-NAME as indicated by the P value in each panel: A, $P < 0.003$; B, $P < 0.001$; C, $P < 0.0099$; D, $P < 0.0009$. BVC, blood vessel count.

tification used, the neovascular response was reduced in L-NAME-treated mice relative to those treated with D-NAME. Tumor-induced neovascularization, measured by Masson's trichrome, was reduced in implants obtained from L-NAME-treated animals when data were expressed as 1) the maximum number of blood vessels per field (L-NAME, 52.3 ± 5.9; D-NAME, 92.3 ± 11.3, $P < 0.003$) and 2) as the average number of blood vessels in three

fields (L-NAME, 42.1 ± 5.4; D-NAME, 83.2 ± 10.2, $P < 0.001$) (Figure 3, A and B, respectively). L-NAME treatment reduced tumor-induced neovascularization, as measured by CD31 immunostaining, when data were expressed 1) as the maximum number of blood vessels per field (L-NAME, 50.8 ± 7.6; D-NAME, 79.9 ± 6.5, $P < 0.0099$) and 2) as the average number of blood vessels in three fields (L-NAME, 40.1 ± 5.6; D-NAME, 69.6 ± 4.8,

Figure 2. Immunohistochemical localization of CD31 antigen is shown at top in tumor-inclusive implants from D-NAME- and L-NAME-treated animals (A and B, respectively), identifying endothelial cells lining the microvasculature within the tumor component of the implants. Neovascularization was reduced in L-NAME-treated animals relative to those treated with D-NAME. Immunohistochemical localization of eNOS antigen is shown at center in tumor-inclusive implants; positive immunostaining and negative control are shown (C and D, respectively). A high proportion of tumor cells and endothelial cells lining the tumor vasculature (inset in C) within implants expressed eNOS, regardless of treatment group. The bottom shows immunohistochemical localization of iNOS antigen in peripheral stroma (E) and healthy tumor (F) bordering necrotic area. Expression of iNOS did not differ between treatment groups. Positive immunoreactivity for iNOS protein was evident in macrophages (large arrows) located in stromal (E) and tumor (F), as well as within central necrotic (not shown) areas of the implants in both treatment groups. Endothelial cells (small arrow) stained positively for iNOS, and some nonspecific staining of stromal tissue was observed in both treatment groups. Scale bars: A–D, 30 μm; E–F, 50 μm; C, inset, 60 μm.

$P < 0.0009$) (Figure 3, C and D, respectively). Results obtained from the duplicate experiment were similar and are not presented.

Quantification of Histologically Distinct Areas within Implants

Quantification of the various tissue compartments contained within tumor cell-inclusive implants indicated that the quantity of peripherally located stromal tissue was reduced in L-NAME relative to D-NAME-treated animals (L-NAME, 4998.5 ± 1055.2 pixels; D-NAME, 9758.3 ± 1515.4 pixels, $P < 0.02$), and the quantity of necrotic tissue was higher in L-NAME relative to D-NAME-treated animals (L-NAME, 73709.5 ± 8638.0 pixels; D-NAME, 38434.5 ± 7918.3 pixels, $P < 0.007$). In addition, the mass of viable tissue (ie, stroma and tumor cells), was lower in L-NAME relative to D-NAME-treated animals (L-NAME, 17.1 ± 3.5%; D-NAME, 28.8 ± 4.0%, $P < 0.04$). Values for the mass of viable tissue were calculated using the following formula: weight of implant (mg) × (1 − necrotic fraction of the implant).

Discussion

Angiogenesis, the development of new blood vessels from the pre-existing vascular bed, is an essential feature of many physiological conditions including wound healing, embryonic development, and endometrial proliferation. Numerous pathological conditions, such as diabetic retinopathy, rheumatoid arthritis, and tumor growth are also characterized by abnormal neovascularization. Growth of solid tumors cannot proceed beyond a microscopic size without the development of an extensive vascular system.[27] Furthermore, because the degree of vascularization often correlates with poor clinical prognosis and increased likelihood of metastasis of a number of human tumors,[28,29] targeting angiogenesis in the therapeutic intervention of cancer has received substantial attention. Although a number of compounds characterized as inhibitors of angiogenesis have entered clinical trials, intense efforts to identify potent angiogenesis inhibitors with improved selectivity continue. However, a consistent limitation of these investigations has been the availability of simple, reproducible, reliable, and easily quantifiable assays that reflect *in vivo* systems for tumor-induced angiogenesis. Overly simplistic cellular *in vitro* systems and technical difficulties of currently used *in vivo* angiogenesis assays are important limiting factors.

In vitro models of angiogenesis[22,30] may not be ideal for measuring tumor-induced angiogenesis because of the inability in providing all of the necessary cells and/or factors that may interact in the *in vivo* tumor environment. The most widely used *in vivo* systems are the rabbit cornea and the chick chorioallantoic membrane (CAM) assays, in which variability of results and subjectivity in quantification remain important limitations.[31] A major concern of the rabbit cornea assay is the potential devel-

opment of xenograft reactions after tumor implantation. Although the cornea is an immunoprivileged site, as it gradually becomes vascularized, the possible contribution of xenograft reactions to the angiogenic response cannot be disregarded. The CAM assay does not present this problem, because the host is naturally immunodeficient. However, major disadvantages of this assay are the time limit of 7 to 10 days imposed by embryo growth and acquisition of immunocompetence[32] and difficulties in objectively quantifying the neovascular response.[31,33] Another potential concern is inherent with properties of the chick chorioallantoic membrane, which is a growing and developing embryonic structure; the relative contribution of vasculogenesis and/or angiogenesis, two discrete processes which are differentially regulated, to the development of new blood vessels may not be clear.

The present *in vivo* model of tumor-induced angiogenesis is devoid of these limitations. The assay is simple, reproducible, and objectively quantifiable. Suspension of tumor cells within the Matrigel matrix serves to effectively immobilize tumor cells; the ensuing angiogenic response is organized, and all stages of the neovascular response can be quantified. Therefore, the kinetics of tumor development and neovascularization may be followed for a considerable length of time (eg, 2 weeks in the present experiment); in separate experiments, we have established that the experimental procedure can be extended (eg, up to 6 weeks). Furthermore, because the developing blood vessels converge within a discrete area, retrieval and quantification of developing blood vessels are simple and complete. Use of a specific inoculation site in the murine model minimizes variation of the angiogenic response. Although we used an inbred mouse strain and its syngeneic tumor, nude mice could appropriately serve as the host for xenografts in other applications of this assay, and in particular, for human tumors.

We used the present assay to evaluate the effects of NO on the angiogenic response by administering L-NAME or D-NAME to mice using osmotic minipumps in two separate experiments. Results from both clearly showed that, irrespective of method of quantification, NOS inhibition dramatically reduced the neovascular response. The growth patterns of histologically distinct areas present within the implants were differentially affected by NOS inhibition. The stromal component of the implants, which supports the vascular supply, was reduced in L-NAME- relative to D-NAME-treated animals. In addition, there was increased necrosis and reduced viable tissue mass within implants obtained from L-NAME relative to D-NAME-treated animals, supporting prior observations of antitumor effects of NOS inhibition in mice transplanted with C3L5 mammary adenocarcinomas.[14,15] Therefore, the antitumor and antimetastatic effects of NOS inhibition, previously attributed in part to reduced tumor cell invasiveness,[16] may also be explained by reduced neovascularization.

Inherent NOS activity of the eNOS-expressing mammary adenocarcinoma cells used in the present research is likely the major source of NO contributing to the NO-mediated induction of angiogenesis. eNOS expression

by endothelial cells, as well as iNOS expression by some macrophages and endothelial cells, may serve as additional minor sources of NO in these tumor implants.

The precise molecular mechanisms responsible for reduced angiogenesis with NOS inhibition in our model remain to be determined. NO is required for endothelial cell proliferation, migration, and organization, key components of the angiogenic cascade.[22,34,35] Using a rabbit cornea assay, it has been shown that NO is a downstream mediator of vascular endothelial growth factor (VEGF)-induced angiogenesis, since it could be blocked by administering L-NAME.[35] Further evidence supports this notion; angiogenesis in response to tissue ischemia (an inducer of VEGF) was reduced in eNOS −/− mice.[36] VEGF-stimulated proliferation of endothelial cells, triggered by NO, was shown to require intracellular signaling via cGMP-dependent protein kinase,[37] Raf-1 kinase,[37] and mitogen- activated protein kinase.[35] Our preliminary results (data not shown) indicate that the C3L5 mammary adenocarcinoma cells used in the present research express VEGF protein *in vitro*. Whether VEGF expression in these cells is induced by endogenous NO remains to be determined; an up-regulation of VEGF mRNA by NO was reported for rat mesangial cells.[38] Co-expression of eNOS and VEGF in C3L5 cells may equip them with a dual advantage in inducing NO-mediated angiogenesis from the host vasculature, VEGF-mediated stimulation of NO in the vascular endothelium and NO produced by tumor cells by activation of eNOS.

References

1. Moncada S, Higgs A: The L-arginine-nitric oxide pathway. N Engl J Med 1993, 329:2002–2012
2. Knowles RG, Moncada S: Nitric oxide synthases in mammals. Biochem J 1994, 298:249–258
3. Thomsen LL, Lawton FG, Knowles RG, Beesley JE, Riveros-Moreno V, Moncada S: Nitric oxide synthase activity in human gynecological cancer. Cancer Res 1994, 54:1352–1354
4. Thomsen LL, Miles DW, Happerfield L, Bobrow LG, Knowles RG, Moncada S: Nitric oxide synthase activity in human breast cancer. Br J Cancer 1995, 72:41–44
5. Dueñas-Gonzalez A, Isales CM, del Mar Abad-Hernandez M, Gonzalez-Sarmiento R, Sangueza O, Rodriguez-Commes J: Expression of inducible nitric oxide synthase in breast cancer correlates with metastatic disease. Mod Pathol 1997, 10:645–649
6. Cobbs CS, Brenman JE, Aldape KD, Bredt DS, Israel MA: Expression of nitric oxide synthase in human central nervous system tumors. Cancer Res 1995, 55:727–730
7. Thomsen LL, Miles DW: Role of nitric oxide in tumor progression: lessons from human tumors. Cancer Metastasis Rev 1998, 17:107–118
8. Klotz T, Bloch W, Volberg C, Engelmann U, Addicks K: Selective expression of inducible nitric oxide synthase in human prostate carcinoma. Cancer 1998, 82:1897–1903
9. Gallo O, Masini E, Morbidelli L, Franchi A, Fini-Storchi I, Vergari WA, Ziche M: Role of nitric oxide in angiogenesis and tumor progression in head and neck cancer. J Natl Cancer Inst 1998, 90:587–596
10. Fujimoto H, Ando Y, Yamashita T, Terazaki H, Tanaka Y, Sasaki J, Matsumoto M, Suga M, Ando M: Nitric oxide synthase activity in human lung cancer. Jpn J Cancer Res 1997, 88:1190–1198
11. Kennovin GD, Hirst DG, Stratford MRL, Flitney FW: Inducible nitric oxide synthase is expressed in tumor-associated vasculature: inhibition retards tumor *in vivo*. Biology of Nitric Oxide, Part 4: Enzymology,
Biochemistry, and Immunology. Edited by S Moncada, M Feelisch, R Busse, EA Higgs. London, Portlant Press, 1994, pp 473–479
12. Edwards P, Cendan JC, Topping DB, Moldawer LL, MacKay S, Copeland EM, Lind DS: Tumor cell nitric oxide inhibits cell growth *in vitro*, but stimulates tumorigenesis and experimental lung metastasis *in vivo*. J Surg Res 1996, 63:49–52
13. Lala PK, Orucevic A: Role of nitric oxide in tumor progression: lessons from experimental tumors. Cancer Metastasis Rev 1998, 17:91–106
14. Orucevic A, Lala PK: N^G-nitro-L-arginine methyl ester, an inhibitor of nitric oxide synthesis, ameliorates interleukin-2-induced capillary leakage, and reduces tumor growth in adenocarcinoma-bearing mice. Br J Cancer 1996, 73:189–196
15. Orucevic A, Lala PK: Effects of N^G-methyl-L-arginine, an inhibitor of nitric oxide synthesis, on IL-2-induced capillary leakage and antitumor responses in healthy and tumor-bearing mice. Cancer Immunol Immunother 1996, 42:38–46
16. Orucevic A, Bechberger J, Green AM, Shapiro RA, Billiar TR, Lala PK: Nitric oxide production by murine mammary adenocarcinoma cells promotes tumor cell invasiveness. Int J Cancer 1999, 81:889–896
17. Chhatwal VJ, Ngoi SS, Chan ST, Chia YW, Moochhala SM: Aberrant expression of nitric oxide synthase in human polyps, neoplastic colonic mucosa and surrounding peritumoral normal mucosa. Carcinogenesis 1994, 15:2081–2085
18. Ambs S, Merriam WG, Bennett WP, Felley-Bosco E, Ogunfusika MO, Oser SM, Klein S, Shields PG, Billiar TR, Harris CC: Frequent nitric oxide synthase-2 expression in human colon adenomas: implication for tumor angiogenesis and colon cancer progression. Cancer Res 1998, 58:334–341
19. Dong Z, Staroselsky AH, Qi X, Xie K, Fidler IJ: Inverse correlation between expression of inducible nitric oxide synthase activity and production of metastasis in K-1735 murine melanoma cells. Cancer Res 1994, 54:789–793
20. Juang SH, Xie K, Xu L, Shi Q, Wang Y, Yoneda J, Fidler IJ: Suppression of tumorigenicity and metastasis of human renal carcinoma cells by infection with retroviral vectors harboring the murine inducible nitric oxide synthase gene. Hum Gene Ther 1998, 9:845–854
21. Ziche M, Morbidelli L, Masini E, Granger HJ, Geppetti G, Ledda F: Nitric oxide promotes DNA synthesis and cyclic GMP formation in endothelial cells from postcapillary venules. Biochem Biophys Res Commun 1993, 192:1198–1203
22. Ziche M, Morbidelli L, Masini E, Amerini S, Granger HJ, Maggi CA, Geppetti P, Ledda F: Nitric oxide mediates angiogenesis *in vivo* and endothelial cell growth and migration *in vitro* promoted by substance P. J Clin Invest 1994, 94:2036–2044
23. Konturek SJ, Brzozowski T, Majka J, Pytko-Polonczyk J, Stachura J: Inhibition of nitric oxide synthase delays healing of chronic gastric ulcers. Eur J Pharmacol 1993, 239:215–217
24. Jenkins DC, Charles IG, Thomsen LL, Moss DW, Holmes LS, Baylis SA, Rhodes P, Westmore K, Emson PC, Moncada S: Roles of nitric oxide in tumor growth. Proc Natl Acad Sci USA 1995, 92:4392–4396
25. Lala PK, Parhar RS: Eradication of spontaneous and experimental adenocarcinoma metastases with chronic indomethacin and intermittent IL-2 therapy. Int J Cancer 1993, 54:677–684
26. Kibbey MC, Grant DS, Kleinman HK: Role of the SIKVAV site of laminin in promotion of angiogenesis and tumor growth: an in vivo Matrigel model. J Nat Cancer Inst 1992, 84:1633–1637
27. Folkman J: Tumor angiogenesis: therapeutic applications. N Engl J Med 1971, 285:82–86
28. Weidner N, Semple JP, Welch WR, Folkman J: Tumor angiogenesis and metastasis-correlation in invasive breast carcinoma. N Engl J Med 1991, 324:1–8
29. Wiggins DL, Granai CO, Steinhoff MM, Calabresi P: Tumor angiogenesis as a prognostic factor in cervical carcinoma. Gynecol Oncol 1995, 56:353–356
30. Brown KJ, Maynes SF, Bezos A, Maguire DJ, Ford MD, Parish CR: A novel in vitro assay for human angiogenesis. Lab Invest 1996, 75:539–555
31. Auerbach R, Auerbach W, Polakowski I: Assays for angiogenesis: a review. Pharmacol Ther 1991, 51:1–11
32. Leighton J: Invasion and metastasis of heterologous tumors in the chick embryo. Prog Exp Tumor Res 1964, 4:98–125

33. Vu MT, Smith CF, Burger PC, Klintworth GK: An evaluation of methods to quantitate the chick chorioallantoic membrane assay in angiogenesis. Lab Invest 1985, 53:499–508

34. Papapetropoulos A, Desai KM, Rudic RD, Mayer B, Zhang R, Ruiz-Torres MP, Garcia-Cardeña G, Madri JA, Sessa WC: Nitric oxide synthase inhibitors attenuate transforming-growth-factor-β1-stimulated capillary organization in vitro. Am J Pathol 1997, 150:1835–1844

35. Ziche M, Morbidelli L, Choudhuri R, Zhang HT, Donnini S, Granger HJ, Bicknell R: Nitric oxide synthase lies downstream from vascular endothelial growth factor-induced but not fibroblast growth factor-induced angiogenesis. J Clin Invest 1997, 99:2625–2634

36. Murohara T, Asahara T, Silver M, Bauters C, Masuda H, Kalka C, Kearney M, Chen D, Symes JF, Fishman MC, Huang PL, Isner JM: Nitric oxide synthase modulates angiogenesis in response to tissue ischemia. J Clin Invest 1998, 101:2567–2578

37. Hood J, Granger HJ: Protein kinase G mediates vascular endothelial growth factor-induced Raf-1 activation and proliferation in human endothelial cells. J Biol Chem 1998, 273:23504–23508

38. Frank S, Stallmeyer B, Kampfer H, Schaffner C, Pfeilschifter J: Differential regulation of vascular endothelial growth factor and its receptor fms-like tyrosine kinase is mediated by nitric oxide in rat renal mesangial cells. Biochem J 1999, 338:367–374